Biohydrogen Production from Crude Glycerol: Process Optimization and Intensification

A
Thesis
Submitted in
Partial Fulfillment of the
Requirements for the Degree of

DOCTOR OF PHILOSOPHY

By

Shyamali Sarma

CENTRE FOR ENERGY
Indian Institute of Technology Guwahati
Guwahati – 781 039, Assam, India
AUGUST 2018

Dedicated

to

My Parents

(Maa & Dewta)

INDIAN INSTITUTE OF TECHNOLOGY GUWAHATI

Centre for Energy

STATEMENT

I do hereby declare that the content embodied in this thesis entitled "*Biohydrogen Production from Crude Glycerol: Process Optimization and Intensification*" is the result of investigations carried out by me in the Centre for Energy, Indian Institute of Technology Guwahati, Guwahati, India, under the guidance of Prof. Vijayanand S. Moholkar and Prof. Vikash Kumar Dubey. In keeping with the general practice of reporting scientific observations, due acknowledgements have been made wherever the work described is based on the findings of other investigators.

Date: Shyamali Sarma

(Roll No.:136151007)

ACKNOWLEDGEMENTS

I take utmost pleasure to express my gratitude to all who made this thesis possible. I owe my deepest gratitude to each one of them who stand by me constantly and dynamically during my research work to make this possible.

I express my prime gratitude to the Lord Almighty for giving me the confidence and strength for the successful completion of the entire Ph.D I acknowledge sincere and grateful thanks to my supervisors ***Prof. Vijayanand S. Moholkar*** and ***Prof. Vikash Kumar Dubey*** for their valuable suggestions, encouragement, and constant support throughout my research work. I sincerely thank them for spending their valuable time for discussion by which I have gained immense skill and knowledge in terms of research and enlightening me the first glance of research. I could not have imagined of having better advisors and mentors for my Ph.D. study. I would also like to express my sincere gratitude to all my doctoral committee members ***Prof. Arun Goyal, Prof. Kannan Pakshirajan***, and ***Dr. Vaibhav Goud*** for their insightful advices, suggestions, and encouragement throughout the research that has led to the successful completion of my thesis.

My sincerely thanks go to the faculty and staff members of **Centre for Energy** and **Department of Chemical Engineering** for their kind help and support. I am thankful to Center for Energy, Department of Chemical Engineering and **Central Instruments Facilities (CIF)** for providing facilities to carry out my research work. I am also thankful to the Indian **Institute of Technology Guwahati** for providing me with the infrastructure and facilities for advanced research.

I place on record my warm gratitude to the **British Council and DBT**, Govt. of India for awarding me with **Newton-Bhaba fellowship, 2017** (Newton Bhaba Ph.D Placement Programme 2017) and funding a part of my research work which gave me an opportunity to work in the esteemed **University of Nottingham, Nottingham, United Kingdom.**

It is my immense pleasure to acknowledge **Prof. Nigel Minton** (Director, Synthetic Biology Research Centre, **Centre for Biomolecular Sciences**, The University of Nottingham, UK) and his group members for the supervision and providing the infrastructure for conducting a part of my research work. I sincerely thank the staff members of Synthetic Biology Research Centre, Centre for Biomolecular Sciences, The University of Nottingham, UK for providing facilities to carry out a part of my research work.

I am immensely thankful to my seniors *Dr. Shuchi Singh, Dr. Sankar Chakma, Dr. Jaykumar B. Bhasarkar, Dr. Maneesh Poddar, Dr. Pritam Dikshit* and research group members, *Arup, Amit, Neha, Niharika, Ritesh, Kuldeep, Philip, Belachew, Dr. Binota, Debarshi, Kajol, Udangshree, Bhaskar, Mayank, STP Bharadwaj, Sushobhan*, *Avinash, Mriganka, Dr. Mousumi, Dr. Ruchika, Dr. Shalini, Ritesh, Kartikeyan, Adarsh, Gundappa, Kamlesh, Dr. Jay.*

I am thankful to my friends *Firdausa Ahmed, Sanjukta Devi and Nilakshi Sarma* for all the love and support throughout my Ph.D.

My Ph.D endeavor would not have been successful without the endless love, trust, support and blessing of these members of my family: Grandmother (*Saru Devi)*; my sisters *Miss Dolly Sharma*, *Mrs. Chinmayee Sarma,* brother *Mr. Pulakesh Sarma* and brother-in law *Mr. Gunajit Goswami* for always standing by me and loving me selflessly. Finally, I would like to express my heartfelt thanks to my affectionate and ever-loving husband and friend *Mr. Rajnish Kumar* who has helped and supported in each and every

step of my Ph.D. endeavor. At last but not the least, I am highly indebted to my parents, ***Mr. Jogeswar Sarma*** and ***Mrs. Hema Prava Devi*** for all their sacrifices they have made for my better future, to have faith in me, and giving me freedom to take my own decision. My Ph.D. endeavor could not be completed without them.

LIST OF ABBREVIATIONS

ATCC	American Type Culture Collection
ATP	Adenosine triphosphate
BSH	Basal solution for hydrogen production
CCD	Central composite design
C. pasteurianum	*Clostridium pasteurianum*
DHA	Dihroxy acetone
dhaD	Glycerol dehydrogenase
dhaK	Dihydroxyacetone kinase
E. coli	*Escherichia coli*
EMP	Embden–Meyerhof–Parnas
Fd	Ferredoxin
H_2	Hydrogen
hydA	Hydrogenase A
KEGG	Kyoto Encyclopedia of Genes and Genomes
MFA	Metabolic Flux Analysis
MT	Megaton
MTCC	Microbial Type Culture Collection
NAD (P)	Nicotinamide adenine dinucleotide phosphate
1,3-PDO	1,3-propanediol
PFOR	Pyruvate Ferredoxin Oxidoreductase
RCM	Reinforced Clostridial Medium
WT	Wild type

CONTENTS

LIST OF TABLES

LIST OF FIGURES

Chapter 1

Introduction and Literature Review

1.1 INTRODUCTION

The world can be regarded as a global village due to the increasing daily requirement of energy by all population across the world which has alarmed energy crisis all around the world. The need for energy and its related services to satisfy human social and economic development, welfare and health is increasing. All societies call for the services of energy to meet basic human needs such as: health, lighting, cooking, space comfort, mobility and communication and serve as generative processes (Edenhofer et al., 2011). It is overwhelming to know that, in today's world 1.4 billion people lack access to electricity, while 85% of them live in rural areas. As a result of this, the number of rural communities relying on the traditional use of biomass is projected to rise from 2.7 billion today to 2.8 billion in 2030 (Kaygusuz, 2012). The dominance of fossil fuel-based power generation (Coal, Oil and Gas) and an exponential increase in population for the past decades have led to a growing demand for energy resulting in global

challenges associated with a rapid growth in carbon dioxide (CO_2) emissions (Asumadu-Sarkodie & Owusu, 2016a). A majority of the communities around the world rely heavily on oil, natural gas and coal for their energy needs. These fuels draw on lots of resources that will eventually diminish, which in turn makes them too expensive or too environmentally damaging to recover.

The total estimated production of crude oil in the world has increased from about 3963.3 MT in 2006-07 to about 4119.2 MT during 2012-13, and further increased to 4361.9 MT during 2015-16 (Table 1.1). The production increased by 3.2% from 2014-15 to 2015-16. Distribution of total world production, according to countries, shows that Saudi Arabia and USA were the first and second highest producers with 13.03% and 13.0% respectively (Energy statistics, 2017). The United States was the largest consumer of crude oil, consuming 19.66% of the world consumption during 2015-16, based on country-wise distribution of consumption data. China was the second largest consumer (12.92%), followed by India (4.51%), Japan (4.38%), Saudi Arabia (3.88%) and Russian federation (3.30%). India was the third largest consumer of crude oil in the world and the second largest crude oil consumer in the Asia-Pacific region after China (Energy statistics, 2017). The above data reveals that Saudi Arabia and USA are the major producers of crude oil accounting for 13% share of total world production. Whereas the estimates of oil consumption in India is much higher than its production. The production rates in India are nearly the same in the last five years but the consumption rate has increased with the growing demands of human needs. So India is highly dependent on import of crude oil. Net imports of crude oil have increased from 111.50 MTs during 2006-07 to 202.85 MTs during 2015-16.

Table 1.1. Global crude oil production and consumption data from the year 2010-2016 (Energy statistics 2017, Ministry of Statistics and Programme Implementation, GOI)

Country/Region	2010-2011	2011-2012	2012-2013	2013-2014	2014-2015	2015-2016	2015-16 % Share of World's Total Production
Estimates of Production of Crude Oil							
Saudi Arabia	473.8	526.0	549.8	538.4	543.4	568.5	13.03
Russian Federation	511.8	518.8	526.1	531.1	534.1	540.7	12.40
USA	332.8	345.0	393.7	448.0	522.8	567.3	13.0
China	203.0	202.9	207.5	210.0	211.4	214.6	4.92
India	41.3	42.9	42.6	42.5	41.6	41.2	0.94
Estimates of Consumption of Crude Oil							
Saudi Arabia	137.1	139.1	146.2	147.3	160.1	168.1	3.88
Russian Federation	133.3	142.2	144.6	144.9	150.8	143	3.30
USA	850.1	834.9	817	832.1	838.1	851.6	19.66
China	447.9	464.2	486.3	507.2	526.8	559.7	12.92
India	155.4	163.0	173.6	175.3	180.8	195.5	4.51

There has been an increase of 7.08% in the net imports of crude oil during 2015-16 over 2014-15, as the net import increased from 189.43 MTs to 202.85 MTs (Energy statistics, 2017). Moreover the natural reserves of coal, crude oil and natural gas, the three main energy source in India are also depleting with time. There was decrease of 2.28% and 1.97% in the estimated reserve of crude oil and natural gas respectively, for the country as a whole during 2015-16 as compared to the position a year ago. These energy statics reveal that the country's fossil fuel reserves are depleting fast which has resulted in high import of energy sources. India is the third-largest importer of crude oil after the United States and China and continues to rely largely on imports. The import volumes grew modestly from 240 billion liters to 278 billion liters over the last four years (Indian Petroleum and Natural gas Statistics, 2015-16). This has not only caused imbalance in our economy but also has adverse effects on climate and environment

resulting in global challenges associated with rapid growth in greenhouse gas emissions. Renewable energy sources hold the key potential to displace greenhouse gas emissions from fossil fuel-based power generating and thereby mitigating climate change (Edenhofer et al., 2011). To achieve the idea of sustainability the best way is to replace fossil fuel-based energy sources with renewable energy sources. There is high potential for generation of renewable energy from various sources such as wind, solar, biomass, hydropower, geothermal, and cogeneration bagasse. The total potential for renewable power generation in the country as on 2016 is estimated at 1198856 MW (Edenhofer et al., 2011). The approximate ratio of different types of renewable energy production is shown in Fig.1.1.

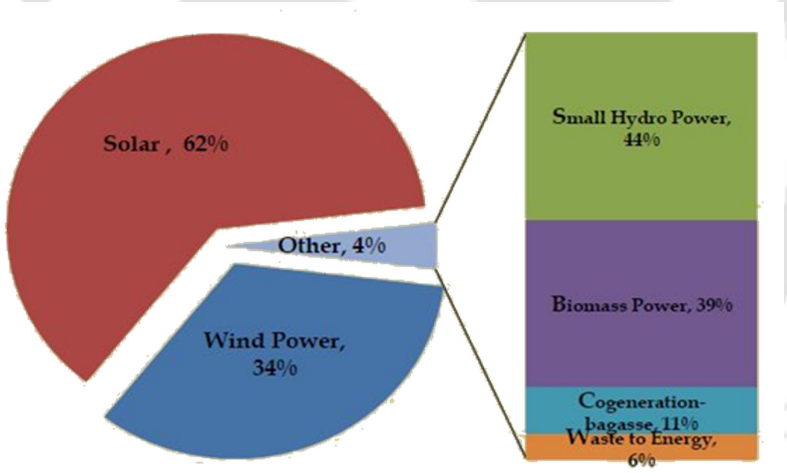

Figure 1.1. Source wise estimated potential of renewable energy in India (adopted from Energy statistics, 2017).

Government of India has implemented few policies and encouraged the use of renewable energy resources as supplement to motor transport fuels to improve India's energy security. An indicative 20 percent target for blending of biofuel for both biodiesel and bioethanol is proposed by end of 12th Five-Year Plan (by 2022). Bio–fuels are

considered as sustainable source of fuel in terms of limiting GHG emission and improving air quality (Delfort et al., 2008). The world biofuel production increased from around 20 billion tones in 2005 to 75 billion tonnes by the end of 2015 (BP Statistical Reviews, 2016). In this period the biofuels production in India increased from 114 million tones oil equivalent to 362 million tones, sharing 0.5% of total global biofuels production (BP Statistical Reviews, 2016).

Among the biofuels, ethanol and biodiesel has gained more importance because of its ease in blending with other conventional fuels and compatible with the same engine configuration. Biodiesel has gained popularity all over the world in many countries such as United States of America, Malaysia, Indonesia, Brazil, Germany, France, Italy and other European countries. Biodiesel has many added advantages over other alternative fuels. It is highly biodegradable with minimal toxicity and almost zero GHG emissions, sulfates, aromatic compounds that are toxic to the environment (Quispe et al., 2013, Vidosh et al., 2011). The wide range of available feedstocks for biodiesel production makes it a more popular biofuel. More than 350 oil-bearing crops has been reported globally for biodiesel production which includes both edible and non-edible crops. Moreover it can be produced via a simple reaction called transesterification which involves reaction of fat or oil with short chain alcohol in the presence of a catalyst to produce biodiesel and glycerol. Glycerol is produced in mass in this reaction and it acts as an important by-product of biodiesel industry. Globally, annual biodiesel production increased from 15 thousand barrel per day in 2000 to 289 thousand barrel per day in 2008 (Silitonga et al., 2011). It is believed that, 85% of biodiesel production comes from the European Union (Ahmad et al., 2011). This energy statistics reveals that biodiesel has a massive potentiality to be a part of a sustainable energy mix in the future which

also increase the availability of the by-product glycerol. With global production of biodiesel reaching 32 billion litres in 2020 with an annual growth of 42%, very large quantities of glycerol will be produced, thereby generating approx. 2.6 million tons (5.9 billion gallons) of crude glycerol (Renewables, 2016). With an estimate of 10 kg of glycerol (crude) produced per 100 kg of biodiesel, 4 billion gallons of crude glycerol is generated as a byproduct. The glycerol from biodiesel industry is contaminated with alcohol (methanol/ethanol) and alkali (NaOH/KOH) used in the transesterification reaction. Due to these contaminations, the waste glycerol is not suitable for conventional applications such as in cosmetics, pharmaceutical and food industry (Sarma et al., 2016). Crude glycerol in large amounts can pose a threat to the environment, so effective disposal of the waste glycerol remains a daunting challenge before biodiesel industry. However, crude glycerol can be effectively used as fermentation substrate for production of several value–added products which would not only save the environment but also add revenue to biodiesel producers. Crude glycerol serves as the raw material for various products such as 1,3-propanediol, succinic acid, biopolymers, poly unsaturated fatty acids, ethanol, hydrogen, *n*-butanol and for different value added industrial products (Khanna et al., 2012).

1.1.1 Conversion of Glycerol to Value-added Products

Crude glycerol can be converted to various value-added products via both catalytic conversion and bioconversion route. Numerous research has been reported for catalytic conversion of glycerol to value-added products through various processes such as oxidation, reduction, condensation, pyrolysis, carboxylation, hydrolysis, esterification, etherification, phase reformation, hydrogenolysis etc. (Bagheri et al., 2015; Nanda et al.,

2016; Pagliaro et al., 2007; Veluturla et al., 2018; Zhou et al., 2013). The principal products and their routes of catalytic conversion are detailed in Fig. 1.2.

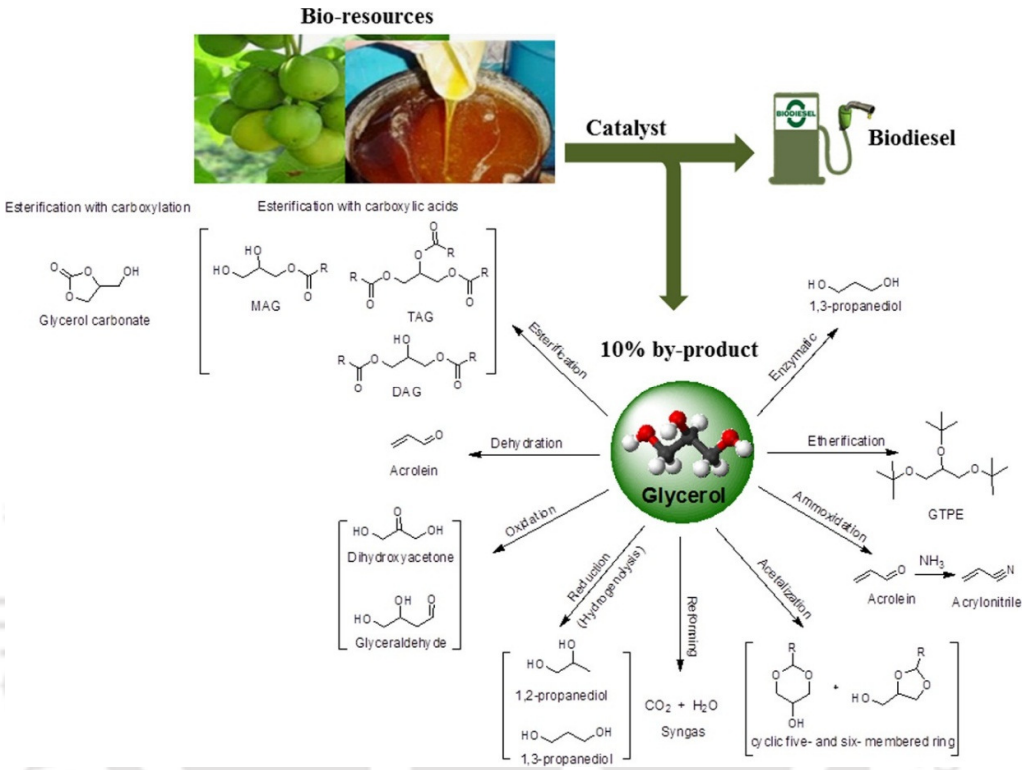

Figure 1.2. Catalytic conversion of glycerol to value added products. (adopted from Bagheri et al., 2015)

However, bioconversion which refers to microbial fermentation has some auxiliary advantage over catalytic conversion in terms of operational conditions and selectivity. Catalytic or chemical route involves harsh conditions in terms of temperature and pressure which is in turn a very energy intensive process. Further the biological route of glycerol conversion is highly selective over the conventional catalytic route which is associated with the production of many undesired byproducts. On the other hand, although the biocatalytic route of glycerol conversion has slower kinetics but it can be operated under ambient conditions with higher selectivity. A wide range of microbial

flora has the ability to utilize glycerol as the carbon source for their growth and metabolism and this involves species belonging to genus *Escherichia*, *Klebsiella*, *Enterobacter*, *Gluconobacter*, *Clostridium*, *Candida*, and *Aspergillus* (Solomos et al., 1995). The generalized metabolic pathway of glycerol conversion by micro–organisms is shown in Fig.1.3.

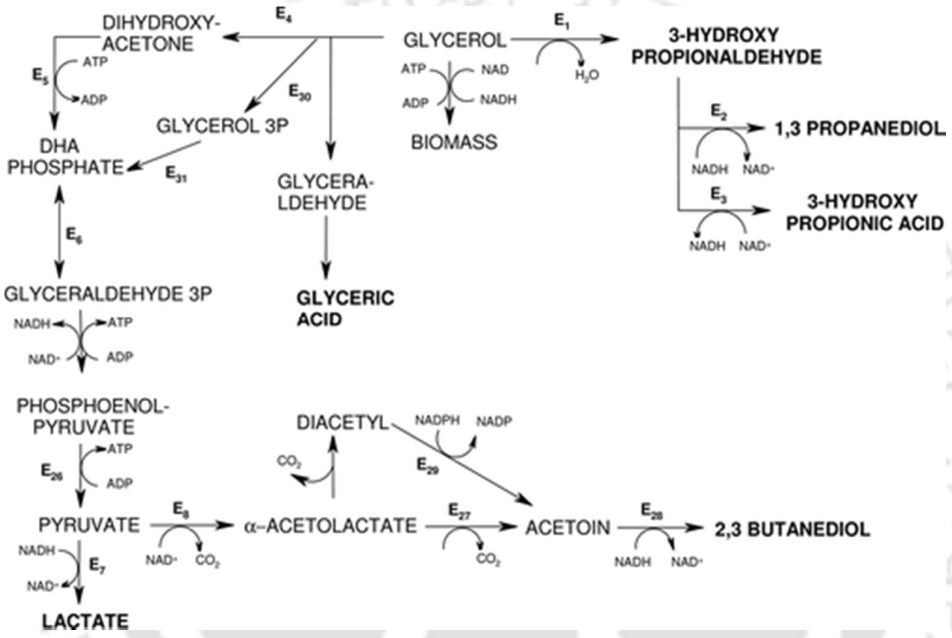

Figure 1.3. Metabolic pathway of glycerol bioconversion: Oxidative and reductive wings of glycerol assimilation (E1–Glycerol dehydratase; E2–1,3 PDO dehydrogenase; E3–Aldehyde dehydrogenase; E4–Glycerol dehydrogenase type 1; E5–Dihydroxy acetone kinase; E6–Triose phosphate isomerase; E7–Lactate dehydrogenase; E8–Pyruvate decarboxylase; E26–Pyruvate kinase; E27– α–Acetolactate decarboxylase; E28–Acetoin reductase; E29–Diacetyl reductase; E31–Glycerol 3–phosphate dehydrogenase)(adopted from Khanna et al., 2012).

Glycerol is utilized as carbon source by microorganisms via two pathways: oxidative and reductive (Yazdani and Gonzalez, 2007). The reductive pathway progresses through the dehydration of glycerol to 3-hydroxypropionaldehyde (3-HPA) which is then reduced to 1,3-propanediol catalyzed by 1,3-propanediol dehydrogenase, regenerating NAD for oxidative pathway. The oxidative branch proceeds by the oxidation of glycerol to

Dihydroxyacetone (DHA) by glycerol dehydrogenase. ATP-dependant DHA kinase then phosphorylates DHA to DHA phosphate which channels glycerol into Embden–Meyerhof–Parnas (EMP) pathway for production of other important metabolites such as butanol, hydrogen, succinic acid, ethanol, citric acid, lactate etc. The range of metabolites produced differs from one microorganism to another, depending on the presence of a particular enzyme or a group of enzymes. Table 1.2 gives a summary of products and the respective micro–organisms used for biochemical conversion of glycerol. Few microorganisms such as *Clostridia*, *Klebsiella*, *Citrobacter* exhibit both oxidative and reductive pathway thereby producing 1, 3-PDO along with other EMP pathway metabolites. Both oxidative and reductive pathways are shown in Fig. 1.3.

Table 1.2. List of micro–organisms capable of utilizing glycerol and the final product of the metabolism (adopted from thesis of Dikshit 2017)

Final product	Micro–organisms
1,3–Propanediol	*Klebsiella*, *Clostridia*, *Citrobacter*, *Enterobacter*, *Lactobacillus*
Butanol	*Clostridium pasteurianum*, *Clostridium acetobutylicum*
Dihydroxyacetone	*Gluconobacter oxydans*, *Acetobacter xylinum*
Citric acid	*Aspergillus niger*, *Yarrowia lipolytica*, *Candida oleophila*
Glyceric acid	*Gluconobacter*, *Acetobacter*, *Gluconacetobacter*
3–Hydroxypropionaldehyde	*Lactobacillus*, *Enterobacter*, *Desulphovibrio*, *Methanospirillum*
Biosurfactants	*Pseudomonas*, *Candida*, *Rhodococcus*
Propionic acid	*Propionibacteria*
Polyhydroxyalkanoates	*Ralstonia eutropha*, *Pseudomonas*, *Cupriavidus necator*
Extracellular polysaccharides	*Pseudomonas oleovorans*
Succinic acid	*Anaerobiospirillum succiniproducens*, *Escherichia coli*, *Actinobacillus succinogenes*
Erythritol	*Y. lipolytica*
Mannitol	*Y. lipolytica*, *Candida magnoliae*, *Candida azyma*
Ethanol	*Enterobacter aerogenes*, *E. coli*
Lactic acid	*Lactobacilli*, *Pediococcus pentosaceus*
Methane	*Methanobacterium sp.*, *Methanosarcina sp.*
Hydrogen	*Clostridia*, *E.coli*, *Enterobacter*
Oxalic acid	*Aspergillus sp.*,
2,3–Butanediol	*Klebsiella oxytoca*, *Klebsiella pneumonia*
3–Hydroxypropionic acid	*Lactobacillus sp.*, recombinant *E. coli*

1.2 PRODUCTION OF HYDROGEN FROM GLYCEROL: A COMPARISION OF CATALYTIC AND BIOCONVERSION

Among all alternative fuels and value-added chemicals produced from crude glycerol (by both chemical and biochemical routes), hydrogen holds great promise because of its high energy content. With heat of combustion of 141.9 MJ/kg (as compared to gasoline 47 MJ/kg and diesel 45 MJ/kg), biohydrogen is the most efficient

fuel. Moreover, it is regarded as the cleanest fuel, as on combustion it produces only water as the by-product. Therefore the engine that is used to burn hydrogen as fuel produces zero pollution. This makes hydrogen to top the list of contenders in the race to discover a green fuel. But a number of challenges exist that have deprived hydrogen to be used as an alternative fuel. It is lighter than air and so can disperse easily into the atmosphere. It is highly flammable and thus easy to ignite. It is odorless, colorless and hence undetectable by human senses. These properties of hydrogen makes it difficult to store. The most common method of storage of hydrogen is in gaseous form in pressurized cylinders/tanks. Storing liquid hydrogen in tanks is safe, however if it escapes in to the environment then it gives rise to many dangerous situations. Despite these limitations hydrogen has paved its way to a number of applications such as vehicles, power plants, fuel cells, electricity etc. This is possible due to proper investigation of the drawbacks by researchers and technological development. Recently in 2015, hydrogen powered tram has been developed by a Chinese company Sifang (CRRC Qingdao Sifang Co. Ltd., 2015). Moreover, intensive research is going on safe storage of hydrogen. A group of researchers at the Lawrence Berkeley National Laboratory of the US, Department of Energy have discovered a material called air-stable magnesium nano-composites that can help in storing hydrogen without complex strategy (AE News, 2016). Further, in India, the Ministry of New and Renewable Energy, GOI, has supported research, development and demonstration projects on various aspects of hydrogen energy including its production, storage and use as a fuel for generation of mechanical/thermal/electrical energy. Hydrogen fuelled small power generating sets, two wheeler (motor cycles), three wheeler and catalytic combustion systems for residential and industrial sectors and fuel cell buses have also been developed and demonstrated.

Hydrogen fuelled 3-wheeler is developed by a research team of IIT-Delhi under the supervision of Prof. L.M. Das jointly with Mahindra & Mahindra. Hydrogen-CNG dispensing station is set up at Faridabad, Haryana and Dwarka, New Delhi. Biological hydrogen production plant is also set up by MCRC, Chennai. Moreover, National Hydrogen Energy Road Map has projected that one million hydrogen fuelled vehicles would be on the Indian roads and 1000 MW aggregate hydrogen based power generating capacity be set up in the country, by 2020 (https://mnre.gov.in/hydrogen-energy). These real time applications of hydrogen as a fuel has not only encouraged researchers to carry out more intensive research on it but also convinced the government to support various hydrogen powered projects.

Hydrogen can be produced by both chemical and biochemical routes and various feed stocks including both renewable and non-renewable sources, are used for its production. It can be produced by catalytic route, directly from fossil fuels or biomass, or by passing electricity through water to break the water into its ingredient components of hydrogen and oxygen. At present, almost 95% of the world's hydrogen is being produced from fossil fuel based feed stocks (Avasthi et al., 2013). But due to the limiting reserves of fossil fuels with growing population has led to the search for some renewable feed stocks for hydrogen production. Glycerol is one such attractive resource for hydrogen production which has drawn great interest over the last few years. Moreover glycerol is the by-product of biodiesel industries which is produced in large quantities. The utilization of waste glycerol as a resource for energy production is itself a very attractive process. This will enhance the revenue of biodiesel industry making it economically attractive. Catalytic conversion of glycerol into hydrogen involves various processes namely steam reforming, auto-thermal reforming, aqueous phase reforming, partial

oxidation or gasification and supercritical water reforming. A detailed review of the catalytic processes for hydrogen production is given in Table 1.3.Globally, about 96% of hydrogen is produced today via steam-reforming of hydrocarbons (Ewan et al., 2005). But steam reforming process and other catalytic routes of hydrogen production has many limitations, which has flagged the way to the biological route of hydrogen production. A detailed comparison of catalytic route (Avasthi et al., 2013) and biological route is given in Table 1.4, which depicts clearly the advantages of fermentative hydrogen production over catalytic conversion of crude glycerol.

Table 1.3. Summary of literature on catalytic processes for hydrogen production from glycerol.

Process	Catalyst	Operating conditions	Remarks	Reference
Steam Reforming	Ir/CeO_2,Ni/CeO_2,Co/CeO_2	Temperature: 400–550 °C; mass of catalyst: 200 mg; particle diameter: 40-60 mesh,$C_3H_8O_3$:H_2O:He = 2:18:80 vol.%; and GHSV = 11,000 mL/g-cat.h	Ir/CeO_2 gave the hydrogen selectivity and glycerol conversion of 85% and 100%, respectively, at 400 °C	Zhang et al., 2007
	Pt/Al_2O_3, Ni/Al_2O_3, Pd/Al_2O_3, Ru/Al_2O_3, Rh/Al_2O_3	Feed flow rate = 0.15–0.5 mL/min; temperatures 600–900 °C; steam/carbon molar ratio (S/C) = 1/3–3.0	About 80% of hydrogen selectivity was obtained with Ni/Al_2O_3, whereas the selectivity was 71% with $Rh/CeO_2/Al_2O_3$ at a S/C = 3, 900 °C temperature, and feed flow rate of 0.15 mL/min	Adhikari et al., 2007
	Pt supported on Al_2O_3, ZrO_2, CeO_2/ZrO_2, MgO/ZrO_2, and Carbon	Temperature = 350 °C; pressure = 1 bar with aqueous glycerol feed solution (30 wt.%) over oxide supported Pt catalysts (1.0 g) or Pt/C catalyst (0.060 g) and a feed flow rate of 0.32 cm^3min^{-1}. Pt/C catalyst was tested at various feed rates and temperatures. Other catalysts tested were Pt–Ru and Pt–Re	Pt/C catalysts showed the superior performance. At 400 °C and pressure = 1 bar, 100% glycerol conversion was achieved at feed rate of 0.32 cm^3min^{-1}	Soares et al., 2006

Table 1.3. (Continued…)

Autothermal reforming	G-91 EW from Sud-Chemie Inc	Temperature 770–810 °C; O/C = 0–0.55 and S/C = 2.0–2.4	4.5 mol of hydrogen was produced per mole of glycerol at O = 0.0 and S = 2.2 and temperature = 804 °C	Douette et al., 2007
	RhCe/γ-Al_2O_3	Temperature 500–1050 °C; C/O = 0.9–1.6; S/C = 0–4.5	100% glycerol conversion and 79% H_2 selectivity was achieved at S/C = 4.5, C/O = 0.9, temperature = 862 °C, GHSV = 10^5 h^{-1}	Dauenhauer et al., 2006
	Pd/Ni/Cu/K supported on γ-Al_2O_3	Temperature 550–850 °C; O/C = 0.3 and S/C = 3.0	Hydrogen yield was ~68% at 850 °C compared to ~42% using steam reforming process under similar conditions	Swami et al., 2006
Aqueous phase reforming	Pt supported on Al_2O_3	Temperature = 250 °C; pressure = 20 bar; glycerol concentration 10 wt.%; feed flow rate = 0.5 mL/min and catalyst = 300 mg (Pt loading = 3 wt.%)	The highest glycerol conversion achieved was 57% and the reaction rate of hydrogen was 7.6×10^{-3} mol/min. g_{cat}	Lehnert et al., 2008
	Pt/γ-Al_2O_3	Temperature = 180–220 °C; pressure = 11–25 bar; feed rate = 0.05–0.1 mL/min; glycerol concentration 5–10 wt.%; catalyst weight = 1–2 g; and Pt loading = 0.3–1.2 wt.%	Al_2O_3 supported Pt catalyst with 0.9 wt.% loading showed the best performance compared to 0.3, 0.6 and 1.2 wt.% loading	Luo et al., 2008
	Pt/γ-Al_2O_3	Temperature 225–265 °C; pressure = 29–56 bar; weight hourly specific velocity (WHSV) = 0.008 g of glycerol/g_{cat}h	The hydrogen selectivity was 65% at 225 °C and 29 bar whereas it dropped to 57% at 265 °C and 56 bar. At higher temperature and pressure, CH_4 selectivity increased	Cortright et al., 2002

Table 1.3. (Continued…)

Supercritical water reforming	Ru/Al_2O_3	Temperature = 700–800 °C; pressure = 241 bar; glycerol concentration 40 wt%; catalyst weight = 2 g	7 mol of hydrogen/mol of glycerol was obtained, which decreases with an increase in the feed concentration. Glycerol was completely gasified to hydrogen, carbon dioxide, and methane along with small amounts of carbon monoxide	Byrd et al., 2008
Gasification (Partial oxidation)	Ni/Al_2O_3	Temperature = 800 °C; steam to glycerol weight ratio 25:75	Pure glycerol was completely converted to gas containing 92 mol% syngas ($H_2/CO \approx 1.94$). Maximum hydrogen, total gas and syngas production of 68.4 mol%, 2.6 L/g of glycerol and 89.5 mol% were obtained.	Valliyappan et al., 2008
	Rh supported on γ-Al_2O_3	Temperature = 1055°C; carbon-to-oxygen ratio (C/O) = 0.43 for glycerol; catalyst = 2.5 wt% Rh;	Catalyst, wash coat, carbon-to-oxygen ratio, and steam-to-carbon ratio were varied to maximize selectivity to H_2. Steam addition increased selectivity to H_2 to79% from glycerol.	Dauenhauer et al., 2006

Table 1.4. Comparison of catalytic and biological route of hydrogen production from crude glycerol.

Sl.No.	Catalytic route (Steam reforming)	Biological route (Fermentation)
1.	It is an endothermic reaction and requires high temperature (800K-1000K) and pressure (10-30 bar).The control of this high temperature is a difficult task and it adds to the operational cost and capital cost of the reactor.	It can be operated at ambient temperature and pressure (upto max. 40°C).
2.	The impurities present in crude glycerol (water, ash, methanol, fatty acids) may affect the chemical reaction and lead to the decrease in the overall cost of the process, as the refining stage of glycerol would be eliminated.	The impurities present in crude glycerol does not have any adverse effect on hydrogen production. Some impurities such as methanol, fatty acids and salt are reported to be beneficial for the growth of microorganisms.
3.	The steam reforming of glycerol apart from producing hydrogen produces 3 moles of carbon dioxide stoichiometrically. It is well known that release of carbon dioxide is an environmental concern, and hence effective utilization of carbon dioxide is required.	Microbial fermentation produces only one mole of CO2 per mole of glycerol along with hydrogen. The production of this minimal amount of CO2 can also be effectively blocked by genetic engineering of the microbes.
4.	The selectivity of the glycerol steam reforming process is low due to the side products such as methane which hinder the production as well as the purity of hydrogen.	The side products of fermentative route are butyric and acetic acids which are a part of the pathway and are further utilized to form butanol and ethanol which are also alternative fuels.
5.	The process also deals with the formation of coke/ carbon during the process. This carbon/coke acts as a poison and clogs the pores of the catalyst and hence deactivates the catalyst thus affecting the process as well as the yield and purity of hydrogen.	No such coke is formed in this process.

Table 1.5. Summary of literature review on hydrogen production from pure and crude glycerol fermentation

Substrates (concentration)	Micro–organism	H_2 yield (mol H_2/mol glycerol)	Fermentation conditions	Salient features of the study	Reference
Crude glycerol	*Enterobacter aerogenes* (EA), *Enterobacter ludwigii* (EL), *Bacillus amyloliquefaciens* (BA)	0.13 ± 0.10, 0.35 ± 0.10 and 0.50 ±0.20 mol H_2/ mol glycerol respectively for the cultures of EA, EL and BA	Temp = 37°C, Initial pH = 6.8, 140 rpm Fermentation mode: Batch	Isolation and characterization of bacteria found in reactors of wastewater and activated sludge treatments that are able to produce biohydrogen from glycerol. *Bacillus amyloliquefaciens* showed highest yield of H_2.	Poleto et al., 2016
Crude glycerol (7.4 g/L)	*Clostridium pasteurianum* MTCC116	0.627	Temp = 36.18°C, Initial pH = 6.7, 150 rpm Fermentation mode: Batch	Optimization of process parameters (temperature, pH, crude glycerol conc.). Higher H_2 production obtained with crude glycerol compared to pure glycerol. Presents kinetic and thermodynamic analysis of crude and pure glycerol. Na^+ ions has positive effect on biohydrogen production.	This study Sarma et al., 2016
Crude glycerol (11.14 g/L)	*Klebsiella sp.* TR17 and *Rhodopseudo–monas palustris* TN1	6.42 mmol H_2/g COD	Temp = 40°C, pH = 8 (dark fermentation) and 30°C, pH = 7 (photo fermentation) Fermentation mode: Batch	Two stage fermentation process using *Klebsiella* sp. for dark fermentation and *R. palustris* for photo fermentation. Dark fermentation effluent was further used for photo fermentation at different dilution rate. The total hydrogen yield for two stage process was 6.42 mmol H_2/g COD consumed.	Chookaew et al., 2015

Table 1.5. (Continued…)

Pure glycerol (20 g/L)	*Bacillus thuringiensis*	0.646 (67%) (Batch) 0.386 (Continuous)	1% ammonium nitrate, Temp = 37°C, pH 7 Fermentation mode: Batch and continuous	H_2 production from crude glycerol was slightly higher than pure glycerol. Cells immobilized on banana leaves to increase H_2 yield.	Kumar et al., 2015
Crude glycerol (1 g/L)	Mixed culture (predominated with *Clostridium* species)	1.41	pH 6.5, Temp = 40°C, 150 rpm Fermentation mode: Batch	Optimization of media components by combination of Plackett–Burman, Box–Behnken and CCD. Optimization of media components enhanced hydrogen yield by 29%.	Mangayil et al., 2015
Mixture of crude glycerol (CG) , cheese whey (CW), buffalo slurry	Mixed culture	111.6 ± 21.8 mL H_2/g Volatile Solids added	Temp = 37°C, Initial pH 6.5, 120 rpm Fermentation mode: Batch	Co–fermentation and optimization of substrate composition and mixing ratio by mixture design RSM. Highest yield was obtained with 66% BS and 33% CW	Marone et al., 2015
Crude glycerol and apple pomace hydro–lyzate (APH) (15 g/L)	Co–culture of *Enterobacter aerogenes* and *Clostridium butyricum*	26.07 mmol H_2/L medium	Crude glycerol 15 g/L, APH 5 g/L and 15% v/v inoculum Fermentation mode: Batch	APH co–fermented with crude glycerol. Shift of glycerol metabolism towards oxidative pathway. APH increased H_2 production and reduced substrate inhibition and by–product production	Pachapur et al., 2015

Table 1.5. (Continued…)

Pure glycerol and formate	*Escherichia coli*	0.75 ± 0.03 mmol H_2 L^{-1} with glycerol, 0.83 ± 0.05 mmol H_2 L^{-1} with formate using wild type strain	Temp = 37°C, Initial pH = 5.5–7.5 Fermentation mode: Batch	H_2 production from mixed carbon source (glycerol and formate) by using wild type and mutant strain of *E. coli*. All *Hyd* enzymes (*Hyd 1–4)* have a significant role for bacterial growth on glycerol	Trchounian et al., 2015a
Pure glycerol and acetate	*Escherichia coli*	5.07 mmol L^{-1} with 5 g/L acetate, pH = 7.5, 5.16 mmol L^{-1} with a mixture of 5 g/L acetate and 10 g/L glycerol, pH 7.5	Temp = 37°C, Initial pH = 5.5–7.5 Fermentation mode: Batch	H_2 production from acetate and mixture of acetate and glycerol at different pHs was evaluated.	Trchounian et al., 2015b
Crude glycerol (10 –30 g/L)	Immobilized *Klebsiella* sp. TR17 in an up-flow anaerobic sludge blanket reactor	H_2 production rate = 242.15 mmol H_2/L·h H_2 yield = 44.27 mmol H_2/g	Temp = 40°C, pH = 8.0 Fermentation mode: Batch	The cells were immobilized over methanogenic granules. The reactor was operated at different hydraulic retention time (HRT) ranging from 2 – 12 h. Decrease in HRT increases the hydrogen yield and production rate.	Chookaew et al., 2014
Pure glycerol	Activated sludge	0.026 L H_2/g COD removed	Fermentation mode: Continuous	Co-digestion of sewage sludge and glycerol. The best operational condition was an organic loading rate (OLR) of 7.82 g COD/L·d, with removal of 93% COD, and H_2 and methane yields of 0.026 L H_2/g COD removed and 0.29 L CH_4/g COD removed, respectively.	Rivero et al. 2014

Table 1.5. (Continued…)

Pure and crude glycerol (10 g/L)	*Clostridium pasteurianum* CH4	0.41 (batch), 0.50 (CSTR– pure glycerol), 0.77 or 48.4% (CSTR – crude glycerol)	Initial pH 7.0, Temp = 35°C, agitation rate 200 rpm, glycerol 10 g/L Fermentation mode: Batch and continuous	H_2 yield improved from 0.50 to 0.77 mol H_2/mol glycerol for crude glycerol as substrate as compared to pure form in continuous process.	Lo et al., 2013
Pure and crude glycerol (25 g/L)	*Enterobacter aerogenes* ATCC 13048	37.1% and 24.2% H_2; H_2 production rate = 9 and 6.2 mmol H_2/L h for pure and crude glycerol respectively	Temp = 37±2°C, Initial pH = 5.5 Fermentation mode: Batch	Biohydrogen production by immobilized cells on heat–treated upflow anaerobic sludge blanket (UASB) granules. Optimization of organic loading rate (OLR). The maximum H_2 were achieved at the optimum OLR of 50 g/L d.	Reungsang et al., 2013
Glycerol from biodiesel waste (2.5 g/L)	Activated sludge	1.1 ± 0.1 (15.2% v/v)	pH 6.5, Temp = 40°C, 1 g/L raw glycerol, 150 rpm Fermentation mode: Batch	H_2 production is associated with acetate, butyrate and ethanol. H_2 production was higher with crude glycerol.	Mangayil et al., 2012
Crude glycerol (22.19 g/L)	Mixed culture	0.30	Sludge 7.16 g–total solid (TS/L), endo–nutrient 2.89 mL/L. Temp = 35±2°C, speed = 150 rpm, pH = 5.5 Batch Fermentation	CCD /RSM for optimization of glycerol conc., sludge conc. and amount of endo–nutrient. Waste glycerol and sludge had individual and interactive effect on HPR.	Sittijunda et al., 2012

Table 1.5. (Continued…)

Crude glycerol (15 g/L)	Activated sludge	0.96	Temp = 37°C, pH 7.9, 120 rpm Fermentation mode: Batch	Plackett–Burman, Box–Behnken with RSM for optimization of pH, temperature and glycerol conc. for H_2 production. Ethanol of 7.92 g/L was also produced.	Varrone et al., 2012
Pure glycerol (15 g/L)	*Enterobacter aerogenes*	0.85	7.5% O_2, 18% ratio of inoculum Fermentation mode: Batch	Box Behnken design/ RSM for optimization of media constituents and oxygen at 37°C and 120 rpm. Min. conc. of O_2 is required to enhance H_2 yield.	Jitrwung et al., 2011
Crude glycerol (20.4 g/L)	*Klebsiella pneumonia* DSM 2026	0.53	Temp = 37°C, pH 6.5, 150 rpm Fermentation mode: Batch	Plackett–Burman design was used to optimize the medium components fermentation conditions	Liu et al., 2007
Pure glycerol (20 g/L)	*Klebsiella pneumonia* GT1	0.61	Controlled conditions: pH = 7, Temp = 35°C Uncontrolled cond -itions: pH 5.5 to 7 Fermentation mode: Continuous	Mainly focus on production of 1,3–propanediol, 2,3–propanediol and ethanol. Hydrogen production as a side product of the process.	Biebl et al., 1998
Pure glycerol (10 g/L)	*Clostridium butyricum* LMG 1212t2 and *Clostridium pasteurianum* LMG 3285	0.87 (continuous process)	pH = 6.5 Temp = 37°C Fermentation mode: Batch and continuous	Both batch and continuous process for production of 1,3–propanediol, n–butanol and ethanol. Increase in acetate concentration resulted in H_2 production along with main products.	Heyndrickx et al., 1991

Abbreviations: RSM = Response surface methodology; Temp. = Temperature

1.2.1 Microbial conversion of glycerol to hydrogen

Biological production of hydrogen is an energy efficient process, and highly economic when produced from waste biomass. Biological process includes microbial conversion of biomass into fuels like ethanol, 1,3-propanediol, hydrogen, methane, biodiesel etc. mainly by two distinct process namely dark fermentation and photo fermentation. Dark fermentation is regarded as the most efficient process due to less hardware requirement, diverse microbial entities and faster hydrogen production rates. Dark fermentation can be carried out by pure or mixed cultures of facultative and strict anaerobes mostly belonging to *Clostridiaceae* or *Enterobacteriaceae* family. Strict anaerobes, which includes *Clostridium sps*. such as *Clostridium acetobutylicum, Clostridium pasteurianum, Clostridium paraputrificum, Clostridium. thermocellum*, are more efficient hydrogen producers compared to facultative organisms, which includes *Bacillus sps., E. coli, Enterobacter sps.*etc. There exists some diversity in the metabolic pathway of hydrogen production in both types of anaerobes. Glycerol metabolism has two phases, viz. acidogenesis (production of organic acids which primarily occurs in exponential growth phase) and solventogenesis (conversion of acid to solvents which occurs in the stationary phase). Glycerol bioconversion commences with conversion of glycerol to dihydroxyacetone (DHA) by enzyme glycerol dehydrogenase followed by further conversion to DHA phosphate, and finally to pyruvate. Pyruvate is then converted to acetyl-coA and then depending on the organism either formate is formed by the PFL (pyruvate formate lyase) pathway or reduced ferredoxin and CO_2, through the PFOR (pyruvate ferredoxin oxidoreductase) pathway (Fig. 1.4). Formate is converted to hydrogen and CO_2 by formate hydrogen lyase, which mostly contains a [NiFe] hydrogenase. Only the PFOR organisms can utilize the NADH formed during glycolysis

to produce hydrogen via NADH dependent [Fe-Fe] hydrogenase. Another class of [Fe-Fe] hydrogenase that produces hydrogen by re-oxidizing ferredoxin, thus called Fd dependent [Fe-Fe] hydrogenase. Reduction of ferredoxin by enzyme hydrogenase results in release of H_2.

Like other biofuels originating from fermentation route, unit cost of production of biohydrogen is strongly influenced by the cost of the substrate. Dark fermentation is remarkable for its ability to utilize a wide variety of feedstock. Monomeric hexose/pentose sugars like glucose and xylose are potential substrate for bio-hydrogen production which can be obtained by pretreatment and enzymatic hydrolysis (or saccharification) of lignocellulosic biomass. However, the entire chain of pretreatment, saccharification and fermentation makes it a lengthy and a cost intensive process of biofuel production. Holding these points in mind, this study aims at using crude glycerol, a byproduct of biodiesel industry as a ***direct*** substrate for hydrogen production which is devoid of above pre-treatment methods. Conversion of waste glycerol to clean energy is itself an economically viable concept. But due to less diversity in microbial cultures capable of utilizing glycerol, this concept is less studied. *Clostridium pasteurianum* is a well-known gram-positive bacterium that can utilize glycerol as a substrate and convert to hydrogen and other metabolites (Lo et al., 2013).

Several earlier authors have studied biohydrogen production from fermentation of either pure or crude glycerol. Some authors have also employed mixtures of glycerol (in either pure or crude form) with other substrates such as cheese whey, buffalo slurry, formate and acetate (Table 1.5). As compared to pure glycerol, studies using crude glycerol as substrate are limited. A review of the previous literature on biohydrogen production using pure and crude glycerol is given in Table 1.5.

A comprehensive review of literature on microbial hydrogen production by bioconversion of crude glycerol has also been published by Sarma et al. (2012). More recently, Hallenbeck and Liu (2016) have reviewed biohydrogen production by photosynthetic bacteria during photo–fermentative growth. Urbaniec and Bakker (2015) have reviewed hydrogen production by dark fermentation using biomass residues (agricultural and agro-industrial solid waste) and other starchy residues. As seen from Table 1.5, most of the previous studies have employed either mixed cultures (in form of activated sludge) or pure cultures of bacteria of *Enterobacteriaceae* family for production of biohydrogen. In addition to the microbial culture, an important factor influencing biohydrogen production is the mode of fermentation. As noted in literature review presented in Table 1.5, several previous authors have used fed-batch and continuous mode of fermentation. The yield of biohydrogen has also been defined in different ways by the previous authors.

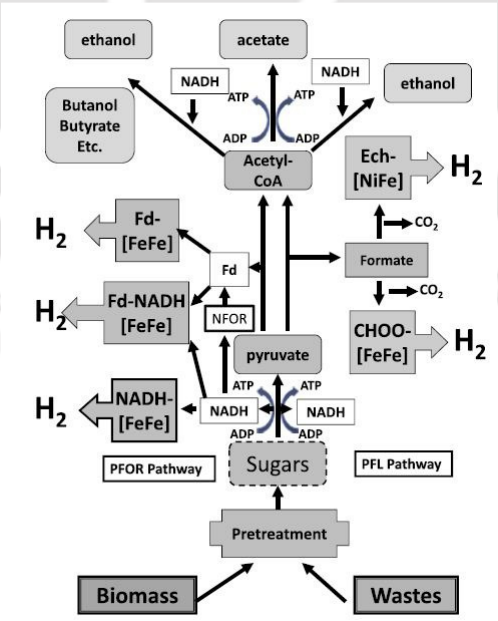

Figure 1.4. Hydrogen production pathways viz. PFOR (pyruvate:ferredoxin oxidoreductase) pathway and PFL (pyruvate:formate lyase) pathway (adopted from Hallenbeck et al., 2012)

1.2.1.1 *Clostridium pasteurianum*

*Clostridium pasteurianum*is a rod-shaped, spore forming Gram-positive obligate anaerobic bacteria which was first described in 1895 by Sergei Nikolayevich Winogradsky (Winogradsky, 1895). It belongs to the phylum Firmicutes, class Clostridia, order Clostridiales, family Clostridiaceae and genus Clostridium. *C. pasteurianum* was initially known for its ability to fix atmospheric nitrogen in a non-symbiotic process (Zelitch, 1951). However, in recent years it has been exploited for the production of acids, solvents and gas from glycerol and other carbohydrates, which was first mentioned by Nakas et al. (1983). The pathway for glycerol utilization in *C. pasteurianum* was proposed by Dabrock et al. (1992) (Fig. 1.5)

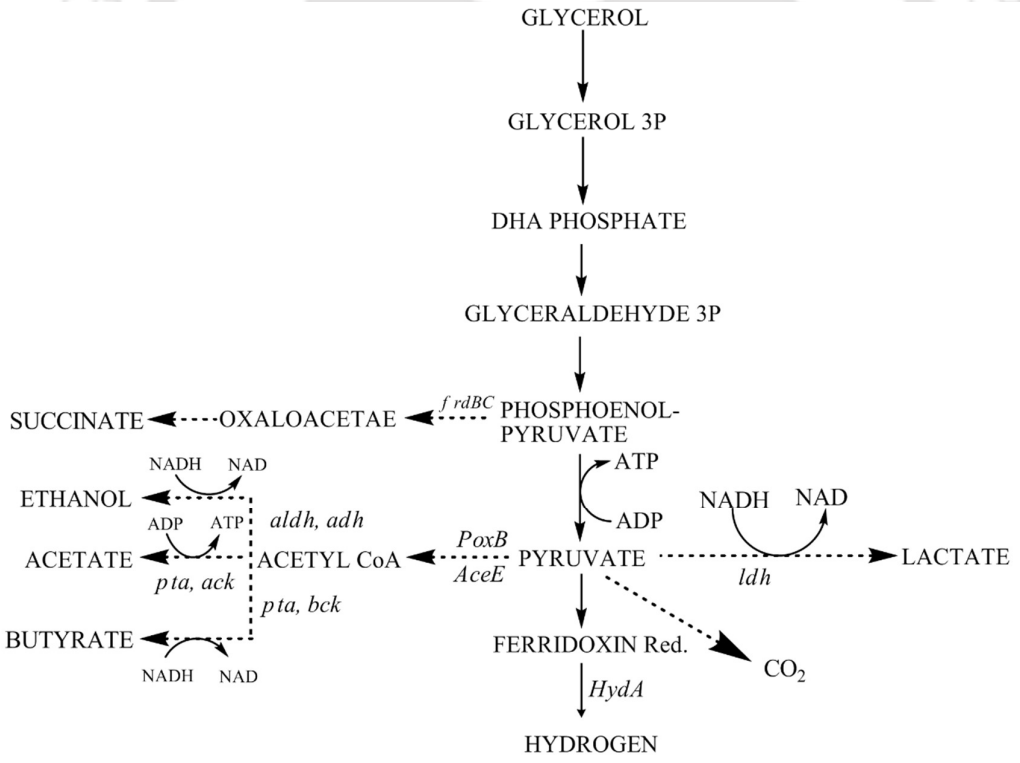

Figure 1.5. Metabolic pathway of *Clostridium pasteurianum* for hydrogen production using glycerol as substrate.

1.2.1.2 Dark fermentation in *C. pasteurianum*

Hydrogen production by the biological processes has been considered as an economical approach and environmentally clean method. Dark fermentation is one of the main biological processes in which microorganisms utilize carbohydrate sources to produce biohydrogen in anaerobic fermentation conditions (Dębowskia et al., 2014). The yield of hydrogen produced depends on metabolic pathway used by microorganisms so that the maximum 4 mol of H_2 can be produced theoretically from one mol of hexose (glucose) as carbon source when acetic acid is the main fermentative byproduct as shown in Eq. (1):

$$C_6H_{12}O_6 + 2H_2O \rightarrow 2C_2H_4O_2 + 2CO_2 + 4H_2 \quad (1)$$

When butyrate is mostly produced as shown in Eq. (2), maximum 2 mol of hydrogen are theoretically produced using one mole of glucose (Sinha et al., 2011).

$$C_6H_{12}O_6 \rightarrow C_4H_8O_2 + 2CO_2 + 2H_2 \quad (2)$$

On the other hand, the highest theoretical hydrogen yield from glycerol is 3 mol H_2/mol glycerol when acetate is the main volatile fatty acid (VFA) as shown in Eq. (3), whereas according to Eq. (4), the production of butyric acid from one mole glycerol results in the maximum theoretical hydrogen yield of 2 mol H_2/mol glycerol (Selembo et al., 2009).

$$\underset{\text{Glycerol}}{C_3H_8O_3} + H_2O \longrightarrow \underset{\text{Acetic acid}}{CH_3COOH} + CO_2 + 3H_2 \quad (3)$$

$$\underset{\text{Glycerol}}{2C_3H_8O_3} \longrightarrow \underset{\text{Butyric acid}}{CH_3CH_2CH_2COOH} + 2CO_2 + 4H_2 \quad (4)$$

The glycerol fermentation pathway in *C. pasteurianum* is divided in two pathways, the reductive and the oxidative pathway. In the oxidative branch glycerol is oxidised by glycerol dehydrogenase to dihydroxyacetone which is further phosphorylated by dihydroxyacetone kinase. Dihydroxyacetone-phosphate enters glycolysis to produce pyruvate in six steps. The oxidation of pyruvate by the pyruvate-ferredoxin oxidoreductase yields acetyl-Coenzyme A (acetyl-CoA). From acetyl-CoA three possible pathways lead to acetate, ethanol or butyrate and butanol in a similar manner to the acetone, butanol, ethanol (ABE)-fermentation pathway in *Clostridium acetobutylicum*. The oxidative pathway is further categorized into two phases, viz. acidogenesis (production of organic acids which primarily occurs in exponential growth phase) and solventogenesis (conversion of acid to solvents which occurs in the stationary phase). Hydrogen is primarily produced during acidogenesis and therefore acetic acid and butyric acid are the associated byproducts of this process (eq. 1-4). Hydrogen production is catalyzed by Fe-hydrogenases. In the reductive branch, glycerol is dehydrated to the toxic intermediate 3-hydroxypropionaldehyde (3-HPA) and further reduced by 1,3-propanediol dehydrogenase to 1,3-propanediol (1,3-PDO). It was shown that at least 9 % of the initial glycerol has to be converted to 1,3-PDO for reducing equivalents of both the fermentative pathway and biomass accumulation to be balanced (Biebl, 2001).

The major products of dark fermentation by *C. pasteurianum* are hydrogen, acetic acid, butyric acid, 1,3-propanediol whereas butanol, ethanol, lactic acid are also associated products.

Hydrogen

Hydrogen is the main product of dark fermentation. *C. pasteurianum* has the ability to ferment glycerol into hydrogen with the aid of hydrogenase (Fe-only) enzyme encoded

by *hydA* gene. It is the most promising alternative fuel as it produces only water as the byproduct on combustion. Hydrogen has a high energy content with calorific value of 142.3 kJ/g which makes it a superior fuel. It is used in hydrogenation of oils and in synthesis of methanol, hydrochloric acid etc. The industrial production of hydrogen occurs by steam reforming of natural gas. The photo fermentation is the oldest known route for hydrogen production by purple non-sulfur photosynthetic bacteria using substrates such as carboxylic acids, sugars etc. The anaerobic production of H_2 is catalyzed by Ni and Fe containing enzyme known as hydrogenases.

Acids

The major volatile fatty acids produced by *C. pasteurianum* during acidogenic phase of dark fermentation includes acetic acid and butyric acid. Stoichiometrically, glycerol fermentation for hydrogen production yields 1 mole of acetic acid or 0.5 mole of butyric acid per mole of glycerol. Acetyl Co-A, an intermediate of glycolysis is converted to acetate by phosphotransacetylase and acetate kinase. Acetyl Co-A is further converted into butyrate by the action of a series of enzymes viz. thiolase, β-hydroxybutyryl CoA dehydrogenase, crotonase, butyryl CoA dehydrogenase, phosphobutyryl transferase and butyrate kinase (Khanna et al., 2012). Acetic acid has wide applications in the food industry in the form of vinegar and for ester production. Butyric acid is of great commercial importance as a starting material for synthesis of esters of lower alcohols used as flavoring agents. Its anhydride is used to produce cellulose butyrate, a useful plastic.

1,3-Propanediol

1,3-Propanediol (1,3-PDO) is one of the major product produced by *C. pasteurianum*. Two enzymes namely, glycerol dehydratase and 1,3-PDO dehydrogenase catalyze the

formation of 1,3-PDO in *C. pasteurianum* via an intermediate 3-hydroxypropionaldehyde. 1,3-PDO is an industrially important monomer used for synthesis of many photostable polymers such as polyesters, polyurethans and polyethers (Biebl et al., 1999)and also finds application in food, cosmetic and pharmaceutical industries. It is also an important starting material for the synthesis of biodegradable plastic, polytrimethylene terephthalate (PTT). It is chemically produced from acrolein or propylene or ethylene derived from petroleum (Khanna et al., 2012).

Butanol

Butanol (C_4H_9OH) is a four carbon alcohol which is considered as a promising alternative fuel due to its comparable combustion characteristics with petrol. Its net heat of combustion (NHOC) is 26.8 MJ/litre compared to 32.3 MJ/litre for petrol. Butanol also acts as the raw material for the production of acrylates, ethers, and butyl acetate which are utilized in paints, resin formulations, and lacquers (Harvey and Meylemans, 2011).This makes butanol an economically valuable product. *C. pasteurianum* is a major producer of butanol and a series of enzymes are involved for its production. The two immediate enzymes namely, butyraldehydedehydrogenase and butanol dehydrogenase catalyze the formation of butanol from butyryl CoA.

Ethanol

Ethanol is a two-carbon alcohol (C_2H_5OH) produced by *C. pasteurianum* from acetyl CoA by the action of acetaldehyde dehydrogenase and alcohol dehydrogenase enzymes. Ethanol serves, apart from drinking alcohol, as a solvent in many pharmaceuticals, cosmetics, household products and flavoring agents (Equistar Chemicals LP, 2003). Bioethanol is currently the major biofuel produced from sugars, starch, or cellulose (Wang et al., 2013; Kocar and Civas, 2013).

1.3 STRATEGIES FOR INTENSIFICATION OF BIOHYDROGEN PRODUCTION

Previous research in intensification of glycerol fermentation for biohydrogen production has adopted several techniques: optimization of media components and process parameters, use of genetically modified microbial strains, efficient reactor design, and better fermentation protocols etc. Each of these techniques are discussed below in detail.

1.3.1 Medium and process optimization

Until recently no genetic tools were available for *C. pasteurianum*, therefore, early research efforts were limited to culture optimization and the deployment of chemical mutagens as a means to isolate the strains with favorable phenotypes**.** Fermentative hydrogen production is influenced by various factors such as substrate concentration, initial pH of media, media components, temperature, inoculum, reactor type and aeration. These factors indirectly affect the activity of enzymes responsible for hydrogen production such as hydrogenase, formate hydrogen lyase, pyruvate formate lyase. In this regard reports exist on increase or decrease in hydrogen yield due to the above factors. An optimum range is defined for all the factors such as an appropriate range of substrate concentration may enhance the hydrogen yield while higher concentrations may inhibit or decrease the yield. Similarly, media components such as nitrogen, phosphate and metal ions, which are essential for activity of enzymes responsible for hydrogen production and growth of bacteria, should also be maintained in optimum range. Temperature and pH are the critical factors which dramatically effects hydrogen production rate. An optimum range of temperature and pH is required for all enzymes and co-factors of bacteria to be active. Thus, optimization of parameters is a key technique to obtain maximum yields. The effects of various factors and their

optimum range can be evaluated by experimental design methods including one-factor-at-a time design, full factorial design, Taguchi design, Plackett-Burman design, central composite design and Box-Behnken design. Many optimization studies have been reported for hydrogen production using Response Surface Methodology, which is a popular method to evaluate the individual effect of variables as well as interactive effects among the variables with minimum error (Wang et al., 2008). In this process certain factors are selected and their individual effects are monitored as response of interest, followed by the analysis of the experimental results. From literature review presented in Table1.5, we can infer that most of the optimization processes for hydrogen production have been carried out by Plackett–Burman and Box–Behnken design or Central Composite Design. Plackett–Burman is a two-level fractional factorial design and is used to screen important factors for further investigation. It uses a first order polynomial model to describe the effects of various factors based on the experimental results. Central composite design (CCD) and Box-Behnken (BB) design are used to estimate the relationship between response and the key factors and evaluate the optimum values based on a second order polynomial. The second order polynomial can be displayed as surface plot or contour plot. Based on analysis of variance (ANOVA) of the model, we can determine the factors which have significant effects on the response.

Very few authors have dealt with biohydrogen production from crude glycerol using *Clostridium* species (Sarma et al., 2012). Lo et al. (2013) have adopted a non–statistical approach for optimization of biohydrogen production, and hence, their study does not reveal the global optimum parameters for biohydrogen production from *Clostridium* species. Moreover, relative influence (significant/insignificant) of each

optimization parameter on biohydrogen production, and the interactions among the parameters are also not revealed in their study.

1.3.2 Metabolic flux analysis

Metabolic flux analysis (MFA) is a technique for the assessment of intracellular metabolic fluxes in a biological system with a central importance to maximize the product yield or to analyze in priori, the effect of targeted genetic modification on the product formation (Nissen et al., 1997, Manish et al., 2007). If the measured fluxes are not sufficient to determine all intracellular fluxes, optimization approaches are applied. This method was mainly established by Edwards et al. (2002) and was named "flux balance analysis" (FBA). The analysis of possible metabolic routes falls into "metabolic network analysis" (MNA). MFA technique has been applied to optimize production of lysine (Vallino et al., 1993), acetate (Delgado et al., 1997), ethanol (Tunahan et al., 2004) etc.

In order to achieve high H_2 production yield, an extensive analysis and understanding of the metabolic pathways in the H_2-producing microorganisms is required which may further aim to redesign or redirect the metabolic pathways towards maximum product formation. The intracellular metabolic fluxes could be calculated by using mass balances across metabolites, stoichiometric reaction models as well as thermodynamics. Metabolic flux analysis (MFA), has been extensively applied in most research over the past decade in predicting changes in the fluxes and rate limiting steps of the specific pathway (Table 1.6).

Table 1.6. Summary of literature on metabolic flux analysis of biohydrogen production utilizing different substrates and microbial strains

Microorganism	Substrate	Salient features	Reference
Clostridium tyrobutyricum	Glucose and lactate/acetate	MFA methodology was applied to study the flux distribution during glucose and lactate/acetate metabolism and effect of HRT and initial substrate concentration. HRT showed significant impact on H_2 production. Increase of HRT increased H_2 production and reduced lactate production	Cheng et al., 2013
Rhodobacter capsulatus	Acetate, lactate, malate and CO_2	Study the flux distribution in the photoautotrophic metabolism of *R. capsulatus* for several substrates. Prediction of knockouts mainly by blockade of Calvin cycle and reduction of formate leading to increase H_2 yield using the constructed flux model.	Golomysova et al., 2011
Klebsiella pneumoniae ECU-15	Glucose	MFA method was used to estimate the effects of various culture conditions (temp, pH, initial glucose conc.) on production and uptake of hydrogen flux. Higher temperature reduced the uptake hydrogen and enhanced H_2 production. pH 7.0-7.5 was optimal for both the H_2 flux and the producing H_2 flux was maximum at 5g/L of initial glucose.	Niu et. al., 2011
Clostridium butyricum W5	Glucose	Metabolic flux analysis (MFA) of fermentative hydrogen with variations in initial glucose concentration and operational pH. The results suggest that pH has more significant effect on H_2 production compared to the glucose concentration.	Cai et al., 2010
Synechocystis sp. PCC6803	Glucose	Metabolic model was implemented for analysis of hydrogen production under three conditions (heterotrophic, autotrophic and mixotrophic) in terms of O_2 production and CO_2 fixation. Two conditions anoxic maximum and anoxic photoreduction	Navarro et al., 2009

Table 1.6. (Continued…)

Citrobacter amalonaticus Y19	Glucose	MetaFluxNet was employed for flux analysis of H_2 production with varying glucose concn. High H_2 yield of 8.7 mol H_2/mol glucose was possible if glucose metabolism is directed to the PP pathway and NAD(P)-linked hydrogenase is used to produce H_2.	Oh et al., 2008
Klebsiella pneumonia	Glycerol	MFA of anaerobic glycerol metabolism for production of 1,3-propanediol. Flux distribution revealed that branch points of glycerol and dihydroxy acetone phosphate were rigid compared to the flexible node of pyruvate and acetyl CoA to various environmental conditions.	Zhang et al., 2008
Escherichia coli	Glucose	Evaluation and comparison of metabolic network of wild and mutant (lacking lactate dehydrogenase) *E.coli* starin for H_2 production. Ethanol and acetate play significant role in H_2 production while lactate and succinate are not necessary.	Manish et al., 2007

Although MFA has been applied for few case studies of Clostridium sp. to study the effect of environmental conditions on H_2 yield (Table 1.6), to the best of our knowledge, investigation of metabolic pathway fluxes of fermentative hydrogen production using *Clostridium pasteurianum* was not found in the literature.

Flux balance analysis (FBA) is a mathematical approach for analyzing the flow of metabolites through a metabolic network. A metabolic network contains all of the known metabolic reactions in an organism and the genes that encode each enzyme. FBA calculates the flow of metabolites through this network, thereby making it possible to predict the growth rate of an organism or the rate of production of an important metabolite. Many reports have been published on FBA analysis of hydrogen production by *Clostridium thermosuccinogenese* (Sridhar et al., 2001); *Clostridium butyricum* W5 (Cai et al., 2010, Cai et al., 2011); *Clostridium acetobutylicum* (Senger et al., 2008). Oh et al., 2008 described flux analysis of hydrogen pathway in *Citrobacter amalonaticus* Y19 and concluded that a high H_2 production yield of 8.7 mol H_2/mol glucose is possible if glucose metabolism is directed to the PP pathway. Similarly Cheng et al., 2013 reported MFA for hydrogen production using *Clostridium tyrobutyricum* and concluded that HRT presents a significant impact on the metabolite flux of H_2production from glucose. In another report, MFA analysis of biohydrogen by *Clostridium butyricum* W5 indicated that operational pH has a significant effect on H_2 yield as well as metabolic flux distribution while initial glucose concentration had less impact on H_2 yield.

1.3.3 Application of Ultrasonication in fermentation

From literature survey it is evident that studies on application of ultrasound on the fermentation process to enhance bio-hydrogen production are very rare. Most of the studies have applied ultrasonication in the pretreatment process such as inoculum

pretreatment or substrate (biomass) pretreatment. Bundhoo et al., 2015, Ramprakash et al., 2015. Leano et al., 2012 reported ultrasonic pretreatment of palm oil mill effluent (POME) which produced 38% more hydrogen than non-sonicated treatments. Till date only one report have been found which has applied ultrasound for optimizing fermentative hydrogen production by Hsia et al., 2014. They optimized ultrasonic energy and its exposure time by Taguchi method and concluded that ultrasound significantly affects hydrogen production efficiency and rate thereby increasing production efficiency by 19.11 % under optimal conditions.

Ultrasound essentially refers to longitudinal acoustic waves beyond upper limit of human hearing range, i.e., 16 Hz – 20 kHz. The frequency range of ultrasound extends from 20 kHz to 20 MHz. Being a longitudinal wave, ultrasound passes through a compressible medium, such as air and water, in the form of alternate compression and rarefaction cycles. Propagation of ultrasound waves in the medium generates periodic variation in bulk pressure as well as density of the medium. Passage of ultrasound wave in the medium sets fluid elements in the medium in oscillatory motion around a mean position (Shah et al. 1999). Ultrasound wave is characterized by physical properties of frequency, velocity and pressure amplitude. During the propagation through medium, the pressure amplitude of the ultrasound wave is attenuated or dampened by various physical mechanisms. These mechanisms include thermal loss, frictional loss and scattering due to bubbles. Frictional loss is a manifestation of finite viscosity of the medium. During oscillatory motion of the fluid elements of the medium, some of the momentum of the fluid elements is dissipated in the medium, which results in their unidirectional (and not truly oscillatory) motion. Thermal loss is attributed to heat conduction between adjacent regions of compression and rarefaction that results in loss of compression work. For

propagation of ultrasound wave through liquid, bubbles present in the medium scatter the ultrasound waves causing severe attenuation. Presence of gas bubbles in the liquid also alters the compressibility of the medium, as a result of which the speed of sound in the medium reduces. The properties of the sound wave in gaseous medium are strongly influenced by the static pressure in the medium. For sound wave propagation in liquids, the static pressure in the medium does not affect much, as the liquid properties are relatively insensitive to static pressures (at least for moderate levels of pressure).

Cavitation can be defined as nucleation, growth, oscillation and transient collapse of gas/vapor bubbles driven by variation in bulk pressure in the medium. The cause leading to variation in bulk pressure could be propagation of an acoustic wave or variation in flow geometry (in case of flow cavitation like hydrodynamic cavitation), or in general, energy dissipation in the system. The efficiency of any physical/chemical/biological process depends on the method of introducing energy into the system. Cavitation has proven to be an efficient tool of introducing energy into the system for intensification of large number of physical/chemical/biological processes. Ultrasound makes available energies on extremely small time and spatial scales that are not available from any other source.

1.3.3.1 Physical effects of ultrasound and cavitation on reaction system

Ultrasound and cavitation has various physical effects on a reaction system. The main manifestation of all of these results is generation of intense micro–convection and micro–mixing in the reaction system. A brief description of all physical effects of ultrasound and cavitation is given below (Leighton 1994; Mason and Lorimer 2002; Shah et al. 1999; Young 1989).

Micro–streaming: It can be defined as oscillatory motion of small amplitude of fluid elements around a mean position, which is induced by propagation of ultrasound wave. For a typical ultrasound wave with pressure amplitude of 120 kPa in water (ρ = 1000 kg/m3, C = 1500 m/s), the micro–streaming velocity = 0.08 m/s.

Acoustic streaming: During transmission of ultrasound wave, the momentum of the wave is absorbed by the medium due to finite viscosity. This results in setting up of low velocity uni-directional currents of the fluid known as acoustic streaming (Kolb and Nyborg 1956; Nyborg 1958).

Microturbulence: The oscillatory motion of fluid induced due to volume oscillations of the bubble is called microturbulence. This phenomenon is explained as follows: in the expansion phase of radial motion of the cavitation bubble, the liquid is displaced away from bubble interface. During the collapse phase the liquid is pulled towards the bubble as it fills the vacuum created in the liquid with size reduction of bubble. The mean velocity of microturbulence depends on the amplitude of bubble oscillation.

Acoustic (or shock) waves: As the cavitation bubble contracts during the compression phase of radial motion, void space is created in the liquid and the fluid element spherically converge (or essentially "gush") in this void space and work is done on the bubble. For a cavitation bubble containing non–condensable gas such as air, the adiabatic compression results in rapid rise of pressure inside the bubble. At the point of minimum radius (or maximum compression), the bubble wall comes to a sudden halt. At this instance, the fluid elements converging towards the bubble are reflected back from the interface. This reflection creates a high pressure shock wave that propagates through the medium. The pressure exerted by the non–condensable gas inside the bubble causes re–bounce of the bubble.

Microjets: As long as the motion of liquid in the vicinity of the cavitation bubble is symmetric and uniform, it maintains spherical geometry during radial motion driven by ultrasound wave and thus there are no pressure gradients. If the bubble is located close to a phase boundary, either solid–liquid, gas–liquid or liquid–liquid, the motion of liquid in its vicinity is hindered, resulting in development of pressure gradient around it. This non–uniformity of pressure results in the loss of spherical geometry of the bubble. During the asymmetric radial motion, the portion of bubble exposed to higher pressure collapses faster than rest of the bubble, which gives rise to the formation of a high speed liquid jet directed towards the boundary. The velocity of these microjets has been estimated in the range of 120–150 m/s (Vogel et al., 1989; Philip et al., 1998), and they can cause severe damage at the point of impact (leading to effects like particle size reduction, microbial cell disruption, degradation of polymer chains etc.). The case of metal surfaces, these microjets can cause erosion of the surface.

1.3.4 Genetic engineering in *C. pasteurianum*

Genetic engineering is one of the approaches to increase the yield of hydrogen gas and maximize substrate utilization. Metabolic engineering strategies provide a way to overcome the limitations that are part of the biochemical pathways involved in hydrogen evolution. There are numerous ways to improve the yield through metabolic engineering such as gene knockout, homologous or heterologous overexpression of competitive genes, addition of synthetic pathways. Many such approaches for increased hydrogen yield has been proposed by researchers that include, addition of a new pathway from heterologous organism or inactivation of genes coding enzymes responsible for production of other side products thereby redirecting the pathway solely towards hydrogen production (Asada et al., 2000, Yoshida et al., 2006, Datsenko et al., 2000,

Kumar et al., 2001, Baba et al., 2006). Another approach is over-expression of few immediate genes responsible for hydrogen production like formate hydrogen lyase in *E. coli* (Yoshida et al. 2005), hydrogenase 3 in *E. coli* (Sode et al., 1998), hydrogenase gene in *Clostridium paraputrificum* (Morimoto et al., 2005). Most of the metabolic engineering studies to maximize hydrogen yield have involved the PFL pathway of *E. coli*, which is again limited to only 2 moles of hydrogen (Abo-Hashesh et al., 2011a, Hallenbeck et al., 2011). *E. coli* have been regarded as the model organism for most genetic studies because of its well-known metabolic pathways and its comprehensive characterization. It has also been explored widely for hydrogen production. In addition, many high hydrogen producing *Enterobacter* sps. have also been explored, which are the result of various genetic engineering approaches While very few studies have been reported till date for modification of the PFOR pathway of *Clostridium*, this is mainly due to lack of efficient methods of genetic engineering for Clostridia as they are gram positive bacteria with a thick cell wall, which is a barrier to transformation techniques. Moreover, the presence of restriction enzyme modification systems in Clostridia inhibits DNA transfer thereby impeding metabolic engineering of the strain. But with recent developments of better genetic tools and electro-transformation techniques has made it possible to construct recombinant strains of clostridia (Pyne et al., 2013, Pyne et al., 2014). Several studies have been published on microbial biohydrogen production from various clostridial strains, but till date few studies have reported biohydrogen from *Clostridium pasteurianum*. Moreover, no study on metabolic engineering has been reported for hydrogen production by *Clostridium pasteurianum*. Although detailed metabolic engineering studies on *C. pasteurianum* for improved solvent production have been reported by Schwartz et al., 2017. The Table1.7 describes genetic engineering

approaches in few species. From the Table 1.7 we can find that research has been widely extended to increase the yield of hydrogen through gene knockouts and over-expression in various bacterial species. Kaji et al. 1999 reported *hydA* gene disruption in *Clostridium perfringens* which completely reduced the hydrogen gas production. This suggested that hydA plays a critical role in the hydrogen pathway. Further research by Morimoto et al. (2005) reported 1.7 times increase in hydrogen yield in *Clostridium paraputrificum* by over-expression of *hydA* gene. This was accompanied by considerable reduction in the lactic acid formation (Morimoto et al. 2005). In the same study, authors conjectured that the over-expression of *hydA* led to over oxidation of NADH to NAD+, thus disrupting the consequent production of lactic acid from pyruvic acid (Morimoto et al. 2005). However, there were contrasting results reported by Klein et al. (2010) who stated that over-expression of hydrogenase did not improve the yield of hydrogen production (Table 1.7). Klein et al. did a comparative study on *Clostridium acetobutylicum* and *Clostridium butyricum* and reported a huge increase in specific hydrogenase activity for *Clostridium butyricum* but only slight increase in the case of *Clostridium acetobutylicum*. Similarly Yoshida et al., showed a 2 fold increase in hydrogen yield on disruption of *ldhA* (lactate dehydrogenase) and *frdBC* (fumarate reductase) pathways which are responsible for side products lactate and succinate. Over-expression of *fhlA* (formate hydrogen lyase activator protein) along with disruption of *ldhA* and *frdBC* resulted in further increase of yield (Yoshida et al., 2006). The acids produced by side reactions have a negative effect on hydrogen production. This was proved by Kumar et al. (2001), who reported 1.5 fold increase in hydrogen yield on disruption of acid producing pathway along with alcohol producing pathways, which directed flux solely towards hydrogen formation.

Table 1.7. Various genetic engineering approaches used to enhance the bio-hydrogen production

Microorganism	Genetic approach	Target gene	Yield (mol H_2/mol substrate)	Reference
Clostridium pasteurianum	Over expression	*hydA* *dhaD1* *dhaK*	1.11 0.93 (0.7 for wild type)	This study
Clostridium acetobutylicum DSM 792	Over expression	*thl* promoter	1.77 (1.79 for wild type)	Klein et al.,2010
Clostridium acetobutylicum DSM 792	Over expression	*hyd*A	1.81 (1.79 for wild type)	Klein et al.,2010
Enterobacter aerogenes ATCC 13408	Over expression	*hyd*A	2.31 (1.18 for wild type)	Zhao et al., 2010
E. coli BL21(DE3)	Over expression	*hup*S+*hup*L	19.68 mL H_2/L/hr (0.94 ml H_2/L/hr for wild type)	Lee et al., 2010
Enterobacter aerogenes IAM1183 Ea	Over expression	*fdh*F	1.16 (0.96 for wild type)	Lu et al., 2009
Enterobacter aerogenes IAM1183 Ea	Over expression	*fhl*A	1.09 (0.96 for wild type)	Lu et al., 2009
Clostridium saccharoperbutylacetonicum N1-4 pNAK1	Knockout	*hup*CBA operon	16.1ml H_2/hr (5.2 for wild type)	Nakayama et al., 2008
Clostridium tyrobutyricum	Knockout	*Ack*	2.16 (1.44 for wild type)	Liu et al.,2006b
Clostridium tyrobutyricum	Knockout	*Pta*	1.08	Liu et al., 2006a

Table 1.7. (Continued…)

E. coli W3110 (SR15 mutant)	Knockout	*ldh*A+*frd*BC	1.82 (1.08 for wild type)	Yoshida et al., 2006a
E. coli W3110 (SR14 mutant)	Knockout and Over expression	*ldh*A+*frd*BC and *fhl*A	1.87	Yoshida et al., 2006a
*Clostridium paraputrificu*m M-21	Over expression	*hyd*A	2.4 (1.4 for wild type)	Morimoto et al., 2005
Enterobacter cloacae IIT BT-08(A3 mutant)	Knockout	Alcohol dehydrogenase + butadienol dehydrogenase	1.65 (2.16 for wild type)	Kumar et al., 2001
Enterobacter cloacae IIT BT-08(DM11 mutant)	Knockout	Alcohol dehydrogenase + butadienol dehydrogenase + acid blocking	3.4 (2.16 for wild type)	Kumar et al., 2001

1.4 OBJECTIVES, APPROACH AND SCOPE OF THE PRESENT THESIS

From an extensive review of literature in the previous sections, it could be inferred that effective utilization of crude glycerol: a by–product of biodiesel industry, is an urgent need of the hour. Conversion of this crude glycerol to energy and value–added product is an effective means of generating revenue for the biodiesel industry to make it economically attractive. Glycerol, with its three carbon atoms, is an excellent fermentation substrate. Unlike other lignocellulosic feedstock, glycerol does not require pretreatment which is a cost intensive step in biofuel process. Many micro–organisms can utilize glycerol as sole carbon and energy source. The prominent value–added products from glycerol fermentation are 1,3–propanediol, butanol, biohydrogen, ethanol, succinic acid etc.

The proposed thesis work is aimed at optimization and intensification of a biochemical process for producing hydrogen from biodiesel–derived crude glycerol. The micro–organism used for in this study is *Clostridium pasteurianum*, which has a higher potential for biohydrogen production. This study aims in enriching H_2 producing *Clostridium pasteurianum* MTCC 116 by optimizing the physio–chemical parameters such as initial pH, incubation temperature and substrate concentration for maximal H_2 production by using central composite design (CCD) of experiments with analysis using response surface method. This is followed by kinetic and thermodynamic analysis of hydrogen production using Haldane substrate-inhibition kinetic model, Arrhenius plots and Eyring equation for both pure and crude glycerol as substrate for fermentation. Similarly statistical optimization of the media components was also considered as one of the approach to intensify H_2 production. Further to maximize valuable metabolite production, extensive analysis and understanding of metabolic pathways is required so as to redirect the cellular metabolic pathways primarily towards its production. An *in silico* metabolic flux model has been formulated for this analysis that determines the complete intracellular fluxes of all metabolites from experimentally measured fluxes. This methodology was used for comparative analysis of mechanical shaking and ultrasound-assisted fermentation for H_2 production. The flux analysis results were further corroborated by targeting the genes involved in glycerol-hydrogen pathway of *C. pasteurianum* which involved overexpression of Fe-only hydrogenase encoded by *hydA* and the enzymes involved in glycerol metabolism encoded by *dhaD1* and *dhaK*. The hydrogen production efficiency was compared between the wild type and recombinant strain of *C. pasteurianum* using crude glycerol as the substrate.

The objectives of the present thesis are listed below:

1. Statistical optimization of process parameters and kinetic-thermodynamic analysis for biohydrogen production from crude glycerol using *C. pasteurianum*

2. Optimization of medium components for biohydrogen production by *C. pasteurianum*

3. Metabolic flux analysis of sonication-induced glycerol fermentation for biohydrogen production by *C. pasteurianum*

4. Genetic engineering (overexpression of *hydA*, *dhaD1*, *dhaK* genes) of *C. pasteurianum* for improved biohydrogen production

The thesis comprises of 6 chapters (including the present one) that address different facets of glycerol fermentation. The brief content of each chapter is outlined below:

- Chapter 1 presents the general introduction to the subject of glycerol conversion to biohydrogen using chemical oxidation and microbial fermentation route. A brief review of literature in various aspects of hydrogen production by *C. pasteurianum*, and techniques for enhancement of biohydrogen yield has been presented followed by description of aim, approach and scope of the thesis.
- Chapter 2 describes the optimization of three different process parameters (pH, temperature, initial glycerol conc.) by response surface methodology (RSM). This study was further extended for studying the thermodynamics of biohydrogen and kinetic analysis of substrate inhibition on growth and biohydrogen production by *C. pasteurianum*.
- Chapter 3 explains the flux analysis of glycerol mediated hydrogen production pathway. A pseudo steady state metabolic flux network model was constructed applying mass balances around intracellular metabolites and analyzed using experimentally measured glycerol uptake rate and metabolite production rates.

The same flux model was used to get insight into ultrasound induced enhancement in biohydrogen production from glycerol fermentation. This study also highlighted the possible aspects of genetic engineering of hydrogen pathway to increase the yield.

- Chapter 4 deals with the statistical optimization of medium components for biohydrogen production by *C. pasteurianum*. The statistical experimental designs comprising six essential medium components were applied in two steps. Four essential medium components were selected by Plackett–Burman design, which were further optimized using Central Composite Design (CCD).
- Chapter 5 presents the fermentation studies using recombinant *C. pasteurianum* under conditions of both optimized fermentation medium (results of chapter 3) and fermentation parameters (results of chapter 4). The recombinant strains are constructed by overexpression of *hydA* encoding hydrogenase enzyme that catalyze the production of hydrogen from acetyl CoA. This study also deals with the overexpression of *dhaD1* and *dhaK* genes involved in glycerol metabolism encoding glycerol dehydrogenase and dihydroxyacetone kinase enzymes respectively.
- Chapter 6 represents the summary of the results and overall conclusion of the thesis. Some suggestions have been made to carry this work forward to an advance level.

References

Abo-Hashesh, M., Wang, R., Hallenbeck, P.C., 2011. Metabolic engineering in dark fermentative hydrogen production; theory and practice. Bioresour. Technol. 102 (18), 8414–8422.

Adhikari, S., Fernando, S., Haryanto, A., 2007. Production of hydrogen by steam reforming of glycerin over alumina supported metal catalysts. Catal Today. 129 (3–4), 355-364.

AE News. 2016, April 18. Hydrogen generation & storage made easy with nanotechnology. (Retrieved from http://www.alternative-energynews.info/hydrogengeneration-storage-nano-technology/).

Ahmad, A.L., Mat Yasin, N.H., Derek, C.J.C., Lim, J.K., 2011. Microalgae as a sustainable energy source for biodiesel production: a review. Renew Sustain Energy Rev. 15(1), 584–593.

Asada, Y., Koike, Y., Schnackenberg, J., Miyake, M., Uemura, I., Miyake, J., 2000. Heterologous expression of clostridial hydrogenase in the cyanobacterium *Synechococcus* PCC7942. Biochim Biophys Acta. 1490, 269-278.

Asumadu-Sarkodie, S., Owusu, P.A., 2016. A review of Ghana's energy sector national energy statistics and policy framework. J Cogent Engineering. Article: 1155274.

Avasthi, K.S., Reddy, R.N., Patel, S., 2013. Challenges in the production of hydrogen from glycerol-a biodiesel byproduct via steam reforming process. Procedia Eng. 51, 423-429.

Baba, T., Ara, T., Hasegawa, H., Takai, Y., Okumura, Y., Baba, M., 2006. Construction of *Escherichia coli* K-12 in frame, single gene knockout mutants: the Keio collection. Mol. Sys Biol. 2. Msb4100050-E1-msb50-E11.

Bagheri, S., Julkapli, N.M., Yehye, W.A., 2015. Catalytic conversion of biodiesel derived raw glycerol to value added products. Renew. Sust. Energ. Rev. 41, 113–127.

Biebl, H., Zeng, A.P., Menzel, K., Deckwer, W.D., 1998. Fermentation of glycerol to 1,3–propanediol and 2,3–butandiol by *Klebsiella pneumonia*. Appl. Microbiol. Biotechnol. 50, 24–29.

Biebl, H., Menzel, K., Zeng, A. P., Deckwer, W. D., 1999. Microbial production of 1,3-propanediol. Appl. Microbiol. Biotechnol. 52(3), 289–297.

Biebl, H., 2001. Fermentation of glycerol by *Clostridium pasteurianum* - batch and continuous culture studies. J of Industrial Microbiol. Biotechnol. 27(1), 18–26.

BP Statistical Review of World Energy June 2016. bp.com/statisticalreview.

Bundhoo, M.A.Z., Mohee, R., Hassan, M.A., 2015. Effects of pretreatment technologies on dark fermentative biohydrogen production: A review. Journal of Env. Manag. 157, 20-48.

Byrd, A.J., Pant, K.K., Gupta, R.B., 2008. Hydrogen production from glycerol by reforming in supercritical water over Ru/Al2O3 catalyst. Fuel. 87, 2956-2960.

Cai, G., Jin, B., Saint, C., Monis, P., 2010. Metabolic flux analysis of hydrogen production network by *Clostridium butyricum* W5: Effect of pH and glucose concentrations. Int. J. Hydrogen Energ. 35, 6681–6690.

Cai, G., Jin, B., Monis, P., Saint, C., 2011. Metabolic flux network and analysis of

fermentative hydrogen production. Biotechnol. Advances. 29, 375–387.

Cheng, H–H., Whang, L–M., Lin, C–A., Liu, I–C., Wu, C–W., 2013. Metabolic flux network analysis of fermentative hydrogen production: Using *Clostridium tyrobutyricum* as an example. Bioresour. Technol. 141, 233–239.

Chookaew, T., O–Thong, S., Prasertsan, P.,2015. Biohydrogen production from crude glycerol by two–stage of dark and photo fermentation. Int. J. Hydrogen Energ. 40, 7433–7438.

Chookaew, T., O–Thong, S., Prasertsan, P.,2014. Biohydrogen production from crude glycerol by immobilized *Klebsiella sp*. TR17 in a UASB reactor and bacterial quantification under non–sterile conditions. Int. J. Hydrogen Energ. 39, 9580–9587.

Cortright, R.D., Davda, R.R., Dumesic, J.A., 2002. Hydrogen from catalytic reforming of biomass-derived hydrocarbons in liquid water. Nature. 418, 964-966.

CRRC Qingdao Sifang Co. Ltd. 2015. China produces first hydrogen fuel cell tram, with Ballard unit. Fuel Cells Bulletin. 4, 5.

Dabrock, B., Bahl, H., Gottschalk, G., 1992. Parameters affecting solvent production by *Clostridium pasteurianum*. Appl Environ Microbiol. 58(4), 1233–1239.

Datsenko, K., Wanner, B.,2000. One step inactivation of chromosomal genes in *Escherichia coli*K-12 using PCR products. Proc Nat AcadSci USA. 97, 6640-6645.

Dauenhauer, P.J., Salge, J.R., Schmidt, L.D., 2006. Renewable hydrogen by autothermal steam reforming of volatile carbohydrates. J Catal. 244, 238-247.

Dębowskia, M., Korzeniewska, E., Filipkowska, Z., Zielinski, M.,Kwiatkowski, R.,2014. Possibility of hydrogen production duringcheese whey fermentation process by different strains ofpsychrophilic bacteria. Int J Hydrogen Energ. 39, 1972-1978.

Delfort, B., Durand, I., Hillion, G., Jaecker‐Voirol, A., Montagne, X., 2008. Glycerin for new biodiesel formulation. Oil Gas Sci. Technol. 63, 395‐404.

Delgado, J., Liao, J.C., 1997. Inverse flux analysis for reduction of acetateexcretion in E. coli. Biotechnol Progr. 13, 361–367.

Dikshit, P.K., 2017. Bioconversion of Crude Glycerol to Dihydroxyacetoneusing Immobilized *Gluconobacter oxydans*:Process Design, Optimization and Intensification. (Ph.D. Thesis)

Dobson, R., Gray, V., Rumbold, K., 2017. Microbial utilization of crude glycerol for the production of value-added products. J. Indust. Microbiol. Biotechnol. 39(2), 217-226.

Douette, A.M.D., Turn, S.Q., Wang, W., Keffer, V.I., 2007. Experimental investigation of hydrogen production from glycerin reforming. Energy Fuel. 21, 3499-3504.

Edenhofer, O., Pichs-Madruga, P., Sokona, Y., Seyboth, K., Matschoss, P., 2011. IPCC Special Report onRenewable Energy Sources and Climate Change Mitigation. Cambridge, UK/New York: Cambridge Univ. (In Press).

Edenhofer, O., Seyboth, K., Creutzig, F., Schloemer, S., 2013. On the sustainability of renewable energy sourcesAnnu. Rev. Environ. Resour. 38, 169-200.

Edwards, J.S., Covert, M., Palsson, B.O., 2002. Metabolic modeling ofmicrobes: the flux-balance approach. Environ Microbiol. 4, 133–140.

Electricity books. 2010. Jatropha for biodiesel. Available from: http://www.electricitybook.com/jatropha-biodiesel/.

Energy Statistics, 2017,24th issue. Central statistics office, Ministry of statistics and Programme Implementation, Government of India.

Ewan, B.C.R., Allen, R.W.K., 2005. A figure of merit assessment of the routes to hydrogen. Int J Hydrogen Energy. 30 (8), 809-819.

Garlapati, V.K., Shankar, U., Budhiraja, A., 2015. Bioconvesion technologies of crude glycerol to value added industrial products. Biotechnol. Rep. 9, 9–14.

Golomysova, A.N., Ivanov, P.S., 2010. Investigation of the anaerobic metabolism of *Rhodobacter capsulatus* by means of a flux model. Biophysics. 56, 74–85.

Hallenbeck, P.C., Ghosh, D., Abo-Hashesh, M., Wang, R., 2011. Metabolic engineering for enhanced biofuels production with emphasis on the biological production of hydrogen. Adv. Chem. Res. 6, 125–154.

Hallenbeck, P.C., Liu, Y.,2016. Recent advances in hydrogen production by photosynthetic Bacteria. Int. J. Hydrogen Energ. 41, 4446–4454.

Harvey, B. G., Meylemans, H. A., 2011. The role of butanol in the development of sustainable fuel technologies. Journal of Chemical Technology and Biotechnol. 86(1), 2–9.

Heyndrickx, M., Vos, P.D., Vancanneyt, M., Ley, J.D., 1991. The fermentation of glycerol by *Clostridium butyricum* LMG 1212t2 and 1213t2 and *Clostridium pasteurianum* LMG 3285. Appl. Microbiol. Biotechnol. 34, 637–642.

Hsia, S.Y., Chou, Y.T., Wang, C.H., 2013. Ultrasound for optimizing dark-fermentive hydrogenproduction. Innovation, Comm. And Engg.-Proceedings Conf. 2, 377-

380.

Indian Petroleum and Natural Gas Statistics. Ministry of Petroleum and Natural Gas, Government of India, 2015‐16.

Jitrwung, R., Yargeau, V., 2011. Optimization of media composition for the production of biohydrogen from waste glycerol. Int. J. Hydrogen Energ. 36, 9602–9611.

Kaygusuz, K., 2012. Energy for sustainable development: A case of developing countries. Renewable and Sustainable Energy Rev. 16, 1116-1126.

Khanna, S., Goyal, A., Moholkar, V.S., 2012. Microbial conversion of glycerol: Present status and future prospects. Crit. Rev. Biotechnol. 32, 235–262.

Klein, M., Ansorge-Schumacher, M.B., Fritsch, M., Hartmeier, W., 2010. Influence of hydrogenase over-expression on hydrogen production of *Clostridium acetobutylicum* DSM 792. Enzyme Microb. Technol. 46, 384–390.

Kocar, G., Civas, N., 2013. An overview of biofuels from energy crops: Current status and future prospects. Renewable & Sustainable Energy Rev., 28, 900–916.

Kolb, J., Nyborg, W.L., 1956. Small scale acoustic streaming in liquids. J. Acoust. Soc. Am. 28, 1237–1242.

Kumar, N., Das, D., 2001. Continuous hydrogen production by immobilized *Enterobacter cloacae* IIT-BT 08 using lignocellulosic materials as solid matrices. Enzyme Microb. Technol. 29, 280–287.

Kumar, P., Sharma, R., Ray, S., Mehariya, S., Patel, S.K., Lee, J.K., 2015. Dark fermentative bioconversion of glycerol to hydrogen by *Bacillus thuringiensis*. Bioresour. Technol. 82, 383–388.

Leano, E.P., Anceno, A.J., Babel, S., 2012. Ultrasonic pretreatment of palm oil mill effluent:Impact on biohydrogen production, bioelectricity generation, and underlying microbial communities. Int. J. Hydrogen Energ. 37(17), 12241-12249.

Lee, S.Y., Lee, H.J., Park, J.M., Lee, J.H., Park, J.S., Shin, H.S., 2010. Bacterial hydrogen production in recombinant Escherichia coli harboring a HupSL hydrogenase isolated from *Rhodobacter sphaeroidesunder* anaerobic dark culture. Int. J. Hydrogen Energ. 35, 1112–1116.

Lehnert, K., Claus, P., 2008. Influence of Pt particle size and support type on the aqueous-phase reforming of glycerol. Catal. Commun. 9, 2543-2546.

Leighton, T.G., 1994. The acoustic bubble. Academic Press, San Diego.

Liu, F., Fang, B., 2007. Optimization of biohydrogen from biodiesel wastes by *Klebsiella pneumonia*. Biotechnol. J. 2, 374–380.

Liu, X., Zhu, Y., Yang, S.T., 2006a. Butyric acid and hydrogen production by *Clostridium tyrobutyricum* ATCC 25755 and mutants. Enzyme Microb. Technol. 38, 521–528.

Liu, X., Zhu, Y., Yang, S.T., 2006b. Construction and characterization of ack deleted mutant of *Clostridium tyrobutyricum*for enhanced butyric acid and hydrogen production. Biotechnol.Prog. 22, 1265–1275.

Lo, Y.C., Chen, X.J., Yuan, Y., Chang, J.S., 2013. Dark fermentative hydrogen production with crudeglycerol from biodiesel industry using indigenous hydrogen producing bacteria. Int. J. Hydrogen Energ. 38, 15815–15822.

Lu, Y., Zhao, H., Zhang, C., Lai, Q., Xing, X.H., 2009. Perturbation of formate pathway for hydrogen production by expressions of formate hydrogen lyase and its transcriptional activator in wild *Enterobacter aerogenes* and its mutants. Int. J. Hydrogen Energ. 34, 5072–5079.

Luo, N., Fu, X., Cao, F., Xiao, T., Edwards, P.P., 2008. Glycerol aqueous phase reforming for hydrogen generation over Pt catalyst–effect of catalyst composition and reaction conditions. Fuel. 87, 3483-3489.

Mangayil, R., Karp, M., Santala, V., 2012. Bioconversion of crude glycerol from biodiesel production to hydrogen. Int. J. Hydrogen Energ. 37, 12198–12204.

Mangayil, R., Aho, T., Karp, M., Santala, V., 2015. Improved bioconversion of crude glycerol to hydrogen by statistical optimization of media components. Renew. Energ. 75, 583–589.

Manish, S., Venkatesh, K.V., Banerjee, R., 2007. Metabolic flux analysis of biological hydrogen production by *Escherichia coli*. Int. J. Hydrogen Energ. 32, 3820–3830.

Marone, A., Varrone, C., Fiocchetti, F., Giussani, B., Izzo, G., Mentuccia, L., Rosa, S., Signorini, A., 2015. Optimization of substrate composition for biohydrogen production from buffalo slurry co–fermented with cheese whey and crude glycerol, using microbial mixed culture. Int. J. Hydrogen Energ. 40, 209–218.

Mason, T.J., Lorimer, J.P., 2002. Applied sonochemistry: The uses of power ultrasound in chemistry and processing. Wiley–VCH, Coventry.

Nakas, J.P., Schaedle, M., Parkinson, C.M., Coonley, C.E., Tanenbaum, S.W., 1983.System development for linked-fermentation production of solvents from algal biomass. Appl. Environ. Microbiol. 46(5), 101723.

Nakayama, S.-i., Kosaka, T., Hirakawa, H., Matsuura, K., Yoshino, S., Furukawa, K., 2008. Metabolic engineering for solvent productivity by downregulation of the hydrogenase gene cluster in *Clostridium saccharoperbutylacetonicum* strain N1-4. Appl. Microbiol. Biotechnol. 78: 483–493.

Nanda, M.R., Yuan, Z., Qin, W., Xu, C., 2016. Recent advancements in catalytic conversion of glycerol into propylene glycol: A review. Catal. Rev. 58(3), 309–336.

Navarro, E., Montagud, A., de Cordoba, P.F., Urchueguia, J.F., 2009. Metabolic flux analysis of the hydrogen production potential in *Synechocystis* sp. PCC6803. Int. J. Hydrogen Energ. 34, 8828–8838.

Nissen, T.L., Schulze, U., Nielsen, J., Villadsen, J., 1997. Flux distributions in anaerobic, glucose-limitedcontinuous cultures of *Saccharomyces cerevisiae*. Microbiology. 143, 203–218.

Niu, K., Zhang, X., Tan, W–S., Zhu, M–L., 2011. Effect of culture conditions on producing and uptake hydrogen flux of biohydrogen fermentation by metabolic flux analysis method. Bioresour. Technol. 102, 7294–7300.

Nyborg, W.L., 1958. Acoustic streaming near a boundary. J. Acoust. Soc. Am. 30, 329–339.

Oh, Y–K., K, H–J., Park, S., Kim, M–S., Ryu, D.D.Y., 2008. Metabolic flux analysis of hydrogen production pathway in *Citrobacter amalonaticus* Y19. Int. J. Hydrogen Energ. 33, 1471–1482.

Pachapur, V.L., Sarma, S.J., Brar, S.K., Bihan, Y.L., Buelna, G., Verma, M., 2015. Biohydrogen production by co–fermentation of crude glycerol and apple pomace hydrolysate using co–culture of *Enterobacter aerogenes* and *Clostridium*

butyricum. Bioresour. Technol. 193, 297–306.

Pagliaro, M., Ciriminna, R., Kimura, H., Rossi, M., Della Pina, C., 2007. From glycerol to value-added products. Angew. Chem. Int. Ed. 46(24), 4434–4440.

Poleto, L., Souza, P., Magrini, F.E., Beal, L.L., Torres, A.P.R., Sousa, M.P., Laurino, J.P., Paesi, S., 2016. Selection and identification of microorganisms present in the treatment of wastewater and activated sludge to produce biohydrogen from glycerol. Int. J. Hydrogen Energ. 41, 4374–4381.

Pyne, M.E., Moo-Young, M., Chung, D.A., Chou, C.P., 2013. Development of an electrotransformation protocol for genetic manipulation of *Clostridium pasteurianum*. Biotechnol. Biofuel. 6, 50.

Pyne, M.E., Moo-Young, M., Chung, D.A., Chou, C.P., 2014. Expansion of the genetic toolkit for metabolic engineering of *Clostridium pasteurianum*: chromosomal gene disruption of the endogenous CpaAI restriction enzyme (2014), Biotechnol. Biofuels. 7, 163.

Quispe, C.A.G., Coronado, C.J.R., Carvalho Jr, J.A., 2013. Glycerol: Production, consumption, prices, characterization and new trends in combustion. Renew. Sust. Energ. Rev. 27, 475‑493.

Ramprakash, B., Muthukumar, K., 2015. Comparative study on the performance of various pretreatment and hydrolysis methods for the production of biohydrogen using *Enterobacter aerogenes* RM 08 from rice mill wastewater. Int. J. Hydrogen Energ. 40, 9106-9112.

Renewables, 2016. Global Status Report, Renewable Energy Indicators, 2015. United

Nations Environment Program, Paris, France, p. 272.

Reungsang, A, Sittijunda, S., O–thong, S.,2013. Biohydrogen production from glycerol by immobilized*Enterobacter aerogenes* ATCC 13048 on heat treated UASB granules as affected by organic loading rate. Int. J. Hydrogen Energ. 38, 6970–6979.

Rivero, M., Solera, R., Perez, M., 2014. Anaerobic mesophilic co–digestion of sewage sludge with glycerol: Enhanced biohydrogen production. Int. J. Hydrogen Energ. 39, 2481–2488.

Sarma, S., Dubey, V.K., Moholkar, V.S., 2016. Kinetic and thermodynamic analysis (with statistical optimization) of hydrogen production from crude glycerol using *Clostridium pasteurianum*. Int. J. Hydrogen Energ. 33, 1471–1482.

Sarma, S., Anand, A., Dubey, V.K., Moholkar, V.S., 2017. Metabolic flux network analysis of hydrogen production from crude glycerol by *Clostridium pasteurianum*. Bioresour. Technol. 242, 169–177.

Sarma, S.J., Brar, S.K., Sydney, E.B., Bihan, Y.L., Buelna, G., Soccol, C.R., 2012. Microbial biohydrogen production by bioconversion of crude glycerol: A review. Int. J. Hydrogen Energ. 37, 6473–6490.

Schwarz, K.M., Grosse-Honebrink, A., Derecka, K., Rotta, C., Zhang, Y., Minton, N.P. 2017. Towards improved butanol production through targeted genetic modification of *Clostridium pasteurianum*. Metabolic Engineering. doi:10.1016/j.ymben.2017.01.009.

Selembo, P.A., Perez, J.M., Lloyd, W.A., Logan, B.E.,2009. High hydrogen production from glycerol or glucose by electrohydrogenesis using microbial electrolysis cells. Int. J. Hydrogen Energ. 34, 5373–5381.

Senger, R.S., Papoutsakis, E.T., 2008. Genome-Scale Model for *Clostridium acetobutylicum*: Part II. Development of specific proton flux states and numerically determined sub-systems. Biotechnol. Bioenng. 101, 1053-1071.

Shah, Y.T., Pandit, A.B. Moholkar, V.S., 1999. Cavitation reaction engineering. Plenum Press, New York.

Silitonga, A.S., Atabani, A.E., Mahlia, T.M.I., Masjuki, H.H., Badruddin, I.A., Mekhilef, S., 2011. A review on prospect of Jatropha curcas for biodiesel in Indonesia. Renew Sustain Energy Rev. 15, 3733–3756.

Sinha, P., Pandey, A.,2011. An evaluative report and challenges forfermentative biohydrogen production. Int J Hydrogen Energ. 36, 7460-7478.

Sittijunda, S., Reungsang, A., 2012. Biohydrogen production from waste glycerol and sludge by anaerobic mixed cultures. Int. J. Hydrogen Energ. 37, 13789–13796.

Soares, R.R., Simonetti, D.A., Dumesic, J.A., 2006. Glycerol as a source for fuels and chemicals by low-temperature catalytic processing. Angew. Chem. Int. Edit. 45, 3982-3985.

Solomos, B., Zeng, A.P., Biebl, H., Schlieker, H., Posten, C., Deckwer, W.D., 1995. Comparison of the energetic efficiencies of hydrogen and oxochemicals formation in *Klebsiella pneumonia* and *Clostridium butylicum* during anaerobic growth on glycerol. J. Biotechnol. 39, 107–117.

Sridhar, J., Eiteman, M.A., 2001. Metabolic flux analysis of *Clostridium thermosuccinogenes*. Appl. Biochem. Biotechnol. 94, 51–69.

Swami, S.M., Abraham, M.A., 2006. Integrated catalytic process for conversion of biomass to hydrogen. Energy Fuel. 20, 2616-2622.

Trchounian. K., Abrahamyan, V., Poladyan, A., Trchounian, A., 2015a. *Escherichia coli* growth and hydrogen production in batch culture upon formate alone and with glycerol co–fermentation at different pHs. Int. J. Hydrogen Energ. 40, 9935–9941.

Trchounian, K., Sargsyan, H., Trchounian, A., 2015b. H_2 production by *Escherichia coli* batch cultures during utilization of acetate and mixture of glycerol and acetate. Int. J. Hydrogen Energ. 40, 12187–12192.

Tunahan, C., Arga, K.Y., Mete, M.A., Kutlu,Ö.Ü., 2004. Flux analysis of recombinant *Saccharomyces cerevisiae* YPB-G utilizing starch for optimal ethanolproduction. Process Biochem. 39, 2097–2108.

Urbaniec, K., Bakker, R.R., 2015. Biomass residues as raw material for dark hydrogen fermentation– A review. Int. J. Hydrogen Energ. 40: 3648–3658.

U.S. Energy Information Administration. 2011.Total biofuels production (thousand barrels perday). Available from: http://tonto.eia.gov/cfapps/ipdbproject/iedindex3.cfm?tid=79&pid=79&aid=1&cid=&syid=2000&eyid=2008&unit=TBPD

Vallino, J.J., Stephanopoulos, G.,1993. Metabolic flux distributions in*Corynebacterium glutamicum* during growth and lysine overproduction.Biotechnol. Bioeng. 41, 633–646.

Valliyappan, T., Ferdous, D., Bakhsi, N.N., Dalai, A.K., 2008. Production of hydrogen and syngas via steam gasification of glycerol in a fixed-bed reactor. Top. Catal. 49, 59-67.

Varrone, C., Giussani, B., Izzo, G., Massini, G., Marone, A., Signorini, A., Wang, A., 2012. Statistical optimization of biohydrogen and ethanol production from crude glycerol by microbial mixed culture. Int. J. Hydrogen Energ. 37, 16479–16488.

Veluturla, S., Archna, N., Rao, D.S., Hezil, N., Indraja, I.S., Spoorthi, S., 2018. Catalytic valorization of raw glycerol derived from biodiesel: a review. Biofuels. 9(3), 305–314.

Vidosh, M., Praksh, V., Alok, Ch., 2011. Impacts of bio‑fuel use: a review. Int. J. Eng. Sci.Technol. 3, 3776‑3782.

Wang, J., Wan, W., 2008. Optimization of fermentative hydrogen production process by response surface methodology. Int. J. Hydrogen Energ. 33, 6976–6984.

Winogradsky, S., 1895. Recherches sur l'assimiltion de l'azote libre de l'atmosph`ere par les microbes. Unknown Binding.

Yang, F., Hanna, M.A., Sun, R., 2012. Value added uses for crude glycerol-a byproduct of biodiesel production. Biotechnol. Biofuel. 5, (doi.org/10.1186/1754-6834-5-13).

Yazdani, S.S., Gonzalez, R., 2007. Anaerobic fermentation of glycerol: a path to economic viability for the biofuels industry. Curr. Opin. Biotechnol. 18,213–219.

Yoshida, A., Nishimura, T., Kawaguchi, H., Inui, M., Yukawa, H., 2005. Enhanced

hydrogen production from formic acid by formate-hydrogen lyase- over-expressing *Escherichia coli* strains. Appl. Environ. Microbiol. 71, 6762-6768.

Yoshida, A., Nishimura, T., Kawaguchi, H., Inui, M., Yukawa, H., 2006. Enhanced hydrogen production from glucose using ldh- and frd-inactivated *Escherichia coli* strains. Appl. Microbiol. Biotechnol. 73, 67–72.

Young, F.R., 1989. Cavitation. McGraw Hill, London.Zelitch, I.H., 1951. Simultaneous use of molecular nitrogen and ammonia by *Clostridium pasteurianum*. Proc Natl Acad Sci U S A. 37(9), 559–565.

Zhang, B., Tang, X., Li, Y., Xu, Y., Shen, W., 2007. Hydrogen production from steam reforming of ethanol and glycerol over ceria-supported metal catalysts. Int J Hydrogen Energ. 32 (13), 2367-2373.

Zhang, Q., Teng, Hu., Sun, Y., Xiu, Z., Zeng, A., 2008. Metabolic flux and robustness analysis of glycerol metabolism in *Klebsiella pneumoniae*. Bioprocess Biosyst Eng. 31, 127–135.

Zhao, J.F., Song, W.L., Cheng, J., Zhang, C., 2010. Heterologous expression of a hydrogenase gene in *Enterobacter aerogenes* to enhance hydrogen gas production. World J. Microbiol. Biotechnol. 26, 177–181

Zhou, C.H., Zhao, H., Tong, D.S., Wu, L.M., Yu, W.H., 2013. Recent advances in catalytic conversion of glycerol. Catal. Rev. 55, 369–453

Chapter 2

Kinetic and Thermodynamic analysis with Statistical Optimization of Hydrogen Production from Crude Glycerol using *Clostridium pasteurianum*

2.1. INTRODUCTION

Although several earlier authors have addressed the matter of glycerol bioconversion to hydrogen, studies using biodiesel–derived crude glycerol are limited. Alkali, alcohol and salt contaminations in crude glycerol could have significant effect on hydrogen production by microbial cells, which needs to be properly investigated. Moreover very few authors have dealt with biohydrogen production from crude glycerol using *Clostridium* species (Sarma et al., 2012). Lo et al. (2013) have adopted a non–statistical approach for optimization of biohydrogen production, and hence, their study does not reveal the global optimum parameters for biohydrogen production from *Clostridium* species. Moreover, relative influence (significant/insignificant) of each

optimization parameter on biohydrogen production, and the interactions among the parameters are also not revealed in their study. Fermentative hydrogen production is influenced by various factors such as substrate concentration, initial pH of media, media components, temperature, inoculum, reactor type and aeration (Wang et al., 2008).

In the present study, we have assessed the potential of crude glycerol as fermentation substrate for biohydrogen production using *Clostridium pasteurianum*. The methodology adopted by us is two–fold, viz. (i) statistical optimization of hydrogen production using central composite design (CCD) of experiments with analysis using response surface method, and (ii) kinetic and thermodynamic analysis of hydrogen production using Haldane substrate-inhibition kinetic model, Arrhenius plots and Eyring equation. For determination of the kinetic and Arrhenius parameters, experiments have been conducted with variation in the required parameter, viz. initial substrate concentration (for the Haldane kinetic model) and temperature (for Arrhenius plots and Eyring equation) with other fermentation parameters held at their optimum conditions determined by the statistical design. The results of these experiments have been compared with pure glycerol as substrate. The relative variations in the kinetic parameters (viz. maximum reaction velocity, V_{max}; Michaelis constant, K_m and inhibition constant, K_I) and thermodynamic parameters (activation energy, E_a; enthalpy, ΔH; entropy, ΔS and Gibbs energy ΔG) for crude and pure glycerol as substrate not only demonstrate feasibility of crude glycerol as fermentation substrate for hydrogen production, but also reveal interesting facets of biomechanics of the fermentation process, as described in the subsequent sections.

2.2. MATERIALS AND METHODS

2.2.1 Materials

Microbial culture of *Clostridium pasteurianum* MTCC 116 (ATCC 6013) was procured from Microbial Type Culture Collection (MTCC), Chandigarh, India. Pure glycerol was procured from Merck, Germany. All other medium components and chemicals used in this study were procured from HiMedia Pvt. Ltd., India.

2.2.2 Synthesis of crude glycerol

The crude glycerol was produced in our laboratory by alkali catalyzed methanolysis of soybean oil. The details of transesterification reaction are as follows: molar ratio (12:1), oil (60 mL), methanol (30 mL), NaOH catalyst (0.54 g, 1% w/v), temperature (65^{o}C), reaction time (1 h). After completion of the reaction, the reaction mixture was kept standing in the separating funnel for 18–20 h. The mixture separated into two layers, viz. upper layer of biodiesel and lower layer of glycerol. Approximately, 27 mL of crude glycerol was produced from the transesterification reaction. The quantities of alkali and alcohol contaminants in crude glycerol were determined as follows: 0.85% w/v of NaOH (calculated by acid base titration) and 0.26% w/v methanol (determined using gas chromatograph).

2.2.3 Inoculum preparation

Freeze dried cultures of *Clostridium pasteurianum* were maintained in Reinforced Clostridial Medium (RCM). The composition of RCM in 1 L of distilled water was as follows: yeast extract 5.0 g, beef extract 10.0 g, peptone 10.0 g, glucose 5.0 g, starch 1.0 g, sodium chloride 5.0 g, sodium acetate 3.0 g, cysteine hydrochloride 0.5 g, agar 0.5 g. The pH of the medium was adjusted to 6.8 ± 0.2 using 1 M NaOH. The medium was inoculated and kept in a rotary incubator shaker (Make: Lab Companion; Model: SI–300R) at 37^{o}C, 150 rpm for 24 h. The 24 h culture was used for streaking over agar plate

having same medium composition with 15 g/L of agar, and the culture was kept at 37ºC in a desiccator containing anaerobic gas pack. The culture broth was used as stock and was sub–cultured every month.

2.2.4 Batch fermentation

The cells from stock culture were grown in fresh RCM medium prior to inoculation under anaerobic conditions (Khanna et al., 2013). Batch experiments were set up by transferring inoculum from mid log phase of culture in 100 mL serum bottle containing BSH (a modified form of Basal solution for hydrogen production) (Chen et al., 2005, Junghare et al., 2012) medium with working volume of 60 mL comprising 6 mL (10% v/v) of *Clostridium pasteurianum* inoculum, 1.2 mL of 3% (w/v) L–cysteine HCl as a reducing agent, and 52.8 mL of fermentation medium (BSH) including substrate glycerol (10 g/L). Resazurin dye (0.1%w/v) was added into medium as an indicator of anaerobic conditions. The BSH medium comprised of following components (concentration, g/L): peptone (2), yeast extract (1), K_2HPO_4 (0.230), KH_2PO_4 (4.035), NaCl (2),in addition to 10 mL trace solution and 10 mL vitamin solution. Trace element solution comprised of following components (concentration, g/L): $MnO_4 \cdot 7H_2O$ (0.01), $ZnSO_4 \cdot 7H_2O$ (0.05), H_3BO_3 (0.01), $N(CH_2COOH)_3$ (4.5), $CaCl_2 \cdot 2H_2O$ (0.01), Na_2MoO_4 (0.01), $CoCl_2 \cdot 6H_2O$ (0.2), $AlK(SO_4)_2$ (0.01), $MgCl_2 \cdot 6H_2O$ (0.2), $FeCl_3$ (0.1), $CuCl_2 \cdot 6H_2O$ (0.05). The composition of vitamin solution was as follows (concentration, g/L): riboflavin (0.025), citric acid (0.02), folic acid (0.01) and para–amino benzoic acid (0.01). The initial pH of the medium was adjusted to 7 using 1 M NaOH. Prior to inoculation, the medium was flushed with pure nitrogen (99.99%) for 15 min, sealed with rubber stoppers, crimped and autoclaved at 121°C, 15 psi for 15 min. The bottles were then inoculated with 10% v/v inoculum and incubated at 37°C and 150 rpm. All treatments were carried out in duplicate. Aliquots of fermentation broth were withdrawn periodically to assess the quantity of

glycerol consumed. Similarly, samples from gaseous phase were collected periodically to quantify H_2 and CO_2 content.

2.2.5 Preliminary experiments

Prior to main experiments for biohydrogen production, initial or preliminary experiments have been conducted for determination of following parameters: (1) incubation time, (2) inoculum size, (3) incubation temperature, (4) initial pH of fermentation, (5) initial glycerol concentration. The approach used in these experiments is "one variable at a time (OVAT)". The results of these experiments have been used to design the main CCD experiments. Procedure and results of these preliminary experiments are described as follows.

2.2.5.1 Incubation period

Optimum incubation period for maximum H_2 production was determined by conducting batch experiments with varying periods with crude glycerol (10 g/L) as the sole carbon source. H_2 content in the gas phase increased from 8.6 ± 0.80% v/v at 4 h to 33.36 ± 0.98% v/v at 15 h (data not shown). Beyond incubation period of 15 h, the H_2 content in the gas phase remained practically constant. On the basis of this result, the optimum incubation period was determined as 15 h.

2.2.5.2 Inoculum size

Batch experiments were conducted with varying inoculum sizes from an overnight–grown culture of *Clostridium pasteurianum.* Inoculum size of 1, 5, 10, 15, 20% (v/v) was used to inoculate freshly prepared anaerobic BSH medium containing 10 g/L crude glycerol as substrate. Incubation was carried out for 15 h at 37°C and 150 rpm, and the gaseous phase was analyzed for H_2 content after completion of incubation. The H_2 content of gas phase increased from 22.5 ± 0.7% v/v for inoculum size of 1% to 32.76 ± 0.45% v/v for inoculum size of 10% (v/v). Thereafter, the H_2 content showed slight

reduction till inoculum size of 20% v/v. Fig. 2.1A depicts the variations in H_2 content of product gas with inoculum size. A probable cause leading to reduction in H_2 content for higher inoculum size is over consumption of the substrate (glycerol) that results in overgrowth of the cells with synthesis of other metabolites like acetate and butyrate. Formation of the acidic side products in the medium results in rapid reduction of the pH (Zhao et al., 2011). Fig. 2.1B depicts the time profiles of pH of the reaction mixture for 5, 10 and 15% v/v inoculum. It could be inferred from Fig. 2.1B that the rate of reduction in pH varies proportionately with the inoculum size. The final pH attended at the end of 24 h fermentation for 5, 10 and 15% v/v inoculum is 5.9, 5.7 and 5.3, respectively. Comparative analysis of biohydrogen yield and pH profiles reveals that hydrogen production is a strong function of the pH in the medium and shows an optimum with the pH. The optimum value of the inoculum was determined as 10% v/v as presented in Figs. 2.1A and 2.1B.

2.2.5.3 pH of fermentation medium

To determine the optimum value of this parameter, experiments have been conducted in serum bottles containing BSH media with initial pH in the range of 5 to 10. Initial pH of the medium was adjusted by addition of 1 M NaOH or 1 N ortho–phosphoric acid. H_2 content in the gas phase increased from 14.3 ± 0.33% v/v at initial pH of 5 to 31.65 ± 0.62% v/v at initial pH of 7. Gradual reduction in H_2 content was observed on further increase in initial pH. These trends have been shown in Fig. 2.1C. Maximum H_2 content of gas phase was obtained at initial pH 7, which is consistent with the previous literature (Zhao et al., 2011; Pan et al., 2008). Lower or higher pH of medium (or cell environment) results in a lower level of ATP in the cell, which in turn inhibits bacterial growth and enzyme activity resulting in reduction in H_2 production (Bowles et al., 1985; Ferchichi et al., 2005).

2.2.5.4 Incubation temperature

To evaluate effect of temperature on H_2 production, batch tests containing BSH media were conducted at various temperatures (30°, 35°, 37°, 40° and 42°C) with other parameters at their optimum values: initial pH 7, crude glycerol concentration 10 g/L and shaking at 150 rpm. Maximum H_2 content of 34.56 ± 0.44% v/v in the gas phase was observed at 37°C, which gradually decreased to 25.0 ± 0.71% v/v at 42°C, as depicted in Fig. 2.1D. The optimum temperature for H_2 production was thus determined as 37°C, which is consistent with results of Zhao et al. (2011).

2.2.5.5 Initial glycerol concentration

Crude glycerol resulting from transesterification reaction for biodiesel synthesis was used as the sole carbon source (or substrate) for hydrogen production. The substrate concentration was varied in the range of 0 to 20 g/L (0.4, 0.8, 1, 2, 4, 6, 10, 15, 17, 20 g/L). The experiments were conducted in serum bottles at pH 7, 37°C and 150 rpm. H_2 content of product gas was found to increase with crude glycerol concentration. The maximum H_2 content of 37.76 ± 0.92% v/v in the gaseous phase was obtained for crude glycerol concentration of 6 g/L, which gradually reduced to 28.92 ± 1.1% v/v (reduction of 23%) at crude glycerol concentration of 20 g/L. The profile of H_2 production with varying initial crude glycerol concentration is shown in Fig. 2.2A, which is consistent with results of Lo et al. (2013). Experiments have also been conducted with varying initial concentrations of pure glycerol as substrate, and the trends in H_2 production are depicted in Fig. 2.2A. For pure glycerol, the highest H_2 content of 31.01 ± 1% v/v in the gas phase was obtained for initial glycerol concentration of 10 g/L.

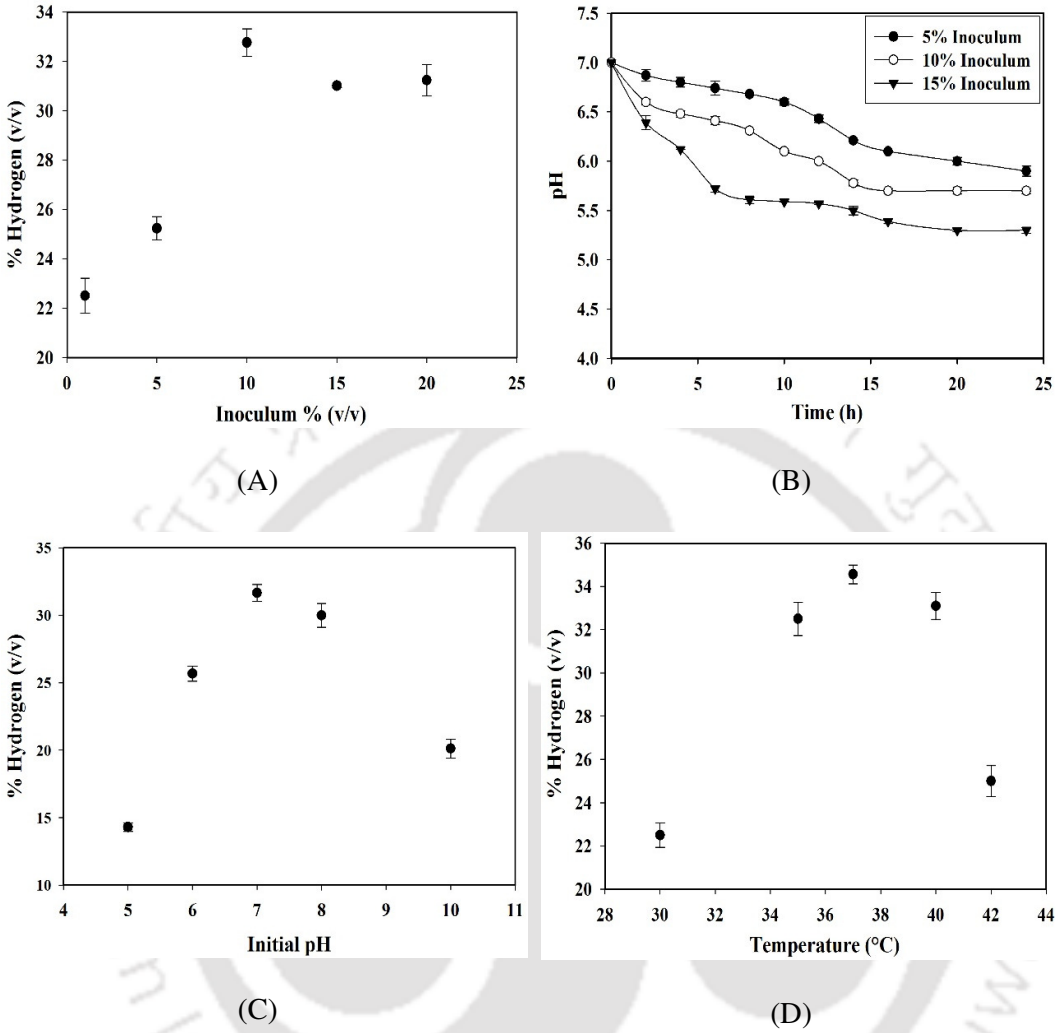

Figure 2.1. Results of preliminary experiments. Effect of various parameters on hydrogen production in batch fermentation for initial crude glycerol concentration of 10 g/L. (A) inoculum size, (B) pH profiles for different inoculums size, (C) initial pH, (D) temperature.

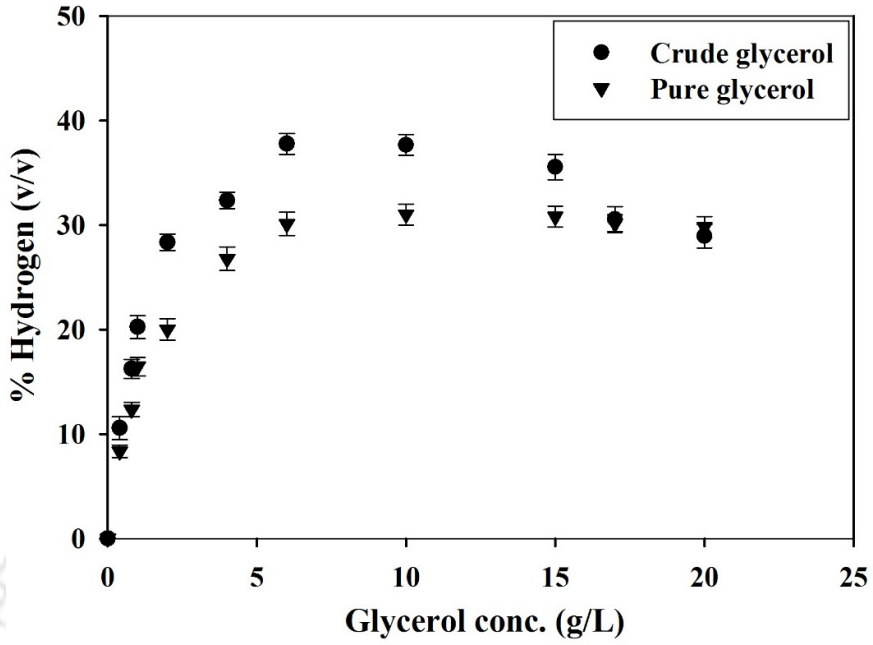

(A)

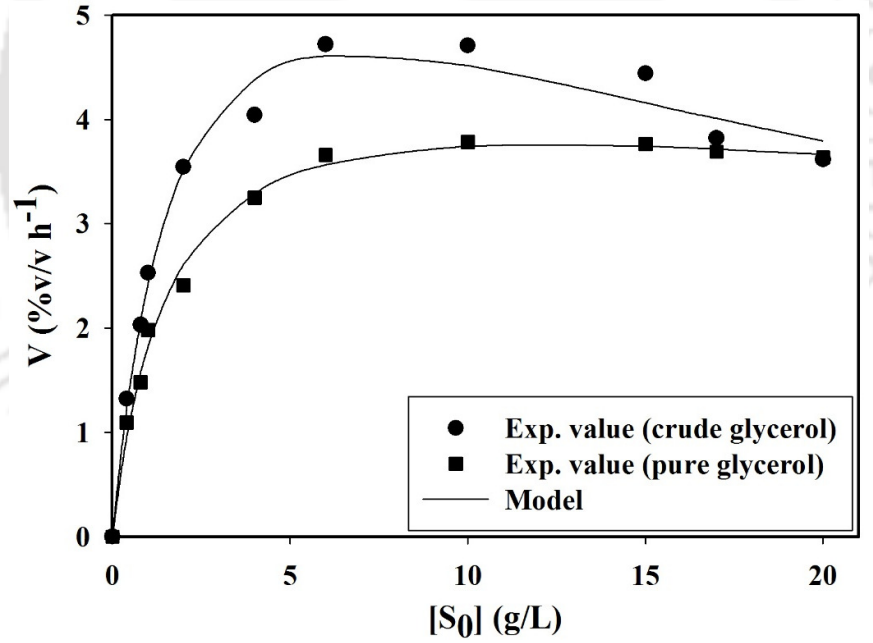

(B)

Figure 2.2. (A) Effect of initial concentration (g/L) of crude and pure glycerol on hydrogen content of product gas. (B) Results of fitting of Haldane substrate–inhibition model to data of initial reaction velocities at different initial concentrations of pure and crude glycerol as substrate.

2.2.6 Main experiments: Optimization using statistical experimental design

It may be inferred from literature review presented in Chapter 1, that fermentative hydrogen production is mainly influenced by temperature, initial pH and glycerol concentration of the fermentation broth (Wang et al., 2009). The main experiments of this study have been aimed at optimizing these variables through a statistical experimental design and its analysis. The protocol of the experiments was same as for the batch fermentation described in preceding section.

2.2.6.1 Experimental design

The optimization of variables influencing biohydrogen production was done by response surface methodology (RSM) with 3–factor CCD of experiments. CCD is commonly used to get insight into the interactions among individual variables while influencing the response (or target) variable. H_2 content (%v/v) of product gas from glycerol fermentation was chosen as the response variable, while temperature, initial pH and crude glycerol concentration of fermentation broth were chosen as three independent variables. These parameters were examined between two levels (listed in Table 2.1A), the range of which has been determined from the initial batch experiments. These variables were used at five coded levels (–α, –1, 0, +1, +α) in the CCD experimental design as described in Table 2.1B. The experimental design constituted 20 individual runs ($= 2^k + 2k + n_o$), where k is the number of independent variables, and n_o is the number of replicate runs at the center point of the variable. The exact experimental design with permutation–combination of levels of different parameters was generated using Minitab statistical software (Release 15.1, Trial Version).

Table 2.1. Details of Central Composite Design of experiments

(A) Factors and their levels used in central composite design matrix

Factors	Levels	
	Low (–α)	High (+α)
(X_1) – Temperature (°C)	30	42
(X_2) – Initial pH	5	8
(X_3) – Crude Glycerol (g/L)	1	10

(B)Central composite design matrix of fermentation parameters

Run order	Temperature (°C) (X_1)*	pH (X_2)*	Initial glycerol concentration (g/L) (X_3)*	% Hydrogen (v/v)	
				Experimental	Predicted
1	–1 (32.43)	–1 (5.61)	–1 (2.82)	16.01±0.707	15.70
2	+1 (39.56)	–1 (5.61)	–1 (2.82)	19.45±0.742	19.45
3	–1 (32.43)	+1 (7.39)	–1 (2.82)	23.91±0.799	23.35
4	+1 (39.56)	+1 (7.39)	–1 (2.82)	25.86±0.502	25.39
5	–1 (32.43)	–1 (5.61)	+1 (8.17)	25.35±0.353	25.55
6	+1 (39.56)	–1 (5.61)	+1 (8.17)	28.02±0.820	28.42
7	–1 (32.43)	+1 (7.39)	+1 (8.17)	29.45±0.629	29.02
8	+1 (39.56)	+1 (7.39)	+1 (8.17)	30.23±0.431	30.19
9	–α (30.00)	0 (6.50)	0 (5.50)	15.78±0.212	16.38
10	+α (42.00)	0 (6.50)	0 (5.50)	20.01±0.466	19.94
11	0 (36.00)	–α (5)	0 (5.50)	28.34±0.622	28.02
12	0 (36.00)	+α (8)	0 (5.50)	34.42±0.452	35.18
13	0 (36.00)	0 (6.50)	–α (1)	26.24±0.820	26.87
14	0 (36.00)	0 (6.50)	+α (10)	40.32±0.502	40.05
15	0 (36.00)	0 (6.50)	0 (5.50)	41.05±0.657	41.54
16	0 (36.00)	0 (6.50)	0 (5.50)	41.56±0.735	41.54
17	0 (36.00)	0 (6.50)	0 (5.50)	41.69±0.325	41.54
18	0 (36.00)	0 (6.50)	0 (5.50)	42.26±0.275	41.54
19	0 (36.00)	0 (6.5)	0 (5.5)	41.34±0.318	41.54
20	0 (36.00)	0 (6.5)	0 (5.5)	41.45±0.120	41.54

* Coded and actual (in parenthesis) values of the parameter

2.2.6.2 Statistical analysis and model fitting

The experimental data given in Table 2.1Bwas fitted to the following quadratic model containing coefficients corresponding to individual and interactive effects of parameters:

$$Y = \beta_0 + \sum_{i=1}^{k} \beta_i X_i + \sum_{i=1}^{k} \beta_{ii} X_i^2 + \sum_{i \neq j} \sum_{i} \beta_{ij} X_i X_j \quad (2.1)$$

Notation: Y – measured response variable (% Hydrogen), k – number of factors or medium components, β_o – intercept (or regression constant), β_i – linear coefficient, β_{ii} – quadratic coefficient, and β_{ij} – interaction coefficient. The coded values (x) of the actual experimental variables were determined using eq. 2.2:

$$X = (x_i - x_o)/\Delta x \quad (2.2)$$

where, i = 1, 2, 3…, X is the dimensionless value of the variables; x_o is the value of the variable x at center point and Δx is the step change. The significance of each parameter in fitted model was determined by signal to noise ratio and by the analysis of variance (ANOVA). The interactive effect of the process parameters was studied by plotting response surface plots and the corresponding contour plots.

2.2.6.3 Validation experiments

For the assessment of the accuracy of the optimum conditions predicted by the statistical analysis, crude glycerol fermentation experiments have been conducted using the parameters resulting from statistical analysis. Reproducibility of fermentation results was checked by performing all validation experiments in triplicate.

2.2.7 Experiments for kinetic and thermodynamic analysis

The kinetic analysis of the biohydrogen production through glycerol fermentation (in pure and crude form) was done by fitting the time profiles of substrate consumption to

Haldane kinetics model for different initial glycerol concentrations. The Haldane kinetic model is written as: $V_o = V_{\max}[S_o] \Big/ \left(K_m + [S_o] + [S_o]^2 / K_I\right)$, where: $V_{\max}$ – maximum reaction velocity or rate of product formation, K_m – Michaelis constant, K_I – inhibition constant, V_o – initial velocity of the reaction, $[S_o]$ – initial substrate concentration. For the kinetic analysis of biohydrogen production, glycerol fermentation experiments have been carried out using following initial glycerol concentrations: 0.4, 0.8, 1, 2, 4, 6, 10, 15, 17 and 20 g/L. The protocol for these experiments was same as for the batch fermentation described previously. The values of other parameters were fixed at their optimum as per the results of preliminary experiments with one–variable–at–a–time (OVAT) approach: Temperature = 37°C, mechanical shaking = 150 rpm, inoculum = 10% v/v, pH = 7. The initial velocity of the glycerol (in both pure and crude form) consumption was determined for different initial substrate concentrations and this data was used to determine kinetic/physiological parameters in the Haldane kinetic equation.

Thermodynamic analysis of the glycerol fermentation was done using Eyring equation compiled with Arrhenius equation. The Eyring equation is written as:

$$\ln\left(\frac{k}{T}\right) = \frac{-\Delta H}{RT} + \ln\frac{k_b}{h} + \frac{\Delta S}{R} \tag{2.3}$$

$$\Delta H = E_a - RT \tag{2.4}$$

$$\Delta G = \Delta H - T\Delta S \tag{2.5}$$

where: k – kinetic constant of reaction, R– universal gas constant (8.314 $JK^{-1}mol^{-1}$), T–temperature.k_b – Boltzmann constant (1.381×10^{-23} J K^{-1}), h – Planck's constant (6.626×10^{-34} J·s). The kinetic constant of reaction, k, can be obtained by fitting a suitable kinetic model to the time profile of substrate consumption. The values of k and E_a obtained from Arrhenius analysis can be substituted in above set of equations to yield thermodynamic

parameters, viz. ΔH (enthalpy change), ΔS (entropy change) and ΔG (Gibbs free energy change), associated with glycerol consumption for H_2 production. The activation energy of H_2 production with pure and crude glycerol as substrate was estimated using Arrhenius plots of *ln k* vs. 1/T based on Arrhenius equation: $k = Ae^{-E_a/RT}$. The Eyring plot of *ln* (k/T) vs $1/T$ reveals the thermodynamic parameters of ΔH and ΔS for glycerol fermentation. For thermodynamic analysis of biohydrogen production batch fermentation experiments were conducted at five temperatures, viz. 23°, 30°, 34°, 37° and 40°C. The protocols for these experiments have been described previously. The other parameters for fermentation were fixed at the global optimum values determined via CCD experiments: pH = 6.7, initial glycerol concentration = 7.4 g/L, inoculum = 10% (v/v) and mechanical shaking = 150 rpm. The time profiles of the substrate (either pure or crude glycerol) were fitted to pseudo 1st order kinetic model to determine the kinetic constants. These kinetic constants have been used to prepare the Arrhenius plots for determination of activation energy.

2.2.8 Analytical methods

Glycerol was quantified by HPLC analysis using a Rezex RCM Monosaccharide calcium–column (300 mm × 8 µm × 7.8 mm, Phenomenex, India) thermostated at 35°C with the help of external column oven (Model– HCO–02, PCI analytics Pvt. Ltd., India). The HPLC apparatus comprised of a pump (Series 200, Perkin Elmer), a refractive index detector (Series 200, Perkin Elmer) and a vacuum degasser (Series 200, Perkin Elmer). Ultra–pure water (18.2 MΩ·cm resistivity at 25°C) was used as the mobile phase at a flow rate of 0.5 mL/min. Reaction mixture samples were centrifuged (12000 rpm, 20 min) and filtered through a 0.2 µm membrane filter, and diluted appropriately prior to injection into HPLC. Standard calibration plots were used to determine residual concentration of glycerol in the samples of reaction mixture.

The composition of product gas of glycerol fermentation was determined using Gas Chromatograph (Make: Thermo scientific, Model: Ceres800 plus) with thermal conductivity detector (TCD) and Porapak Q (60/80 mesh) column employing argon as carrier gas at a flow rate of 30mL/min. The operational temperature at the column oven was 45°C and the injector and detector temperatures were maintained at 200°C. Gas samples were taken from the bottles and used to determine the contents of hydrogen and carbon dioxide. Hydrogen gas production was calculated from the headspace measurements and the total volume of gas produced for each time interval using the mass balance equation.

$$V_{H,i} = V_{H,i-1} + C_{H,i}(V_{G,i} - V_{G,i-1}) + V_H (C_{H,I} - C_{H,i-1}) \quad (2.6)$$

$V_{H,i}$ and $V_{H,i-1}$ are the cumulative hydrogen gas volumes at current (i) and previous time interval (i–1), respectively; $V_{G,i}$ and $V_{G,i-1}$ are total biogas volume at the current and previous time intervals; $C_{H,i}$ and $C_{H,i-1}$ are the fraction of hydrogen gas in the headspace at the current and previous time intervals; V_H is the volume of headspace of vials. The volume of product gas used for analysis was also taken into account during hydrogen mass balance.

2.3. RESULTS AND DISCUSSION

2.3.1 Optimization of process parameters

Fitting of the experimental data of response variable (i.e. % v/v H_2 content of product gas) to the quadratic regression model using coded values of independent variables listed in Table 2.1B yielded following equation:

$$Y = 40.897 + 1.097X_1 + 2.334X_2 + 3.917X_3 - 0.374X_1X_2 - 0.208X_1X_3 - 1.108X_2X_3 - 8.264X_1^2 - 3.514X_2^2 - 2.629X_3^2 \quad (2.7)$$

The values of the response variable predicted by the quadratic response model have also been given in Table 2.1B. It could be seen from Table 1B that experimental and model

predicted values of the response variable are in close agreement, which indicates the best fit of the model to experimental data. The statistical analysis of the quadratic response model is given in Table 2A that lists the coefficients of the model (given in eq. 2.1) along with their *p*– and *t*–values. Analysis of variance (ANOVA) of the quadratic model is given in Table 2.2B. ANOVA results show that regression model was highly significant ($p < 0.01$), while the lack of fit was not significant ($p > 0.05$). Coefficient of determination (R^2) was 0.998, which indicated that 99.8% variation in the response variable could be explained using the model. $R^2 = 0.998$ also indicated best fit of the model to the experimental data, which is also corroborated by close agreement of the experimental and model–predicted values of response variable.

The *t*–test, *F*–values and *p*–values of quadratic model coefficients indicate relative significance of corresponding independent variables. A large *t*–stat value and *p*–value < 0.05 indicates significance of the coefficient and the corresponding independent variable. Relative *F*–values of linear, interaction and quadratic coefficient indicate significance of the individual effects of independent variables and the magnitude of interaction between them. As per ANOVA results given in Table 2B, *F*–value of overall regression is 537.36, while *F*–value of linear coefficient is 285.95. *F*–value of 10.61 for interaction coefficients is much smaller than *F*–value for linear coefficients, which implies relatively standalone or unrelated effect of independent variables on the % v/v H_2 content of product gas. *p*–values of all linear and quadratic coefficients are < 0.05 with large absolute *t*–values, which indicates that all variables have significant effect on % v/v H_2 content of product gas. The *t*–values of interaction coefficients are relatively smaller than linear and square coefficients indicating their relative less significance. Moreover, *p*–values of interaction coefficients between temperature and pH; and temperature and initial glycerol concentration is > 0.05, which further confirms that the interaction between these variables

is insignificant or in other words, these variables have independent effect on the response variable. The *p*–value of the interaction coefficient between pH and initial glycerol concentration is < 0.05, which signifies that these variables have an inter–related effect on response variable. Relatively small *F*–value of 3.03 for The Lack of Fit with *p*–value of 0.124 implies that Lack of Fit is not significant as compared to the pure error, or in other words the model was significant.

Table 2.2. Results of central composite design for optimization of fermentation parameters

(A) The coefficients of quadratic regression model and their *t*– and *p*– values

Model term	Coefficient	*t*–value	*p*–value Prob >*F*
Intercept (A_0)	40.897	169.802	0.000*
Linear coefficients			
Temperature (X_1)	1.097	7.477	0.000*
pH (X_2)	2.334	14.885	0.000*
Glycerol (X_3)	3.917	24.091	0.000*
Square coefficients			
Temperature (X_1^2)	–8.264	–57.284	0.000*
pH (X_2^2)	–3.514	–23.114	0.000*
Glycerol (X_3^2)	–2.629	–16.532	0.000*
Interaction coefficients			
Temperature and pH ($X_1 \times X_2$)	–0.374	–2.066	0.066
Temperature and Glycerol ($X_1 \times X_3$)	–0.208	–1.071	0.309
pH and Glycerol ($X_2 \times X_3$)	–1.108	–5.140	0.000*

(B) ANOVA for quadratic model

Source	DF	SS	MS	*F*–value	*p*–value Prob >*F*
Regression	9	1622.99	180.33	537.36	0.000*
Linear	3	345.67	95.96	285.95	0.000*
Square	3	1266.63	422.21	1258.11	0.000*
Interaction	3	10.68	3.56	10.61	0.002*
Residual (Error)	10	3.36	0.34		
Lack of fit	5	2.52	0.50	3.03	0.124
Pure error	5	0.83	0.17		
Total	19	1626.34			

* Significant *p* values, $p \leq 0.05$; $R^2 = 0.998$; Predicted $R^2 = 0.987$; Adjusted $R^2 = 0.996$

(C) Analysis of the contour plots

Fixed parameter (Center point value)	Variable parameter #		H_2 (% v/v)#
Temperature = 36°C	pH = 6.69	Glycerol = 7.38 g/L	42.406
Initial pH = 6.5	Temp. = 36.2°C	Glycerol = 7.5 g/L	42.259
Glycerol = 5.5 g/L	Temp. = 36.2°C	pH = 6.79	41.070
Global optimum values of variable parameters: 1. Parameter actual (coded) values: Temperature = 36.18°C (0.72), pH = 6.7 (0.22), Glycerol conc. = 7.4 g/L (0.70); 2. H_2 conc. (% v/v): 42.54; 3. Regression coefficients: R^2 = 99.8%; R^2 (adj) = 99.6%			

Values of variable parameters corresponding to max. H_2 conc. for centre point value of third parameter

Figs. 2.3A, B, C show contour plots that reveal interactions among any two independent variables for the % v/v H_2 content of product gas. The contour plots (which essentially are graphical representation of regression eq. 2.7) represent infinitive number of combinations of two test variables, with the third variable maintained at its zero (or center point) level. Analysis of the contour plots is given in Table 2.2C. The shapes of response surface contours, whether elliptical, circular, or saddle point, explain the magnitude of interaction between independent variables (Tanyildizi et al., 2005; Ravikumar et al., 2005). For strong interactions among the variables, the contour plots have perfectly elliptical shape. The surface confined in the smallest contour represents parameter space for maximum value of response variable. A peculiar facet of the contour plots shown in Fig. 2.3is that each of these plots has a clear highest point, which means that the maximum hydrogen production could be achieved inside the design boundary. The contour plots in Figs. 2.3A (temperature vs. initial pH) and2.3B (temperature vs. initial glycerol conc.) have circular shape, which points to relatively individual effect (or insignificant interactions) between the parameters. This is also corroborated by *p*–value > 0.05 for the interaction coefficients for these variables, as noted earlier. On the other hand, the contour plot between pH and glycerol shown in Fig. 2.3C has elliptical shape, which reveals significance of interaction between these variables. This result is also corroborated by the ANOVA results, i.e. *p*–value < 0.05 for the interaction coefficient of glycerol and pH. The parameter space corresponding to maximum % v/v H_2 for any two variables (with value of the third variable held at its center point) is given in Table 2.2C. Values of all independent variables corresponding to global optimum of maximum % v/v H_2 content of product gas are also listed in Table 2.2C. In the given range of optimization parameters, the highest H_2 content of 42.54% v/v in product gas is obtained for crude glycerol concentration = 7.4 g/L, pH = 6.7 and temperature = 36.18^{o}C.

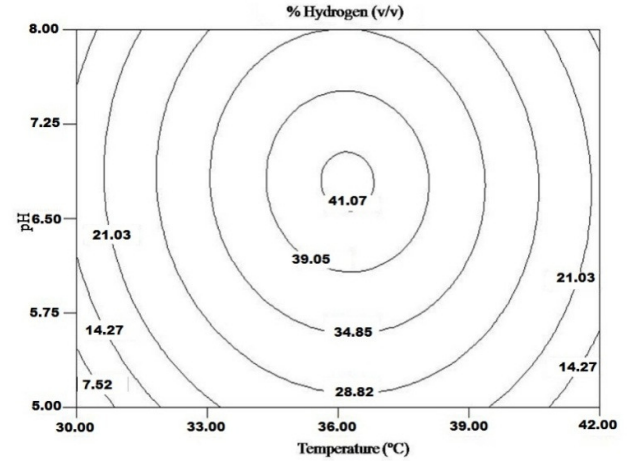

(A)

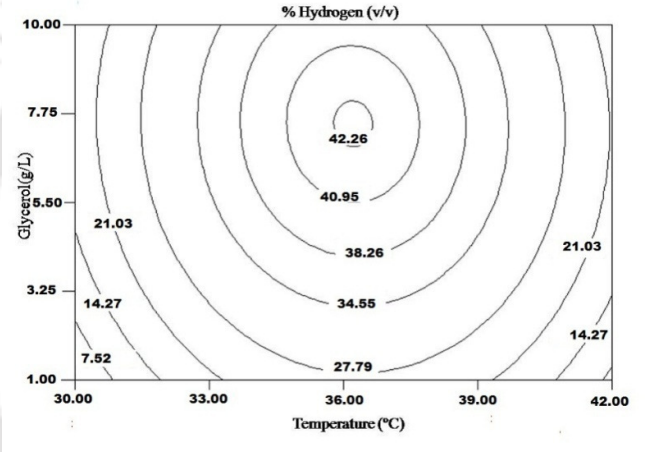

(B)

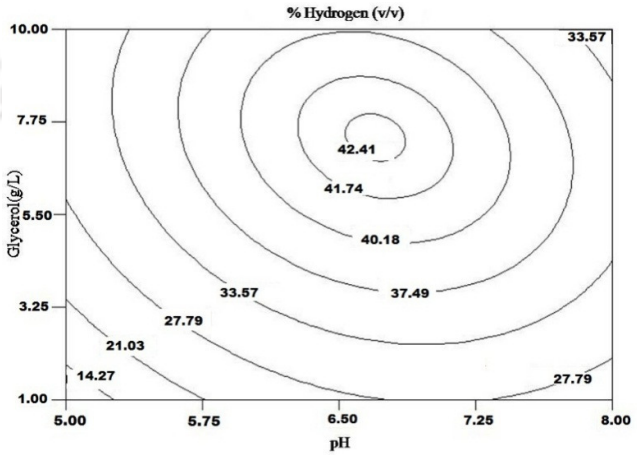

(C)

Figure 2.3. Cotour plots for interactive effects of different parameters on hydrogen content of product gas. (A) temperature and initial pH (B) temperature and crude glycerol (C) initial pH and crude glycerol

It is noteworthy that optimum values of temperature and initial pH for maximum H_2 content of product gas with crude glycerol as substrate are very similar to those for other substrates such as palm oil effluent (Chong et al., 2009) and glucose (Ghosh et al., 2010; Mullai et al., 2013). However, as seen from literature summary in Table 1 from Chapter 1, the optimum crude glycerol concentration in our study (7.4 g/L) is much smaller than the optimum pure glycerol concentration of 15 to 20 g/L reported by previous authors (Kumar et al., 2015; Jitrwung et al., 2011; Sittijunda et al., 2012).

2.3.2 Validation experiments

Optimum conditions of maximum H_2 content in product gas predicted by the CCD experiments and RSM analysis have been corroborated by validation experiments of crude glycerol fermentation. The validation experiments were conducted in triplicate to ascertain reproducibility of results. Batch fermentations were carried out under strict anaerobic conditions at initial pH = 6.7, temperature = 36°C and crude glycerol concentration = 7.4 g/L. The time profiles of glycerol consumption, H_2 and CO_2 production in the validation experiment have been depicted in Fig. 2.4and the summary of the results is given in Table 2.3that lists the cumulative total volume of the product gas, molar yield of hydrogen and the hydrogen production rate. The time profile of biomass or microbial cell concentration in the fermentation mixture is also shown in Fig.2.4. As noted earlier, the metabolic pathway of glycerol fermentation comprises of two phase, viz. acidogenesis and solventogenesis. The acidogenesis phase is essentially hypothesized to be the growth-associated process, while solventogenesis occurs during the stationary phase. H_2 and CO_2

are the side products of the acidogenesis (or acid formation) phase as described by following equations:

$$\underset{\text{Glycerol}}{C_3H_8O_3} + H_2O \longrightarrow \underset{\text{Acetic acid}}{CH_3COOH} + CO_2 + 3H_2 \quad (2.8)$$

$$2\,\underset{\text{Glycerol}}{C_3H_8O_3} \longrightarrow \underset{\text{Butyric acid}}{CH_3CH_2CH_2COOH} + 2CO_2 + 4H_2 \quad (2.9)$$

Table2.3. Results of validation experiment

Time (h)	Glycerol consumption (g/L)	% H_2 in product gas (v/v)	Volume of total gas (mL)	Cumulative H_2 (mL)	H_2 yield (mole H_2/mole glycerol)	H_2 production rate (mmol H_2/L·h)
3	2.38	7.50 (± 1.10)	15(±3)	5.63	0.192	1.54
6	3.24	13.59 (± 1.01)	35(±4)	11.99	0.295	1.64
12	5.31	43.07 (± 0.96)	55(±6)	37.06	0.552	2.57
15	5.87	44.02 (± 1.00)	76(±4)	47.42	0.627	2.59

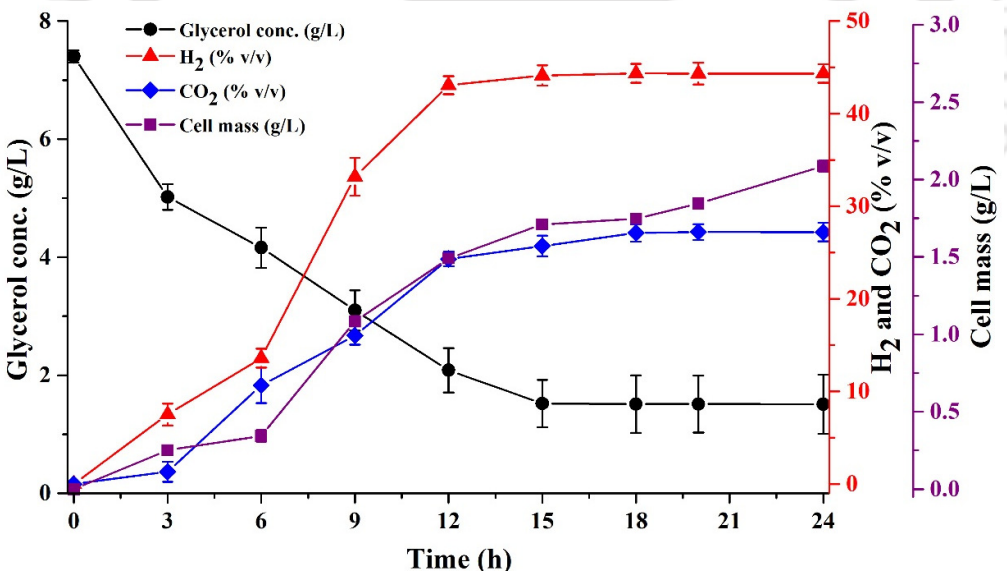

Figure 2.4. Results of validation experiments: Time profiles of substrate consumption (crude glycerol), microbial cell concentration (g/L), H_2 and CO_2 concentration (% v/v) in product gas. Fermentation parameters: initial glycerol concentration = 7.4 g/L, temperature = 36°C, initial pH = 6.7, and mechanical shaking = 150 rpm.

The time profiles of H_2, CO_2 and biomass concentrations in the fermentation broth, as shown in Fig. 2.4, have proportionate variations. These results essentially corroborate the hypothesis that acidogenesis phase (leading to formation of H_2 and CO_2) is a growth associated process.

In these experiments, maximum H_2 content of 44.05 ± 0.43% v/v was obtained in the gaseous phase, which corresponded to yield of 0.627 moles H_2/ moles of glycerol. The experimentally obtained hydrogen concentration in gas phase was in close agreement to the model predicted value of 42.54% v/v, which confirms the validity of statistical model used in this study. Comparing this result with literature summary in Table 1.5 from Chapter 1, reveals that optimum H_2 concentration in product gas obtained in present study is higher than most of the previously reported values with either pure or crude glycerol as substrate.

2.3.3 Kinetic and thermodynamic parameters

The results of the kinetic analysis of biohydrogen production from pure and crude glycerol are given in Fig. 2.2B and Table 2.4A. Fig. 2.2B depicts the trends in initial reaction velocity with initial glycerol concentration. Table 2.4A lists the values of the kinetic parameters obtained after fitting of Haldane substrate–inhibition model to the data of initial reaction velocity (V_o) versus initial substrate concentration ([S_o]). Fig. 2.2B also shows the Haldane kinetic model predicted trends of V_o versus S_o. It could be inferred fromFig. 2.2B that the experimental and model predicted trends match well. It could be inferred from Table 2.4A that the reaction velocity for crude glycerol as substrate is significantly higher than pure glycerol. The Michaelis constant K_m increases marginally for crude glycerol indicating reduction in enzyme-substrate activity. Moreover, the inhibition constant K_I shows marked reduction for crude glycerol, which indicates enhanced susceptibility of the cells to substrate inhibition at much lower concentrations.

The trends in K_m and K_I with pure and crude glycerol as substrate are attributed to the impurities in glycerol that reduce substrate affinity and enhance substrate inhibition. The increase in V_{max} is however attributed to the alkali contamination, as discussed in greater details subsequently. Figs. 2.6A and B show the plots of pseudo 1st order kinetic model fitted to the time profiles of substrate consumption during fermentation of pure and crude glycerol at five temperatures, viz. 23°, 30°, 34°, 37°, 40°C. The regression coefficients of these plots indicate that the model fits well for both pure and crude glycerol fermentation. It could be inferred from Table 2.4B that the kinetic constants are higher for crude glycerol for all temperatures of fermentation, which is in concurrence with the results of Haldane kinetic model. The results of the kinetic and thermodynamic analysis (i.e. the Arrhenius and Eyring plots) for pure and crude glycerol are presented in Figs. 2.6A and B, and 2.6C and D, respectively, and the summary of the results is given in Table 2.4C that lists the values of activation energy and thermodynamic parameters of enthalpy, entropy and Gibbs energy change associated with glycerol bioconversion. The kinetic constant used in the pseudo 1st order model is Arrhenius type: $k = A\exp(-E_a/RT)$, where A is the pre–exponential or frequency factor, while E_a is the activation energy (or activation enthalpy).

Table 2.4. Results of kinetic and thermodynamic analysis of hydrogen production by *C. pasteurianum*

(A) Haldane kinetic parameters

Substrate	V_{max} (%v/v·h^{-1})	K_m (g/L)	K_I (g/L)	SSD
Pure glycerol	4.74	1.59	93.87	0.11
Crude glycerol	7.20	1.93	24.93	0.33

(B) Kinetic constants

Substrate	Pseudo 1st order kinetic constants at different temperatures (k, s^{-1})				
	23°C	30°C	34°C	37°C	40°C
Pure Glycerol	0.28×10^{-6}	6.11×10^{-6}	2.89×10^{-5}	2.39×10^{-5}	1.78×10^{-5}
Crude Glycerol	1.39×10^{-6}	9.17×10^{-6}	3.39×10^{-5}	3.03×10^{-5}	2.61×10^{-5}

(C) Thermodynamic parameters

Substrate	Process	E_a (absolute) kJ·mol^{-1}·K^{-1}	ΔH kJ·mol^{-1}	ΔS kJ·mol^{-1}·K^{-1}	ΔG kJ·mol^{-1}
Pure glycerol	Fermentation	320.23	317.73	0.703	105.46
	Thermal deactivation	64.59	–67.14	–0.550	103.50
Crude glycerol	Fermentation	217.18	214.68	0.368	103.58
	Thermal deactivation	34.69	–37.27	–0.452	102.85

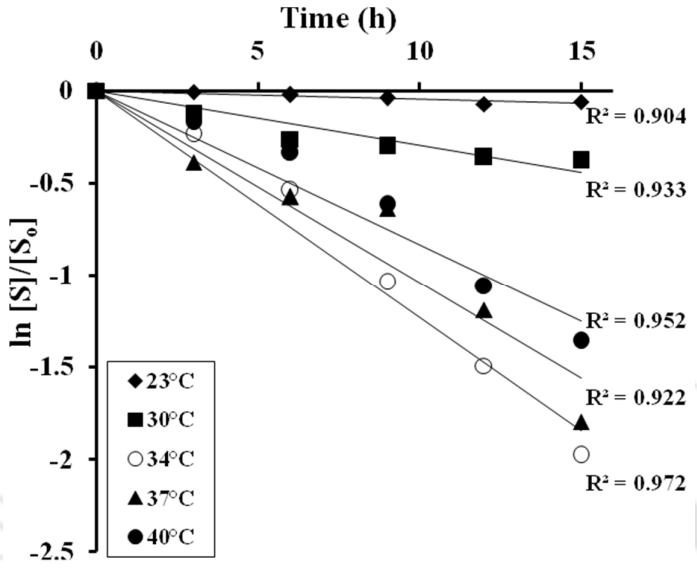

(A)

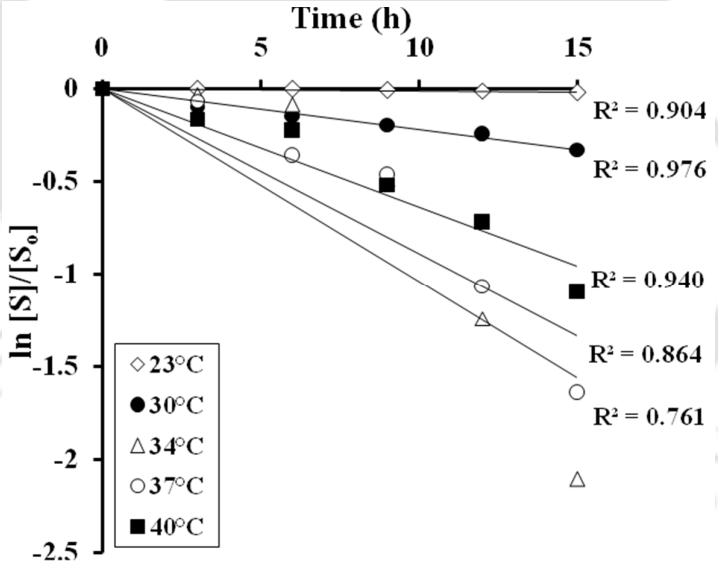

(B)

Figure 2.5. Fitting of the pseudo 1st order kinetic model to the time profiles of substrate consumption during glycerol fermentation at different temperatures. (A) Pure glycerol, (B) Crude glycerol

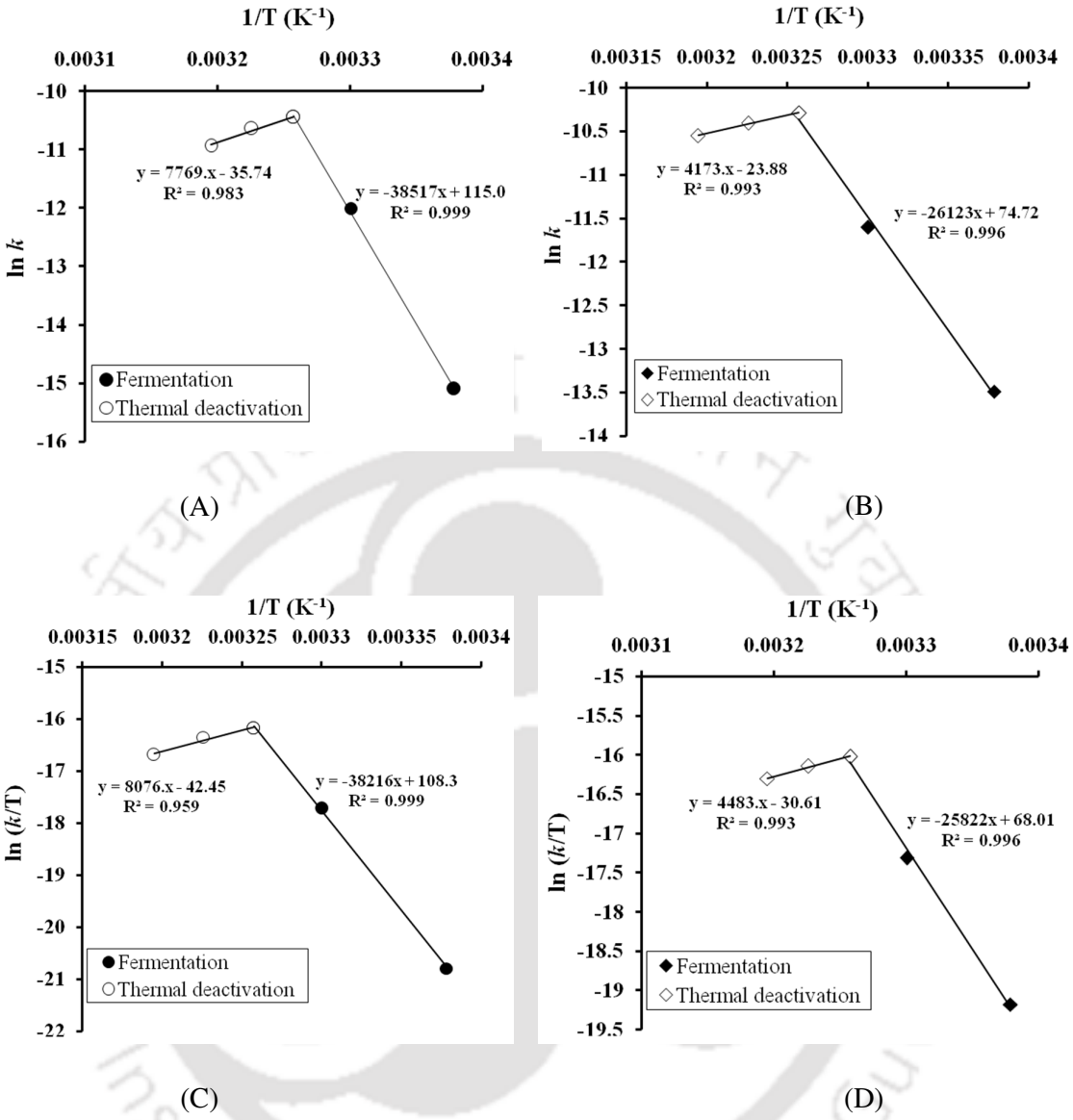

Figure 2.6. Kinetic and thermodynamic analysis of biohydrogen production. Arrhenius plots: (A) pure glycerol as substrate, (B)crude glycerol as substrate; Eyring plots: (C) pure glycerol as substrate, (D)crude glycerol as substrate.

The Arrhenius kinetic constant is based on the hypothesis that reactant molecules are in a state of random (Brownian) motion, and the collisions among them lead to reaction and formation of products. The minimum energy required to be associated with the collision in order to reach the transition state (before formation of the product) is essentially the activation energy. The frequency and amplitude of the random motion of reactants, and the energy associated with intermolecular collisions rises with temperature, hence the Arrhenius kinetic constant is also expected to rise with temperature.

However, some of the results shown in Fig. 2.6 and Table 2.4B and C depict an incongruent trend. For the temperature range between 23°–34°C, the kinetic constant of glycerol conversion increases with temperature, while for the temperature range 34°–40°C, the kinetic constant reduces with temperature. This trend is consistent for both pure and crude glycerol. The Arrhenius parameters of pre–exponential factor and activation energy have been determined using the Arrhenius plots of ln k vs. $1/T$. The slope of this plot ($-E_a/RT$) gives the activation energy. Fig. 7A and B depicts the Arrhenius plot for pure and crude glycerol fermentation. It could be seen that the slope of the Arrhenius plot is negative (indicating positive activation energy) in the temperature range of 23°–34°C due to rise in kinetic constant with temperature. However, for the temperature range of 34°–40°C, the slope of Arrhenius plot is positive (indicating negative activation energy) due to reduction in kinetic constant with increase in temperature. Reduction in kinetic constant with increasing temperature, which is an aberration of the Arrhenius hypothesis, essentially is a consequence of denaturation of the enzymes in glycerol metabolism at higher temperatures. Such observation has also been reported by Fabiano and Perego (2002) for biohydrogen production using starch hydrolyzate as substrate. Thus, the

absolute value of activation energy in the temperature of range of 34°–40°C corresponds to the activation energy of thermal deactivation or denaturation of the intracellular enzymes.

On the basis of these results, we have defined two regimes for thermodynamic analysis, viz. fermentation regime (in the range of 23°–34°C) and deactivation regime (in the range of 34°–40°C). Figs. 2.7C and D show the Eyring plot for pure and crude glycerol in the two regimes. E_a for crude glycerol for fermentation regime is significantly lower than pure glycerol, which indicates easier and faster reactivity requiring lesser energy input. The values of thermodynamic parameters also corroborate this conclusion. Crude glycerol has lesser ΔH and ΔG values than pure glycerol indicating smaller energy input required for bioconversion. The positive values of ΔS (entropy change) for biohydrogen production from both pure and crude glycerol is indicative of marginal rise in the randomness of the tertiary structure of enzyme during formation of enzyme–substrate complex (or formation of the activated or transition state) during the reaction. E_a and ΔG values for crude glycerol in the thermal deactivation regime are higher than pure glycerol. These values indicate greater resistance and stability of the intracellular enzymes towards deactivation with crude glycerol as substrate. ΔH and ΔS in the thermal deactivation regime are negative for both pure and crude glycerol, which indicates disruption of the secondary structure of the enzyme and the concurrent reduction in the tendency for enzyme-substrate complex formation.

2.3.4 Analysis

The results of statistical optimization, in addition to comparative analysis of the kinetic and thermodynamic parameters for pure and crude glycerol fermentation, provide an insight into the biomechanics of the hydrogen production. A peculiar result of present

study is higher yield of hydrogen using crude glycerol as compared to pure glycerol. This result has also been reported in previous studies by (Lo et al., 2013; Mangayil et al., 2015). This result is quite a typical, as one would expect the impurities in crude glycerol to inhibit the fermentation leading to lower yields of biohydrogen. Indeed, lowering of the yield of other fermentation products such as 1,3– propanediol and butanol using *Clostridium pasteurianum* due to impurities present in crude glycerol has been reported in previous studies (Venkataramanan et al., 2012; Khanna et al., 2012; Khanna et al., 2013). The main impurities in crude glycerol are short chain alcohols (usually methanol or ethanol), alkali (NaOH/KOH), inorganic salts ($NaCl/Na_2SO_4/KCl/K_2SO_4$ etc.) and unsaturated fatty acids. Each of these impurities has effect on growth and metabolism of *Clostridia*. Previous studies have investigated the effect of impurities in glycerol on fermentation (in terms of yield/selectivity of products) using different microbial cultures (Venkataramanan et al., 2012; Xiaolong et al., 2006; Cao et al., 2009; Khanna et al., 2011; Chatzifragkou et al., 2012;). In the context of present study, the influence of various impurities on hydrogen production vis–à–vis their concentrations in crude glycerol is discussed below:

Alcohols and unsaturated fatty acids: Alcohols are known to enhance the fluidity of the membrane. Ingram et al. (1976) has reported that bacterial membrane fluidity is significantly affected by alcohol only for concentrations ≥ 1% w/v. In the present study, the concentration of alcohol in glycerol is 2.6 g/L (or 0.26% w/v), which is far lower than the limit reported (Ingram et al., 1976). Hence, influence of alcohol impurity on glycerol metabolism is expected to be minimal. Venkataramanan et al. (2012), have given an account of the effect of fatty acids on growth/ metabolism of *Clostridia*. As a result, the diffusive mass transfer is affected. More unsaturated fatty acids containing two or more double bonds create hindrance to mass transfer of nutrients and metabolites through the membrane leading to inhibitory effect. In the context of present study, however, the

adverse effect of fatty acids is expected to be minimal, as the substrate used for transesterification was refined soybean oil, with very little content of fatty acids.

Alkali metals, salts and ions: Monovalent salts can cause swelling of the cell membrane due to weakening of Vander Waal's forces between lipid tails of the membrane. This affects the energy barrier within lipid bilayer of the cells, which results in obstruction of substrate transport across the membrane. In the present study, the probability of formation of metal salts is rather miniscule due to pure version of the chemicals used.

The alkali contamination in glycerol is a source of sodium ions, which have marked effect on biohydrogen production, as reported by previous studies. Cao and Zhao (2009) have reported enhancement in hydrogen concentration and yield in anaerobic fermentation of food waste in presence of sodium ions. Typically, sodium ion concentrations below 14 g/L promoted biohydrogen synthesis. Cao and Zhao (2009) have proposed that sodium can build a Na–K–ATP enzyme pump to transfer nutrients and substrates such as glucose or glycerol to the intracellular region to improve the bioreactions leading to biohydrogen production. This is manifested in terms of reduction in activation energy, increase in V_{max} and 1st order kinetic constant. Impurities in crude glycerol, however, may affect the intracellular enzymes in glycerol metabolism making them more susceptible to inhibition, which is reflected in terms of reduction in K_I. The inhibition substrate concentration (24.93 g/L) predicted by the Haldane kinetic model for crude glycerol is significantly higher than the optimum concentration (7.4 g/L) predicted by the CCD experimental design, and hence, substrate inhibition effect is expected to be minimal for crude glycerol fermentation at optimum conditions.

Xiaolong et al. (2006) have studied effect of sodium ion concentration on hydrogen production from sucrose. The optimum sodium ion concentration reported by Xiaolong et al. (2006) is in the range of 1–2 g/L. Xiaolong et al. (2006) have also reported marked

reduction in hydrogen production for Na^+ concentrations above 4 g/L. This reduction is attributed to adverse effect of high Na^+ concentration on microbial enzyme activities such as dehydrogenase activity, alkaline phosphatase and adenosine tri phosphate. Khanna et al. (2011) have assessed the effect of sodium ions on hydrogen production. Sodium ion concentration up to 250 mM has been found to be beneficial for metabolism and growth of hydrogen producing bacteria. The maximum Na^+ concentration in fermentation mixture in present study is 35.2 mM, which is below the limit of 250 mM given by Cao and Zhao (2009) and Khanna et al. (2011). The Na^+ ions contributed by alkali in crude glycerol can help enhance biohydrogen production, as compared to pure glycerol.

2.3.5 Confirmation of hypothesis of Na^+–induced enhancement

The beneficial effect of Na^+ ions on enhancing the transfer of substrate and nutrients to intracellular regions was confirmed with additional batch experiments on fermentation of pure glycerol supplemented with externally added Na^+ ions. The procedure followed in these experiments was similar as described in section 2.2.4except that the concentration of NaCl in the BSH medium was varied. Batch experiments have been conducted in 100 mL serum bottles containing BSH medium supplemented with pure glycerol (7.4 g/L), peptone (2 g/L), yeast extract (1 g/L), K_2HPO_4 (0.23 g/L), KH_2PO_4 (4.04 g/L), trace element solution (10 mL/L medium). The fermentation medium was also supplemented with known quantities of Na^+ ions in the form of NaCl salt in the range of 0 to 6 g/L. The trends in the H_2 content (% v/v) of fermentation gas in these experiments are shown in Fig. 2.7. The hydrogen content of gas resulting from fermentation of pure glycerol (without addition of NaCl) was negligible. However, with addition of NaCl, the H_2 content of product gas showed marked enhancement. As seen from Fig. 2.7, the % v/v H_2 content of product gas increased till 1.25 g/L NaCl in fermentation medium, and gradually decreased thereafter till 6 g/L NaCl. The highest H_2 concentration of 40.38% v/v

in the product gas was obtained for 1.25 g/L NaCl, which corresponds to Na^+ concentration of 21.3 mM. These experiments essentially corroborate the hypothesis of enhancement of crude glycerol fermentation by Na^+ ions.

The role of alkali metal ions in enhancing fermentation of crude glycerol was further ascertained by external addition of K^+ ions in the form of KCl to the fermentation mixture. The BSH medium used in these experiments had same composition as mentioned in section 2.2.4. Thus, the medium already contained 2 g/L NaCl. Other parameters for fermentation were as follows: glycerol = 7.4 g/L, pH = 6.7, temperature = 36°C. The concentration of KCl in the fermentation medium was varied in the range of 0 to 6 g/L. The experimental results presented in Fig. 2.7reveal that H_2 production enhanced only marginally (≈ 10%) with addition of K^+ ions.

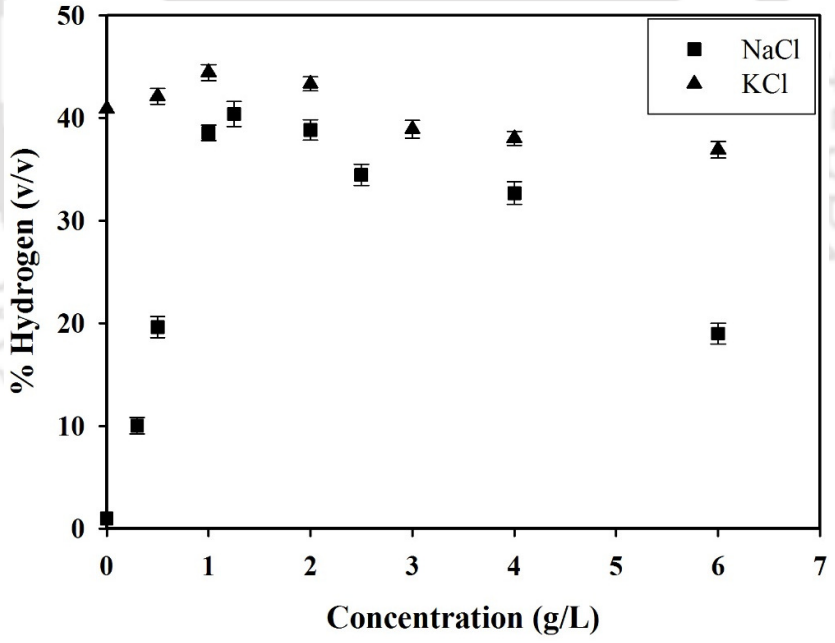

Figure 2.7. Effect of external addition of sodium (Na^+) and potassium ions (K^+) in pure glycerol on biohydrogen production.

The highest H_2 content of 44.43% v/v in the product gas has been obtained for KCl concentration of 1 g/L which corresponds to K^+ ion concentration of 13.41 mM.

2.3.6 Comparative analysis with literature

Table 1.5 presents comparative accounts of the results of the present study with the earlier literature on bioconversion of pure and crude glycerol. A direct quantitative comparison of the results of different studies is difficult due to wide variation in fermentation conditions, mode of fermentation, type of microbial cultures employed etc. However, comparing among batch processes, the biohydrogen yield of 0.627mol H_2/ mol glycerol obtained in the present study is higher than several previous studies (Liu et al., 2007; Poleto et al., 2016; Sittijunda et al., 2012). With further optimization of operating conditions and use of either fed–batch or continuous mode of fermentation, the biohydrogen yield is expected to improve further. For the comparative analysis of the kinetic and thermodynamic parameters of crude glycerol fermentation determined in present study, there is a limitation. To the best of our knowledge, there is no previous study on kinetic and thermodynamic analysis of fermentative biohydrogen production by *Clostridium pasteurianam* with pure or crude glycerol as substrate. Therefore, we are unable to present comparative accounts of our results with published literature.

2.4. CONCLUSIONS

Potential of crude glycerol (originating as side-product of biodiesel industry) as fermentation substrate for biohydrogen production has been reported in previous literature. The kinetic and thermodynamic analysis of biohydrogen production presented in this study has given quantitative substantiation of this proposition. Under statistically optimized conditions of pH, initial substrate concentration and temperature, crude glycerol fermentation gives biohydrogen yield of 0.627 mol H_2/mol glycerol with H_2 content of 44% v/v in product gas. The parameters of Haldane substrate inhibition model show

significant enhancement in reaction velocity (albeit with increased susceptibility for substrate inhibition) for crude glycerol fermentation as compared to pure glycerol. Thermodynamic parameters of activation energy and Gibbs energy change also confirm potential of crude glycerol for less energy intensive biohydrogen production. Both activation energy and Gibbs energy change for crude glycerol fermentation (viz. 217.18 kJ/mol and 103.58 kJ/mol, respectively) are smaller than those for pure glycerol. This study has also highlighted some important mechanistic aspects of biohydrogen production from crude glycerol. Beneficial effect of Na^+ ions on crude glycerol fermentation has been experimentally demonstrated, as Na^+ ions work towards faster trans–membrane transport of nutrients and substrate to intracellular region, which essentially improves enzymatic reactions in glycerol metabolism resulting in higher hydrogen production. We believe that the insights into biohydrogen production from fermentation of crude glycerol obtained in the present study will give crucial inputs for further research in this area.

References

Chatzifragkou, A., Papanikolaou, S., 2012. Effect of impurities in biodiesel–derived waste glycerol on the performance and feasibility of biotechnological processes. Appl. Microbial. Biotechnol. 95, 13–27.

Cao, X., Zhao, Y., 2009. The influence of sodium on biohydrogen production from food waste by anaerobic fermentation. J. Mater. Cycles Waste Manag. 11, 244–250.

Chen, W.M., Tseng, Z.J., Lee, K.S., Chang, J.S.,2005. Fermentativehydrogen production with *Clostridium butyricum* CGSS isolated from anaerobic sewage sludge. Int J HydrogenEnerg.30, 1063-1070.

Chong, M.L., Rahman, N.A.A., Rahim, R.A., Aziz, S.A., Shirai, Y., Hassan, M.A.,2009. Optimization of biohydrogen production by *Clostridium butyricum* EB6 from palm

oil mill effluent using response surface methodology. Int. J. Hydrogen Energ. 34, 7475–7482.

Fabiano, B., Pergo, P.,2002. Thermodynamic study and optimization of hydrogen production by *Enterobacter aerogenes*. Int. J. Hydrogen Energ. 27, 149–156.

Ghosh, D., Hallenbeck, P.C.,2010. Response surface methodology for process parameter optimization of hydrogen yield by the metabolically engineered strain *Escherichia coli* DJT135. Bioresour. Technol. 101, 1820–1825.

Ingram, L.O., 1976. Adaptation of membrane lipids to alcohols. J. Bacteriol.125, 670–678.

Jitrwung, R., Yargeau, V., 2011. Optimization of media composition for the production of biohydrogen from waste glycerol. Int. J. Hydrogen Energ. 36, 9602–9611.

Junghare, M., Subudhi, S., Lal., B. 2012. Improvement of hydrogen production under decreased partialpressure by newly isolated alkaline tolerant anaerobe,*Clostridium butyricum* TM-9A: Optimization of processparameters. Int J Hydrogen Energ. 37, 3160-3168.

Khanna, N., Kotay, S.M., Gilbert, J.J., Das, D., 2011. Improvement of biohydrogen production by *Enterobacter cloacae* IIT–BT 08 under regulated pH. J. Biotechnol. 152, 9–15.

Khanna, S., Goyal, A., Moholkar, V.S.,2012. Bioconversion of biodiesel derived crude glycerol by immobilized *Clostridium pasteurianum*: Effect of temperature. Int. J. Chem. Biol. Eng. 6, 301–304.

Khanna, S, Goyal, A., Moholkar, V.S.,2013a. Effect of fermentation parameters on bio–alcohols production from glycerol using immobilized *Clostridium pasteurianum*: an optimization study. Prep. Biochem. Biotechnol. 43, 828–847.

Khanna, S., Goyal, A., Moholkar, V.S.,2013b. Production of n–butanol from biodiesel derived crude glycerol using *Clostridium pasteurianum* immobilized on amberlite.

Fuel. 112, 557–561.

Kumar, P., Sharma, R., Ray, S., Mehariya, S., Patel, S.K., Lee, J.K., 2015.Dark fermentative bioconversion of glycerol to hydrogen by *Bacillus thuringiensis*. Bioresour. Technol. 82, 383–388.

Liu, F., Fang, B., 2007. Optimization of biohydrogen from biodiesel wastes by *Klebsiella pneumonia*. Biotechnol. J. 2, 374–380.

Lo, Y.C., Chen, X.J., Yuan, Y., Chang, J.S., 2013. Dark fermentative hydrogen production with crudeglycerol from biodiesel industry using indigenous hydrogen producing bacteria. Int. J. Hydrogen Energ. 38, 15815–15822.

Mangayil, R., Aho, T., Karp, M., Santala, V.,2015. Improved bioconversion of crude glycerol to hydrogen by statistical optimization of media components. Renew. Energ. 75, 583–589.

Mullai, P., Yogeswari, M.K., Sridevi, K., 2013. Optimization and enhancement of biohydrogen production using nickel nanoparticles – A novel approach. Bioresour. Technol. 141, 212–219.

Poleto, L., Souza, P., Magrini, F.E., Beal, L.L., Torres, A.P.R., Sousa, M.P., Laurino, J.P., Paesi, S., 2016. Selection and identification of microorganisms present in the treatment of wastewater and activated sludge to produce biohydrogen from glycerol. Int. J. Hydrogen Energ. 41, 4374–4381.

Ravikumar, K., Pakshirajan, K., Swaminathan, T., Balu, K., 2005. Optimization of batch process parameters using response surface methodology for dye removal by a novel adsorbent. Chem. Eng. J. 105, 131–138.

Sarma, S.J., Brar, S.K., Sydney, E.B., Bihan, Y.L., Buelna, G., Soccol, C.R., 2012. Microbial biohydrogen production by bioconversion of crude glycerol: A review. Int. J. Hydrogen Energ. 37, 6473–6490.

Sittijunda, S., Reungsang, A., 2012. Biohydrogen production from waste glycerol and sludge by anaerobic mixed cultures. Int. J. Hydrogen Energ. 37, 13789–13796.

Tanyildizi, M.S., Ozer, D., Elibol, M., 2005. Optimization of α–amylase production by *Bacillus sp.* using response surface methodology. Process. Biochem. 40, 2291–2296.

Venkataramanan, K.P., Boatma, J.J., Kurniawan, Y., Taconi, K.A., Bothun, G.D., Scholz, C., 2012. Impact of impurities in biodiesel–derived crude glycerol on the fermentation by *Clostridium pasteurianum* ATCC 6013. Appl. Microbiol. Biotechnol. 93, 1325–1335.

Xiaolong, H., Minghua, Z., Hanqing, Y., Qinqin, S., Lecheng, L., 2006. Effect of sodium ion concentration on hydrogen production from sucrose by anaerobic hydrogen–producing granular sludge. Chinese J. Chem. Eng. 14, 511–517.

Wang, J., Wan, W., 2008. Optimization of fermentative hydrogen production process by response surface methodology. Int. J. Hydrogen Energ. 33, 6976–6984.

Wang, J., Wan, W., 2009. Factors influencing fermentive hydrogen production: a review. Int. J. Hydrogen Energ. 34, 799–811.

Chapter 3

Metabolic Flux Network analysis of Hydrogen Production from Crude Glycerol by *Clostridium pasteurianum*

3.1 INTRODUCTION

Fermentation processes are limited by slow kinetics. The kinetics of fermentation can be boosted by optimization of the process conditions (such as pH, temperature, agitation rate etc.) or by use of recombinant or genetically engineered microbial cultures (Mu et al., 2009; Wang et al., 2008; Liu et al., 2008; Morimoto et al., 2005). Another effective means of enhancing the fermentation kinetics is application of ultrasound irradiation or sonication to fermentation mixture. Ultrasound and cavitation make energy available on extremely small temporal and spatial scales (Moholkar and Warmoskerken, 2003).The physical and chemical effects of ultrasound can boost fermentation kinetics through enhancement of cellular transport and inducing conformational changes in secondary structure of enzymes (Singh et al., 2015a, 2015b; Bhasarkar et al., 2015a,

2015b; Borah et al., 2016). In our previous work, we have demonstrated effective use of ultrasound in boosting glycerol fermentation to butanol and 1,3–propanediol (Khanna et al., 2012b, 2013c). The metabolic pathway of glycerol bioconversion by *Clostridium sp.* is well established and is depicted in Fig. 3.1. Glycerol metabolism has two phases, viz. acidogenesis and solventogenesis. The initials steps in glycerol bioconversion are formation of dihydroxyacetone (DHA) by enzyme glycerol dehydrogenase with further conversion of DHA to DHA phosphate and finally to pyruvate. Conversion of pyruvate yields lactic acid or acetyl–CoA and CO_2through pyruvate–ferredoxin (Fd) oxidoreductase, which occurs simultaneously with reduction of ferredoxin (Fd). Reduction of Fd by enzyme hydrogenase results in formation of H_2. The end products of acetyl–CoA conversion are acetic and butyric acid. Thus, the H_2 production is associated with formation of end products like acetate, butyrate and lactate. The actual H_2 yield from glycerol fermentation is, however, lesser than theoretical yield. This result is essentially attributed to formation of lactate and other solvent products. Thus, in order to achieve high H_2 yield, degree of engagement of various pathways in overall cellular functions and metabolic processes needs to be properly studied. In other words, quantification of the magnitude of pathway fluxes *in vivo* is essential for maximizing production of the valuable metabolites. The intracellular metabolic fluxes can be estimated using stoichiometric reaction models and mass balances for the metabolites. Metabolic flux analysis (MFA) is an useful methodology for determination of the fluxes in metabolic pathways. MFA is also an effective tool for understanding cell physiology and regulation of metabolism in different microorganisms (Ahrens et al., 1997; Cirana et al., 2004; Hadicke et al., 2011; Mathews et al., 2009). To the best of our knowledge, no study has been published on metabolic flux analysis of glycerol fermentation by *C. pasteurianum*. In present study, we

have addressed this important issue with focus on biohydrogen yield from glycerol fermentation. A review of the previous literature on MFA of biohydrogen production by various microbial strains is given in Table 1.6. The present study essentially aims at utilizing the experimentally measured fluxes of certain metabolites (under steady state conditions) to estimate the complete intracellular fluxes and identify robustness of branch points (or nodes) of anaerobic glycerol metabolism in *C. pasteurianum* using MFA. An *in silico* metabolic flux model has been formulated for this analysis that determines the complete intracellular fluxes of all metabolites from experimentally measured fluxes. Batch mode fermentation of glycerol has been carried out with mechanical shaking (control experiments) and sonication (test experiments) using pre–optimized conditions of pH, temperature and initial glycerol concentration (Sarma et al., 2016). Comparative analysis of the metabolic fluxes in the control experiments and ultrasound–assisted (or test) experiments has given insight into the influence of ultrasound on glycerol metabolism and H_2 yield.

3.2. MATERIALS, METHODS AND MODEL

3.2.1. Microorganism and fermentation conditions

Microbial culture of *Clostridium pasteurianum* MTCC 116 (ATCC 6013)was procured from Microbial Type Culture Collection (MTCC), Chandigarh, India. Pure glycerol was procured from Merck, Germany. All other medium components and chemicals used in this study were procured from HiMedia Pvt. Ltd., India. The standards of acetic acid, butyric acid, lactic acid, succinic acid and1,3–PDO were of HPLC grade and procured from HiMedia Pvt. Ltd., India.

Freeze dried cultures of *C. pasteurianum* were maintained in Reinforced Clostridial Medium (RCM). The composition of RCM in 1 L of distilled water was as

follows: yeast extract 5.0 g, beef extract 10.0 g, peptone 10.0 g, glucose 5.0 g, starch 1.0 g, sodium chloride 5.0 g, sodium acetate 3.0 g, cysteine hydrochloride 0.5 g, agar 0.5 g. The pH of the medium was adjusted to 6.8 ± 0.2 using 1 M NaOH. The medium was inoculated and kept in a rotary incubator shaker (Make: Lab Companion; Model: SI–300R) at 37°C, 150 rpm for 24 h. The 24 h culture was used for streaking over agar plate containing 15 g/L of agar in medium with same composition as stated above. The culture was kept at 37°C in a desiccator containing anaerobic gas pack. The culture broth was used as stock and was sub–cultured every month.

The cells from stock culture were grown under anaerobic conditions in fresh RCM prior to inoculation. Batch fermentation experiments were set up in 100 mL serum bottles containing BSH medium at pre-optimized conditions (pH = 6.7, temperature = 36°C, crude glycerol concentration = 7.4 g/L) (Sarma et al., 2016). The total working volume of fermentation mixture was 50 mL with following composition: 5 mL (or 10% v/v) of *C. pasteurianum* inoculum (containing microbial cells in mid–log phase), 1 mL of 3% w/v L–cysteine HCl as a reducing agent, and 44 mL of fermentation medium (BSH) including substrate crude glycerol (7.4 g/L). The crude glycerol employed as fermentation substrate was produced in–house through alkali catalyzed methanolysis of soybean oil. This glycerol had contaminations of alkali (NaOH, 0.85% w/v) and alcohol (methanol, 0.26% w/v). The levels of these impurities were determined by either acid–base titration or gas chromatograph (Sarma et al., 2016). Resazurin dye (0.1% w/v) was added to fermentation medium as indicator of anaerobic conditions. The BSH medium comprised of following components (concentration, g/L): peptone (2), yeast extract (1), K_2HPO_4 (0.230), KH_2PO_4 (4.035), NaCl (2) in addition to 10 mL trace solution and 10 mL vitamin solution. Trace element solution comprised of following components (concentration, g/L): $MnO_4 \cdot 7H_2O$ (0.01), $ZnSO_4 \cdot 7H_2O$ (0.05), H_3BO_3 (0.01), $N(CH_2COOH)_3$ (4.5), $CaCl_2 \cdot 2H_2O$ (0.01),

Na_2MoO_4 (0.01), $CoCl_2 \cdot 6H_2O$ (0.2), $AlK(SO_4)_2$ (0.01), $MgCl_2 \cdot 6H_2O$ (0.2), $FeCl_3$ (0.1), $CuCl_2 \cdot 6H_2O$ (0.05). The composition of vitamin solution was as follows (concentration, g/L): riboflavin (0.025), citric acid (0.02), folic acid (0.01) and para–amino benzoic acid (0.01). The initial pH of the medium was adjusted to 6.7 using 1 M NaOH. Prior to inoculation, the medium was flushed with pure nitrogen (99.99%) for 15 min, sealed with rubber stoppers, crimped and autoclaved for 15 min at 121°C and 15 psi. Further, 10% v/v inoculum was added to the serum bottles, and the fermentation mixture was incubated at 36°C and 150 rpm. All experiments were carried out in duplicate. Aliquots of fermentation broth were withdrawn periodically for assessment of residual glycerol and other metabolites. Similarly, samples of gas phase products (accumulated above fermentation mixture) were collected periodically to quantify H_2 and CO_2 content.

3.2.2 Ultrasound–assisted glycerol fermentation

Ultrasound–assisted glycerol fermentation was carried out in an ultrasound bath (Make: Elma, Germany; Model: Transsonic T–460, Capacity: 2 L; Frequency: 35 kHz; Rated power input: 35 W). The bath was filled with water which acted as medium for propagation of ultrasound. Fermentation experiments were carried out in a 100 mL serum bottle with 50 mL working volume. The composition of the fermentation mixture was same as stated earlier. The serum bottle was placed at the center of the ultrasound bath and the flask was immersed in about 50% of its height in the water (Bhasarkar et al., 2015a; Khanna et al., 2012b; Singh et al., 2015b). The temperature of the water in the bath was maintained at 36°±2°C by circulating water bath. Sonication was applied in the duty cycle of 20% (i.e. 2 min ON and 8 min OFF in every 10 min of treatment). Prior to fermentation experiments, the ultrasound bath was characterized for acoustic power dissipation. Using calorimetric techniques, the amplitude of the ultrasound waves generated in the bath was determined as 1.5 bar.

3.2.3. *In silico* model construction and MFA

The *in silico* metabolic network of *C. pasteurianum* was constructed from experimental results, KEGG database of metabolic pathways (http://www.genome.jp/keg), and data reported in previous literature. The metabolic network was constructed with 26 reactions and 21 intracellular metabolites. Cellular composition of microbial culture *C. pasteurianum* MTCC 116 (ATCC 6013) used in present study was assumed to be the same as other Clostridial species reported in the literature (Cai et al., 2010; Jiang et al., 2013; Papoutsakis, 1984). Biomass formation (growth flux) was included into the model to account for the drain of intermediate metabolites into biomass. Metabolic fluxes of *C. pasteurianum* during glycerol fermentation were analyzed on the basis of glycerol metabolic pathway, with comparative assessment of numerical and experimental results. The specific rates of glycerol uptake and production of four metabolites, viz. acetate, butyrate, succinate and 1,3–PDO, were measured during the exponential phase of batch fermentation. The experimentally measured values of metabolite production were used as constraints in the *in silico* MFA. The specific hydrogen production rate was used as the criterion to evaluate the results, and to assess the concurrence between *in silico* MFA and experiments. The *in silico* MFA model used in this study was solved using MATLAB R2015a.

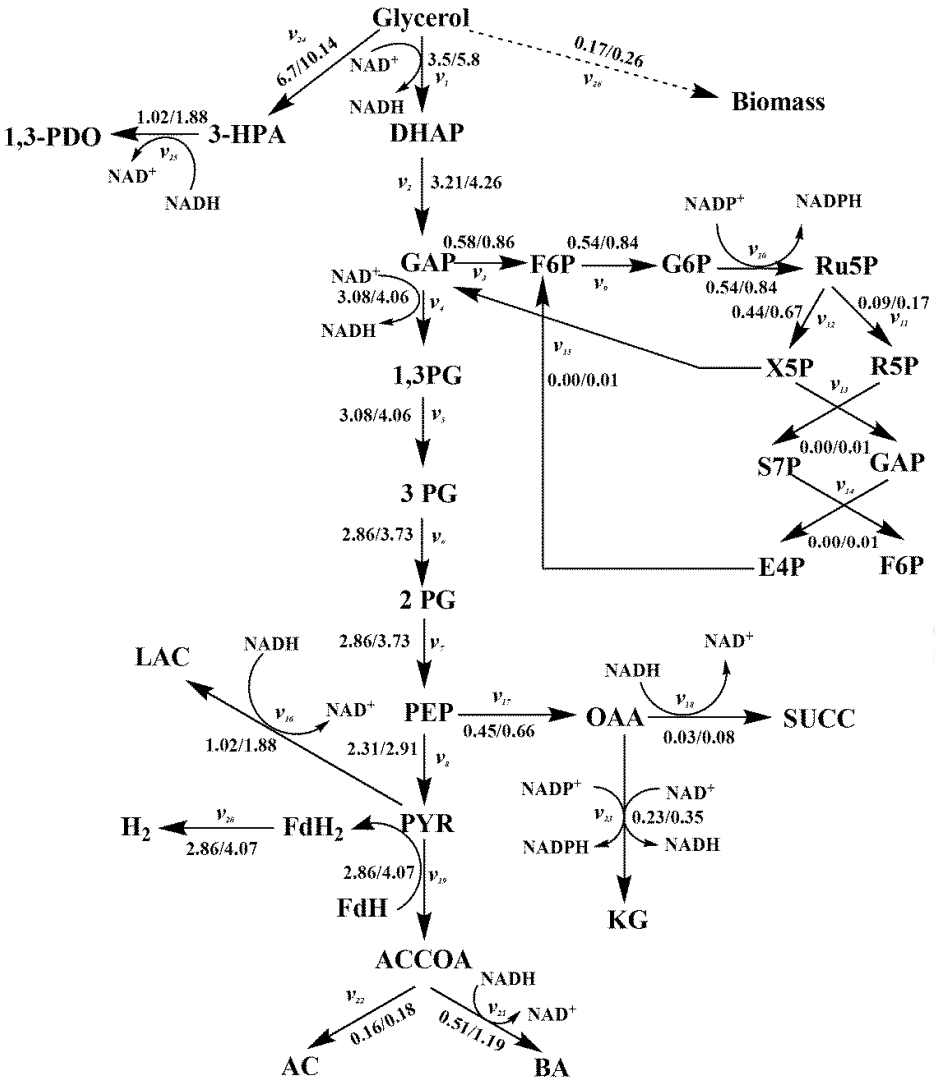

Figure 3.1. Metabolic flux distribution of hydrogen production pathway in *C. pasteurianum* with glycerol as the substrate in control (mechanical shaking)/test (mechanical shaking with intermittent ultrasound) experiments.

***Metabolic flux model*:** Metabolic flux analysis (MFA) is essentially a measure to determine steady–state reaction rates of different steps of substrate metabolism in microorganism. Input for the MFA is the stoichiometry matrix of intracellular metabolic reactions. MFA makes assumption of pseudo steady state for the intermediate metabolites, in which their net concentration at steady state is assumed to remain constant. The reaction

rates or the metabolic fluxes are determined on the basis of molar balances of all intracellular metabolites. The boundary conditions for the analysis are experimentally measured values of the substrate consumption rate and formation rates of certain extracellular metabolites. The general equation for MFA that relates intracellular metabolite concentrations, reaction fluxes, and the matrix of stoichiometric coefficients is written as:

$$dx/dt = S \cdot v \tag{3.1}$$

The above equation is essentially a dynamic mass balance equation for all metabolites. The LHS of above equation is m × 1 matrix of the time profiles of concentrations (x) of metabolites. The RHS has two matrices, viz. stoichiometric matrix S with dimensions m × r and reaction rate matrix v with dimensions r × 1. Element of the i^{th} row and j^{th} column in matrix S represents the stoichiometric coefficient of species i in reaction j. As per assumption of pseudo steady state, the intracellular concentrations (x) of all metabolites remain constant, and thus, equation 3.1 is written as:

$$S \cdot v = 0 \tag{3.2}$$

The degrees of freedom of the reaction system represented by eq. 3.2 is given as: $F = r - m$, where r = number of reactions, and m = number of intracellular metabolites. This necessitates that some of the elements in the matrix v are experimentally measured, so that remaining elements are determined by solving equation 3.2. In order to have unique solution of reaction system describe by eq. 3.2, experimental measurement of fluxes of F number of metabolites is needed. Manish et al., (2007) have suggested a simple procedure for determination of the remaining intracellular fluxes as follows:

The original vector v can be split into two components, viz. vector v_m that contains measured fluxes, and vector v_c containing the remaining fluxes. The original matrix of stoichiometric coefficient S can also be partitioned accordingly into two parts, viz. matrix

S_m comprising of coefficients of measured reactions and matrix S_c containing the remaining reactions. Eq. (3.2) is then transformed as follows:

$$S_m.v_m + S_c.v_c = 0 \tag{3.3}$$

It may be noted that S_c is a square matrix (of dimensions m × m), as F (= $r - m$) number of fluxes are experimentally measured. Inversion of the S_c matrix yields the fluxes in vector v_c as follows:

$$v_c = -(S_c)^{-1}.S_m.v_m \tag{3.4}$$

The present system of glycerol metabolism comprises of 26 reactions with 21 metabolites. These reactions have been listed in Appendix A. Fig. 3.1 depicting the metabolic pathway of glycerol also shows the intermediate metabolites along with the metabolic reactions and the corresponding fluxes. The mass balance of all metabolites is depicted in Appendix B using which the stoichiometric matrix S was constructed (Table 3.1).

Table 3.1. Stoichiometric matrix S for MFA analysis

	v_1	v_2	v_3	v_4	v_5	v_6	v_7	v_8	v_9	v_{10}	v_{11}	v_{12}	v_{13}	v_{14}	v_{15}	v_{16}	v_{17}	v_{18}	v_{19}	v_{20}	v_{21}	v_{22}	v_{23}	v_{24}	v_{25}	v_{26}
PEP	0	0	0	0	0	0	1	–1	0	0	0	0	0	0	0	0	–1	0	0	0	0	0	0	0	0	–0.611
G6P	0	0	0	0	0	0	0	0	1	–1	0	0	0	0	0	0	0	0	0	0	0	0	0	0	0	–0.0016
PYR	0	0	0	0	0	0	0	1	0	0	0	0	0	0	0	–1	0	0	–1	0	0	0	0	0	0	–2.6666
F6P	0	0	1	0	0	0	0	0	–1	0	0	0	0	1	1	0	0	0	0	0	0	0	0	0	0	–0.1788
DHAP	1	–1	0	0	0	0	0	0	0	0	0	0	0	0	0	0	0	0	0	0	0	0	0	0	0	0
GAP	0	1	–1	–1	0	0	0	0	0	0	0	0	1	–1	0	0	1	0	0	0	0	0	0	0	0	0
1,3–PG	0	0	0	1	–1	0	0	0	0	0	0	0	0	0	0	0	0	0	0	0	0	0	0	0	0	0
3–PG	0	0	0	0	1	–1	0	0	0	0	0	0	0	0	0	0	0	0	0	0	0	0	0	0	0	–1.239
2–PG	0	0	0	0	0	1	–1	0	0	0	0	0	0	0	0	0	0	0	0	0	0	0	0	0	0	0
Ru5P	0	0	0	0	0	0	0	0	0	1	–1	–1	0	0	0	0	0	0	0	0	0	0	0	0	0	0
R5P	0	0	0	0	0	0	0	0	0	0	1	0	–1	0	0	0	0	0	0	0	0	0	0	0	0	–0.5726
X5P	0	0	0	0	0	0	0	0	0	0	0	1	–1	0	0	0	–1	0	0	0	0	0	0	0	0	0
S7P	0	0	0	0	0	0	0	0	0	0	0	0	1	–1	0	0	0	0	0	0	0	0	0	0	0	0
E4P	0	0	0	0	0	0	0	0	0	0	0	0	0	1	–1	0	0	0	0	0	0	0	0	0	0	0
OAA	0	0	0	0	0	0	0	0	0	0	0	0	0	0	0	0	1	–1	0	0	0	0	–1	0	0	–1.4452
FdH_2	0	0	0	0	0	0	0	0	0	0	0	0	0	0	0	0	0	0	1	–1	0	0	0	0	0	0
AcCoA	0	0	0	0	0	0	0	0	0	0	0	0	0	0	0	0	0	0	1	0	–1	–1	0	0	0	–20.29
α–KG	0	0	0	0	0	0	0	0	0	0	0	0	0	0	0	0	0	0	0	0	0	0	1	0	0	–1.3285
NADH	1	0	0	1	0	0	0	0	0	0	0	0	0	0	0	–1	0	–1	0	0	–2	0	1	0	–1	–10.75
NADH	0	0	0	0	0	0	0	0	0	2	0	0	0	0	0	0	0	0	0	0	0	0	1	0	0	–7.6152
3–HPA	0	0	0	0	0	0	0	0	0	0	0	0	0	0	0	0	0	0	0	0	0	0	0	1	–1	0

3.2.4 *Analytical methods*

The concentrations of metabolites in the samples withdrawn from fermentation broth were quantified by HPLC analysis using a Hi–Plex H column (300 mm × 8 µm × 7.7 mm, Agilent, India) thermostated at 60°C with the help of external column oven (Model: HCO–02, PCI analytics Pvt. Ltd., India). 0.01 M H_2SO_4 in ultra–pure water (18.2 MΩ·cm resistivity at 25°C) was used as the mobile phase at a flow rate of 0.5 mL/min. Residual glycerol content of the fermentation samples was quantified by HPLC analysis using a Rezex RCM Monosaccharide calcium–column (300 mm × 8 µm × 7.8 mm, Phenomenex, India) thermostated at 35°C with the help of external column oven (Model– HCO–02, PCI analytics Pvt. Ltd., India). Ultra–pure water (18.2 MΩ·cm resistivity at 25°C) was used as the mobile phase at a flow rate of 0.5 mL/min. The HPLC apparatus comprised of a pump (Series 200, Perkin Elmer), a refractive index detector (Series 200, Perkin Elmer) and a vacuum degasser (Series 200, Perkin Elmer). Reaction mixture samples were centrifuged (12,000 rpm, 20 min) and filtered through a 0.2 µm membrane filter, and diluted appropriately prior to injection into HPLC. Standard calibration plots were used to determine concentrations of the metabolites and glycerol in the samples of fermentation mixture.

The composition of product gas from glycerol fermentation was determined using Gas Chromatograph (Make: Thermo scientific, Model: Ceres800 plus) with thermal conductivity detector (TCD) and Porapak Q (60/80 mesh) column employing argon as carrier gas at a flow rate of 30 mL/min. The operational temperature of the column oven was 45°C, and the injector and detector temperatures were maintained at 200°C. Gas samples were withdrawn from fermentation serum bottles and the molar/volumetric content of H_2 and CO_2 in the gas was determined. Hydrogen gas production was calculated from measurement of headspace of fermentation bottles (above surface of fermentation

mixture).The total volume of gas produced in each time interval can be determined using the mass balance equation.

$$V_{H,i} = V_{H,i-1} + C_{H,i}(V_{G,i} - V_{G,i-1}) + V_H\,(C_{H,i} - C_{H,i-1}) \quad (3.5)$$

$V_{H,i}$ and $V_{H,i-1}$ are the cumulative hydrogen gas volumes at present (i) and previous (i–1) time interval, respectively; $V_{G,i}$ and $V_{G,i-1}$ are total product gas volume at the current and previous time intervals; $C_{H,i}$ and $C_{H,i-1}$ are the volume or mole fractions of hydrogen gas in the headspace at the current and previous time intervals; V_H is the volume of headspace of vials. The volume of product gas used for analysis was also taken into account during hydrogen mass balance.

3.3. RESULTS AND DISCUSSION

3.3.1 Carbon mass balance for glycerol fermentation by *C. pasteurianum*

The carbon mass balance of glycerol fermentation by *C. pasteurianum* was examined by monitoring the time profiles of various metabolites such as CO_2, acetate, butyrate, succinate and 1,3–PDO for both control (mechanical shaking) and test (mechanical shaking with intermittent sonication) experiments. The carbon mass balance for control and test experiments is summarized in Table 3.2and 3.3, respectively. It can be inferred from data presented in Tables 3.2 and 3.3 that butyrate and 1,3–PDO were the main intermediates of glycerol metabolism. This also implies that hydrogen production from glycerol metabolism in *C. pasteurianum* is mainly associated with formation of butyrate. In addition to acetate and butyrate, the major fraction of carbon is distributed in the form of biomass or cell growth itself. Our previous results (Sarma et al., 2016) have shown that biomass growth and H_2 production are concurrent processes, which also supports the conclusion that biohydrogen is a cell growth associated product. Comparative analysis of Table 3.2 and 3.3reveals marked influence of ultrasound in enhancing the glycerol metabolism. It could be observed that glycerol consumption rate increases by ~ 50% with

application of sonication, as 80% of initial glycerol is consumed within 12 h in test experiments as against 18 h in control experiments. Nonetheless, production rates of all metabolites show non–uniform enhancement with sonication. The highest enhancement of > 70% is seen in production of succinate, followed by butyrate (> 50%). Production rate of 1,3–PDO, however, shows only marginal improvement of ~ 20% with sonication. Another significant influence of sonication on glycerol fermentation is in terms of carbon distribution to biomass formation. With application of sonication, the carbon distribution towards biomass growth drops by ~ 20%. Cai et al., (2010) and Cheng et al., (2013) have outlined the significance of butyrate to acetate ratio (B/A ratio) for H_2 production. Greater production of H_2 is favored by higher B/A ratio or higher butyrate yield. On the other hand, lactate formation has adverse effect on H_2 production due to lack of re– oxidation and consumption of NADH (Santilal et al., 2015). In the present study, the B/A ratio is found to increase with application of ultrasound. This is manifested in terms of ~40% rise in the H_2 yield (0.869 mol H_2/mol glycerol) in the test experiments as compared control experiments (0.622 mol H_2/mol glycerol). As per the glycerol metabolism reactions 2.8 and 2.9, the acetate route of glycerol metabolism yields 3 mol H_2/mol glycerol, while butyrate route of glycerol metabolism yields 2 mol H_2/mol glycerol. This stoichiometric relation points to reduction in H_2 yield with increasing B/A ratio. However, experimental results violate the stoichiometric prediction and show opposite trend of H_2 yield with B/A ratio.

Table 3.2. Carbon mass balance for glycerol fermentation (control experiment with mechanical shaking) by *C.pasteurianum*

Time (h)	Glycerol (mg)	Acetate (mg)	Butyrate (mg)	1,3-PDO (mg)	Succinate (mg)	CO_2 (mg)	Biomass (mg)	Total carbon (mg)	Carbon balance (%)
0	370.00	0.	0.	0.	0.	0.	0.	370.00	100.00
3	291.50±0.01	2.75±0.02	15.53±0.12	39.58±0.33	2.59±0.11	1.55±1.20	16.57±0.01	370.06	100.02
6	232.75±0.13	5.34±0.13	20.92±0.32	44.30±0.23	3.14±0.22	6.54±1.11	32.12±0.01	345.11	93.27
9	199.67±0.11	7.04±0.11	22.17±0.15	58.69±0.06	3.25±0.02	13.80±0.96	54.17±0.55	358.79	96.97
12	147.36±0.32	8.76±0.18	29.47±0.16	59.98±0.17	3.45±0.21	20.69±0.98	74.54±0.19	344.23	93.04
15	112.01±0.01	7.50±0.11	32.78±0.02	62.01±0.11	3.43±0.06	33.83±1.23	85.53±0.04	337.08	91.10
18	74.01±0.50	9.01±0.01	40.12±0.04	69.76±0.02	3.36±0.07	35.12±0.99	92.24±0.01	323.61	87.46
24	65.35±0.40	8.88±0.01	44.32±0.50	68.13±0.30	3.33±0.35	33.21±1.01	104.25±0.11	327.26	88.45
Carbon distribution (%)	20.00	2.43	10.84	18.85	0.91	9.49	24.92		

Table 3.3. Carbon mass balance for glycerol fermentation (test experiment with ultrasound-irradiation) by *C.pasteurianum*

Time (h)	Glycerol (mg)	Acetate (mg)	Butyrate (mg)	1,3-PDO (mg)	Succinate (mg)	CO_2 (mg)	Biomass (mg)	Total carbon (mg)	Carbon balance (%)
0	370.	0.	0.	0.	0.	0.	0.	370.	100.
3	252.30±0.01	5.21±0.32	30.06±0.26	49.10±0.16	5.27±0.19	1.67±1.1	15.04±0.11	358.65	96.93
6	190.21±0.13	7.34±0.10	47.52±0.21	57.81±0.08	6.96±0.15	6.88±0.98	36.12±0.03	352.84	95.36
9	108.01±0.11	7.04±0.02	62.42±0.06	85.17±0.11	5.80±0.12	15.78±2.1	52.13±0.06	336.35	89.91
12	75.12±0.03	7.82±0.05	62.91±0.11	86.01±0.30	5.70±0.02	34.12±2.3	73.12±0.03	344.80	83.19
Carbon distribution (%)	20.3	2.11	17.00	22.24	1.54	9.22	19.76		

Two plausible explanations for this result have been given by Cheng et al., (2012) as follows:

(1) Consumption of acetate and lactate for production of butyrate and H_2 in anaerobic fermentation leading to higher H_2 yield at higher B/A ratio.

(2) H_2 and CO_2 or butyrate consumption for acetate production through acetogenesis resulting in lower H_2 yield at lower B/A ratio.

3.3.2 Metabolic flux analysis

The *in silico* metabolic network of *C. pasteurianum* was constructed using the reaction scheme given in Appendix A. Intracellular fluxes of *C. pasteurianum* in glycerol fermentation were determined using metabolic network and experimentally measured rates of formation/consumption of certain metabolites/substrates. As noted earlier, the specific rates of glycerol uptake and production rates of four metabolites, viz. acetate, butyrate, succinate and 1,3–PDO during exponential phase of fermentation have been experimentally measured. These rates form the constraints or boundary conditions for solving the pseudo–steady state metabolic flux balance given by eq. 3.6. The results of the metabolic flux analysis are shown in Table 3.4. It can be inferred from Table 3.4that experimental (measured) and *in silico* (calculated by MFA model) results on specific H_2 production rate matched very well. The biomass formation equation was obtained from cellular composition of *C. butyricum* and *C. acetobutylicum*, as no detailed information about *C. pasteurianum* cells was available in published literature. The results of metabolic flux analysis are depicted in Fig. 3.1 for the control and test experiments. According to the MFA results shown in Fig. 3.1, the flux through the Embden–Meyerhof (EM) pathway is about five times as much as that through the pentose phosphate (PP) pathway. This indicates predominance of glycerol metabolism through EM pathway

resulting in formation of pyruvate. Pyruvate is subsequently converted to lactate or acetyl–CoA with co–generation of reduced ferredoxin, from which hydrogen is formed directly by the action of hydrogenase. In order to get insight into the influence of ultrasound on carbon flux distribution in *C. pasteurianum*, MFA was performed under both control and test experiments. As seen from Fig. 3.1, application of ultrasound influenced the metabolic fluxes at three key nodes, viz. PEP, pyruvate and acetyl–CoA. At the PEP node, the fraction of carbon flux towards pyruvate was higher as compared to the flux towards OAA. Marked increase of 47% in the metabolic flux towards OAA in test is a possible consequence of modifications in the secondary structure of PEP carboxylase enzyme due to intermittent sonication which increases its affinity towards the substrate PEP. At the pyruvate node, the fraction of carbon flux to acetyl–CoA and H_2 was higher as compared to the flux towards lactate. Smaller flux distribution towards lactate favors H_2 production, as confirmed by several previous authors (Cai et. al., 2010; Oh et al., 2007). With application of ultrasound, the fraction of carbon flux towards lactate increased by 84% from 1.02 to 1.88. However, this flux is still far less as compared to the sum total of fluxes (8.14) towards AcCoA and H_2. At the pyruvate node, three enzymes compete for pyruvate as substrate, viz. pyruvate:pyruvate ferredoxin oxidoreductase, pyruvate dehydrogenase and lactate dehydrogenase. The relative values of fluxes mentioned above indicate most flux is directed to reduced ferredoxin (FdH_2) and acetyl–CoA, both of which are associated with maximum H_2 production. It was also observed that, most of the flux from glycerol was directed towards 3–HPA formation, which is an intermediate for 1,3–propanediol. This is in accordance with the experimental results, which have revealed 1,3 PDO to be the major product of glycerol metabolism (refer to Table 3.2 and 3.3).

Table 3.4. Experimental metabolic rates and constraints used in *in silico* MFA

	Component	Control (Mechanical shaking)		Test (Ultrasound assisted)	
		Measured	Calculated	Measured	Calculated
Specific uptake rate (mmol/L/h)	Glycerol	3.50	--	5.80	**--**
Specific production rate (mmol/L/h)	Acetate	0.17	--	0.18	**--**
	Butyrate	0.51	--	1.19	--
	1,3-PDO	1.02	--	1.88	--
	Succinate	0.03	--	0.08	--
	H_2	2.70	2.80	3.85	4.07
H_2 yield (mol/mol glycerol)		0.63	0.70	0.89	0.95
Specific growth rate (h^{-1})		0.10	0.17	0.12	0.26

Table 3.5. Product yields under different operational conditions (Control: Mechanical shaking, Test: Ultrasound assisted)

	Product yields (mol/mol glycerol)						Butyrate/Acetate
	Acetate	Butyrate	1,3-PDO	Succinate	CO_2	H_2	
Control	0.046	0.142	0.285	0.008	0.248	0.622	3.086
Test	0.041	0.216	0.312	0.015	0.242	0.869	5.268

Carbon flux distribution at the acetyl–CoA node was greatly affected by sonication as the flux towards butyrate increased by 133% in test experiments, whereas flux towards acetate increased by ~ 11%. The yields of major products from glycerol metabolism are shown in Table 3.5. The yield of biohydrogen showed marked rise (~ 40%) in test experiments. The MFA results indicate that enhancement in H_2 yield from ultrasound–assisted glycerol fermentation is manifestation of enhanced flux towards butyrate. This conclusion is also corroborated by higher butyrate/acetate ratio in the test experiments as shown in Table 3.5.

3.3.3 Contemplations for enhancing H_2 production and their assessment with MFA

Despite enhancement in H_2 yield with application of ultrasound in glycerol fermentation, the yield of 0.869 mol H_2/mol glycerol obtained in present study is far lower than the H_2 yield from conventional processes such as catalytic steam reforming of glycerol (typical yield of ~ 6 mol H_2/mol glycerol). Several causes contribute to lowering of the H_2 yield in dark fermentation. One of the main causes leading to reduction in H_2 yield is accumulation of fermentation end products in fermentation broth which inhibit hydrogen production. The main metabolites of dark fermentation are acetic acid and butyric acid which leads to acidification of the fermentation broth. Reduction in pH of the fermentation broth initiates solventogenesis and results in lowering of the H_2 yield. The stoichiometry of glycerol fermentation (equation 2.9) suggests that hydrogen yield is 2 mole H_2 per mole of glycerol, when butyrate was the sole by–product. It was also found that butyrate had inhibitory effects on hydrogen production (Chin et al., 2003). The butyrate formation pathway is considered as the main competing pathway during H_2 production because it consumes more NADH than other pathways, reducing the yield of H_2 (Saint–Amas et al., 2001; Kumar et al., 2001; Hallenbeck et al., 2009). Despite these theoretical contemplations, experimental results presented in preceding sections have indicated increasing H_2 yield with butyrate/acetate ratio, and we have outlined some possible causes leading to this discrepancy. Nonetheless, it can also be conjectured that elimination of the butyrate pathway and the increased production of acetate may increase the H_2 yield per unit substrate consumption in *Clostridial* fermentation (Hallenbeck et al., 2009; Cai et al., 2011).

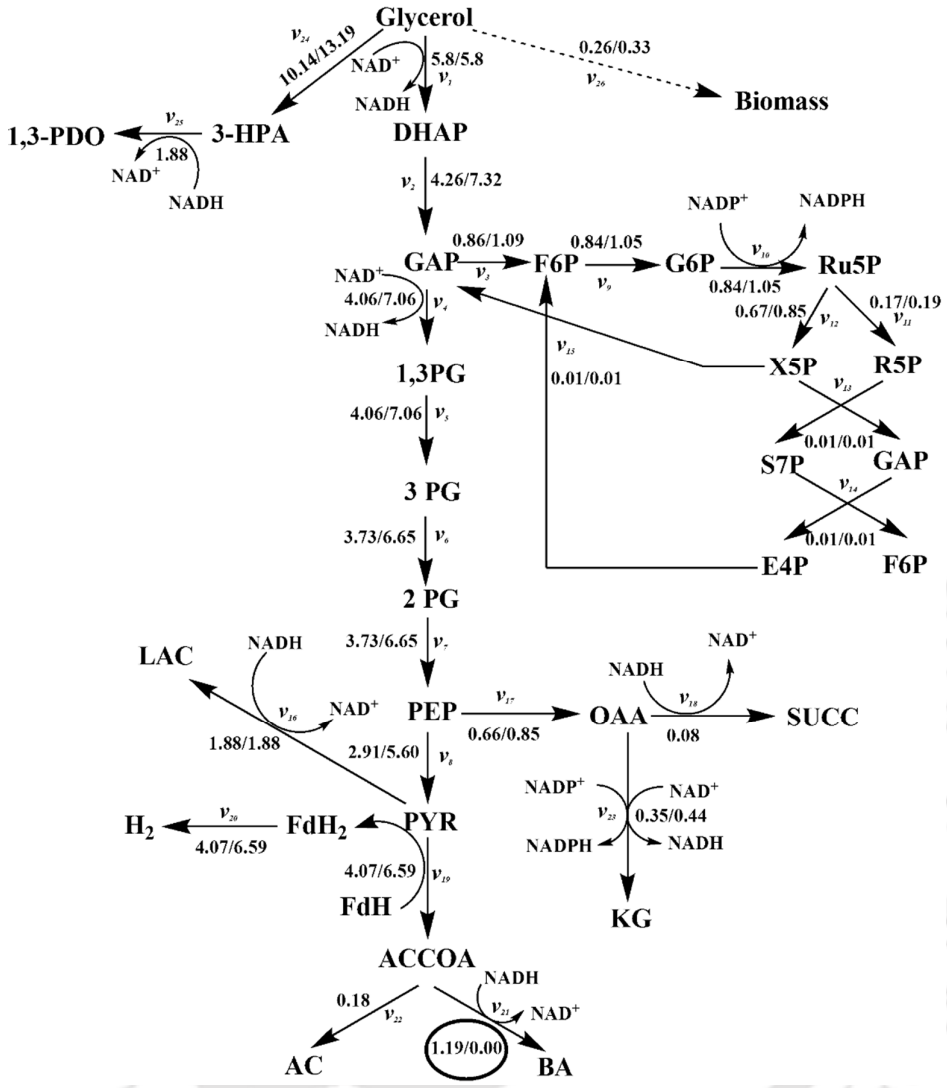

Figure 3.2. Metabolic flux distribution of hydrogen production pathway in *C. pasteurianum* with glycerol as the substrate when v_{21}=0 i.e. butyrate production assumed to be zero.

In this study, we have made assessment of two theoretical contemplations for further enhancement of H_2 yield (simultaneously with application of ultrasound) using the MFA model for glycerol metabolism by *C. pasteurianum*:

(i) Elimination of butyrate pathway in the *in silico* metabolic network of *Clostridium pasteurianum*: In this case, the flux from acetyl–CoA to butyrate, denoted as v_{21}, was assumed to be nullified (v_{21}= 0) and the effect on H_2 flux was analysed by MFA.

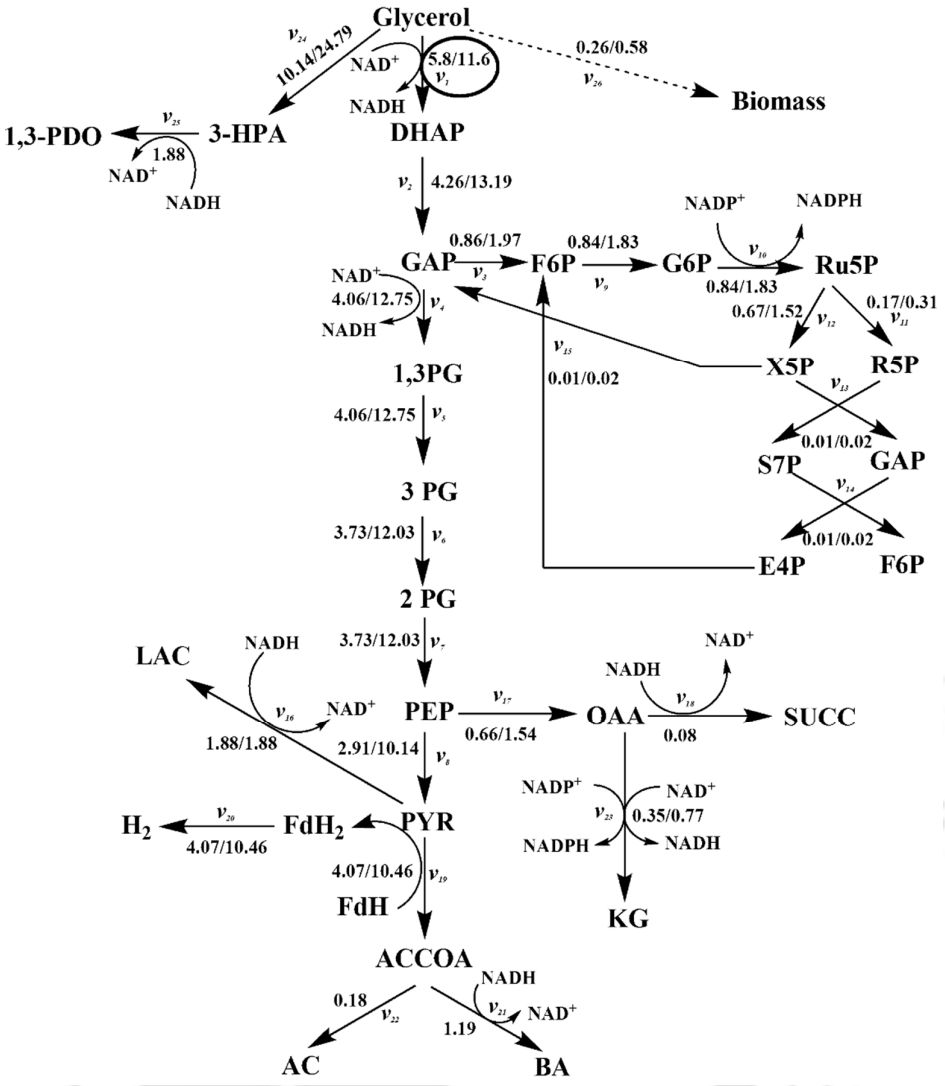

Figure 3.3. Metabolic flux distribution of hydrogen production pathway in *C. pasteurianum* with glycerol as the substrate when v_1=2x i.e. glycerol uptake rate is doubled.

(ii) MFA analysis shown in Fig. 2 revealed that for v_{21}= 0, flux towards hydrogen (v_{20}) increased significantly. The increase in $v_{20}$was 37% in control experiments (employing mechanical shaking), and 62% in test experiments (employing sonication). The elimination of the butyrate pathway is possible *in vivo* by knockout of genes encoding the enzymes involved in the butyrate formation pathway, viz. β–hydroxy butyryl–CoA

dehydrogenase (BHBD), 3–hydroxy–CoA dehydratase (CRT), butyryl–CoA–dehydrogenase (BCD), phosphotransbutyrylase (PTB), and butyrate kinase (BK).

(iii) Doubling the glycerol uptake rate in *C. pasteurianum*: The glycerol uptake rate can be enhanced *in vivo* by high–level expression of genes encoding enzymes involved in the *dha* (dihydroxyacetone) system composed of glycerol kinase (GK) and glycerol dehydrogenase (GDH). In this case, the flux from glycerol to DHAP (v_1) was assigned a value 2× the experimental value. This exercise was done for both test and control experiments. Results of MFA analysis depicted in Fig. 3 revealed that doubling the glycerol uptake rate enhances the flux towards H_2 approx. 2.5× times for both control and test experiments. These two theoretical approaches to enhance H_2 yield can provide valuable insights for construction of *C. pasteurianum* mutants lacking butyrate pathway or having over–expressed genes for higher glycerol uptake.

3.4 CONCLUSIONS

MFA of glycerol fermentation has provided insight into influence of ultrasound on intracellular carbon flux in *C. pasteurianum*. Glycerol uptake flux and butyrate flux at acetyl–CoA node showed increase of ~50% and ~133%, respectively, with sonication. ~40% increase in biohydrogen yield with sonication is accompanied by >65% rise in butyrate/acetate ratio. Thus, greater biohydrogen generation is attributed to higher carbon flux at acetyl–CoA node flowing to butyrate. Hypothetical MFA of ultrasound–assisted fermentation with nullifying of butyrate flux (or complete carbon partitioning to acetate at acetyl–CoA node) or doubling of glycerol uptake flux predicted further increase in biohydrogen yield.

Appendix A: Reaction system of glycerol metabolism

1. $Gly + NAD \longrightarrow DHAP + NADH$
2. $DHAP \longrightarrow GAP$
3. $GAP + DHAP \longrightarrow F6P$
4. $GAP + NAD^{+} \longrightarrow 1,3PG + NADH$
5. $1,3PG \longrightarrow 3PG$
6. $3PG \longrightarrow 2PG$
7. $2PG \longrightarrow PEP$
8. $PEP \longrightarrow PYR$
9. $F6P \longrightarrow G6P$
10. $G6P + 2NADP^{+} \longrightarrow Ru5P + 2NADPH$
11. $Ru5P \longrightarrow R5P$
12. $Ru5P \longrightarrow X5P$
13. $X5P + R5P \longrightarrow S7P + GAP$
14. $S7P + GAP \longrightarrow E4P + F6P$
15. $E4P + X5P \longrightarrow F6P + GAP$
16. $PYR + NADH \longrightarrow LAC + NAD^{+}$
17. $PEP \longrightarrow OAA$
18. $OAA + NADPH \longrightarrow SUCC + NAD^{+}$
19. $PYR \longrightarrow ACCOA$
20. $FdH_2 \longrightarrow H_2$
21. $ACCOA + 2NADH \longrightarrow BA + 2NAD^{+}$
22. $ACCOA \longrightarrow AC$
23. $OAA + NADP^{+} + NAD^{+} \longrightarrow \alpha - KG + NADPH + NADH$
24. $Gly \longrightarrow 3HPA + H_2O$
25. $3HPA + NADH \longrightarrow 1,3 - PDO$
26. $0.0016G6P + 0.1788F6P + 0.5726R5P + 1.2393PG + 0.611PEP + 2.6666PYR + 20.29AcCoA + 1.4452OAA + 10.75NADH + 7.6152NADPH + 1.3285\alpha - KG \longrightarrow BIOMASS$

Appendix B: Mass balances of metabolites

1. PEP: $v_7 - v_8 - v_{17} = 0$
2. G6P: $v_9 - v_{10} = 0$
3. PYR: $v_8 - v_{16} - v_{19} = 0$
4. F6P: $v_3 - v_9 + v_{14} + v_{15} = 0$
5. DHAP: $v_1 - v_2 - v_{24} = 0$
6. GAP: $v_2 - v_3 - v_4 + v_{13} - v_{14} + v_{17} = 0$
7 .1,3 PG: $v_4 - v_5 = 0$
8. 3PG: $v_4 - v_5 = 0$
9. 2PG: $v_6 - v_7 = 0$
10. Ru5P: $v_{10} - v_{11} - v_{12} = 0$
11. R5P: $v_{11} - v_{13} = 0$
12. X5P: $v_{12} - v_{13} - v_{17} = 0$
13. S7P: $v_{13} - v_{14} = 0$
14. E4P: $v_{14} - v_{15} = 0$
15. OAA: $v_{17} - v_{18} - v_{23} = 0$
16. FdH_2 : $v_{19} - v_{20} = 0$
17. ACCOA: $v_{19} - v_{21} - v_{22} = 0$
18. α-KG: $v_{23} = 0$
19. NADH: $v_1 + v_4 - v_{16} - v_{18} - 2v_{21} + v_{23} - v_{25} = 0$
20. NADPH: $2v_{10} + v_{23} = 0$
21. LAC: $v_{16} = 0$

Appendix C: List of abbreviations

DHAP	Dihydroxyacetone phosphate
3–HPA	3–Hydroxypropionaldehyde
1,3–PDO	1,3–Propanediol
GAP	Glyceraldehyde 3–phosphate
F6P	Fructose 6–phosphate
G6P	Glucose 6–phosphate
Ru5P	Ribulose 5–phosphate
R5P	Ribose 5–phosphate
X5P	Xylulose 5–phosphate
E4P	Erythrose 4–phosphate
S7P	Sedoheptulose 7–phosphate
1,3 PG	1,3–bisphosphoglycerate
3PG	3–phosphoglycerate
2PG	2–phosphoglycerate
PEP	Phosphoenolpyruvate
PYR	Pyruvate
ACCOA	Acetyl coenzyme A
AC	Acetate
BA	Butyrate
OAA	Oxaloaceate
SUCC	Succinate
LAC	Lactate
KG	α Ketoglutarate
Fd	Ferredoxin
FdH_2	Reduced Ferredoxin
H_2	Hydrogen
NADPH	Nicotinamide adenine dinucleotide phosphate(reduced form)
NADH	Nicotinamide adenine dinucleotide (reduced form)

References

Ahrens, K., Menzel, K., Zeng, A.P., Deckwer, W.D., 1997. Kinetic, Dynamic, and Pathway Studies of Glycerol Metabolism by *Klebsiella pneumoniae* in Anaerobic Continuous Culture: III. Enzymes and Fluxes of Glycerol Dissimilation and 1,3–Propanediol Formation. Biotechnol. and Bioeng. 59, 544–552.

Bhasarkar, J.B., Dikshit, P.K., Moholkar, V.S., 2015a. Ultrasound assisted biodesulfurization of liquid fuel using free and immobilized cells of *Rhodococcus rhodochrous* MTCC 3552: A Mechanistic Investigation. Bioresour. Technol. 187, 369–378.

Bhasarkar, J.B., Borah, A.J., Goswami, P., Moholkar, V.S., 2015b. Mechanistic analysis of ultrasound assisted enzymatic desulfurization of liquid fuels using horseradish peroxidase. Bioresour. Technol. 196, 88–98.

Borah, A.J., Agarwal, M., Poudyal, M., Goyal, A., Moholkar, V.S., 2016. Mechanistic investigation in ultrasound induced enhancement of enzymatic hydrolysis of invasive biomass species. Bioresour. Technol. 213, 342–349.

Cheng, H–H., Whang, L–M., Lin, C–A., Liu, I–C., Wu, C–W., 2013. Metabolic flux network analysis of fermentative hydrogen production: Using *Clostridium tyrobutyricum* as an example. Bioresour. Technol. 141, 233–239.

Chin, H., Chen, Z., Chou, C.P., 2003. Fedbatch operation using *Clostridium acetobutylicum* suspension culture as biocatalyst for enhancing hydrogen production. Biotechnol. Prog. 19, 383–388.

Cai, G., Jin, B., Monis, P., Saint, C., 2011. Metabolic flux network and analysis of fermentative hydrogen production. Biotechnol. Advances. 29, 375–387.

Ciranna, A., Pawar, S.S., Santala, V., Karp, M., van Niel, E.W.J., 2014. Assessment of

metabolic flux distribution in the thermophilic hydrogen producer *Caloramator celer* as affected by external pH and hydrogen partial pressure. Microb. Cell. Fact. 13, 48.

Hadicke, O., Grammel, H., Klamt, S., 2011. Metabolic network modelling of redox balancing and biohydrogen production in purple non sulfur bacteria. BMC Syst. Biol. 5, 150.

Hallenbeck, P.C., 2009. Fermentative hydrogen production: principles, progress, and prognosis. Int. J. Hydrogen Energ. 34, 7379–7389.

Jiang, L., Song, P., Zhu, L., Li, S., Hu, Y., Fu, N., Huang, H., 2013. Comparision of metabolic pathway for hydrogen production in wild type and mutant *Clostridium tyrobutyricum* starin based on metabolic flux analysis. Int. J. Hydrogen Energ. 38, 2176–2184.

Jitrwung, R., Yargeau, V., 2011. Optimization of media composition for the production of biohydrogen from waste glycerol. Int. J. Hydrogen Energ. 36, 9602–9611.

Khanna, S., Goyal, A., Moholkar, V.S., 2012a. Microbial conversion of glycerol: present status and future prospects. Crit. Rev. Biotechnol. 32, 235–262.

Khanna, S., Jaiswal, S., Goyal, A., Moholkar, V.S., 2012b. Ultrasound enhanced bio-conversionof glycerol by *Clostridium pasteurianum*: A mechanistic investigation. Chem. Eng. J. 200–202, 416–425.

Khanna, S., Goyal, A., Moholkar, V.S., 2013a. Effect of fermentation parameters on bio–alcohols production from glycerol using immobilized *Clostridium pasteurianum*: an optimization study. Prep. Biochem. Biotechnol. 43, 828–847.

Khanna, S., Goyal, A., Moholkar, V.S., 2013b. Production of n–butanol from biodiesel

derived crude glycerol using *Clostridium pasteurianum* immobilized on amberlite. Fuel. 112, 557–561.

Khanna, S., Goyal, A., Moholkar, V.S., 2013c. Mechanistic investigation of ultrasonic enhancement of glycerol bioconversion by immobilized *Clostridium pasteurianum* on silica support. Biotechnol. and Bioeng. 110, 1637–1645.

Khanna, S., Shukla, A., Goyal, A., Moholkar, V.S., 2014. Alcoholic Biofuels production from biodiesel derived glycerol by *Clostridium pasteurianum* whole cells immobilized on silica. Waste and Biomass Valorization. 5, 789–798.

Kumar, N., Ghosh, A., Das, D., 2001. Redirection of biochemical pathways for the enhancement of H_2 production by *Enterobacter cloacae*. Biotechnol. Lett. 23, 537–541.

Liu, X., Ren, N., Song, F., Yang, C., Wamg, A., 2008. Recent advances in fermentative biohydrogen production. Progress in Natural Science 18, 253–258.

Oh, Y–K., K, H–J., Park, S., Kim, M–S., Ryu, D.D.Y., 2008. Metabolic flux analysis of hydrogen production pathway in *Citrobacter amalonaticus* Y19. Int. J. Hydrogen Energ. 33, 1471–1482.

Mangayil, R., Karp, M., Santala, V., 2012. Bioconversion of crude glycerol from biodiesel production to hydrogen. Int. J. Hydrogen Energ. 37, 12198–12204.

Mangayil, R., Aho, T., Karp, M., Santala, V., 2015. Improved bioconversion of crude glycerol to hydrogen by statistical optimization of media components. Renew. Energ. 75, 583–589.

Manish, S., Venkatesh, K.V., Banerjee, R., 2007. Metabolic flux analysis of biological hydrogen production by *Escherichia coli*. Int. J. Hydrogen Energ. 32, 3820–3830.

Mathews, J., Wang, G., 2009. Metabolic pathway engineering for enhanced biohydrogen production. Int. J. Hydrogen Energ. 34, 7404–7416.

Marone, A., Varrone, C., Fiocchetti, F., Giussani, B., Izzo, G., Mentuccia, L., Rosa, S., Signorini, A., 2015. Optimization of substrate composition for biohydrogen production from buffalo slurry co–fermented with cheese whey and crude glycerol, using microbial mixed culture. Int. J. Hydrogen Energ. 40, 209–218.

Moholkar, V.S., Warmoeskerken, M. M. C. G., 2003.Integrated approach to optimization of an ultrasonic processor. AIChE J. 49(11), 2918–29

Morimoto, K., Kimura, T., Sakka, K., Ohmiya, K., 2005. Overexpression of a hydrogenase gene in *Clostridium paraputrificum* to enhance hydrogen gas production. FEMS Microbiol. Lett. 246, 229–234.

Mu, Y., Zheng, X–J, Yu, H–Q., 2009. Determining optimum conditions for hydrogen production from glucose by an anaerobic culture using response surface methodology (RSM). Int. J. Hydrogen Energ. 34, 7959–7963.

Papoutsakis, E.T., 1984. Equations and calculations for fermentations of Butyric acid bacteria. Biotechnol. Bioeng. 26, 174–187.

Saint–Amans, S., Girbal, L., Andrade, J., Ahrens, K., Soucaille, P., 2001. Regulation of carbon and electron flow in *Clostridium butyricum* VPI 3266 grown on glucose–glycerol mixtures . J. Bacteriol. 183, 1748–1754.

Sarma, S., Dubey, V.K., Moholkar, V.S., 2016. Kinetic and thermodynamic analysis (with statistical optimization) of hydrogen production from crude glycerol using *Clostridium pasteurianum*. Int. J. Hydrogen Energ. 33, 1471–1482.

Singh, S., Agarwal, M., Sarma, S., Goyal, A., Moholkar, V.S., 2015a. Mechanistic insight into ultrasound induced enhancement of simultaneous saccharification

and fermentation of *Parthenium hysterophorus* for ethanol production. Ultrason. Sonochem. 26, 249–256.

Singh, S., Sarma, S., Agarwal, M., Goyal, A., Moholkar, V.S., 2015b. Ultrasound enhanced ethanol production from *Parthenium hysterophorus*: A mechanistic investigation. Bioresour. Technol. 188, 287–294.

Stephanopoulos, G.N., Aristidou, A.A., Nielsen, J., 2012. Metabolic Engineering–Principles and Methodologies, Academic Press, Diego, 1998 (Chapter 8: Metabolic flux analysis, pp. 313–350).

Wang, J., Wan, W., 2008. Optimization of fermentative hydrogen production process by response surface methodology. Int. J. Hydrogen Energ. 33, 6976–6984.

Chapter 4

Optimization of Medium Components for Biohydrogen Production from Biodiesel-derived Waste Glycerol

4.1 INTRODUCTION

In order to achieve efficient production of hydrogen, optimum environmental factors such as temperature, pH, inoculum size and media compositions are necessary. Optimum media components are needed for the growth of micro-organisms and the hydrogenase enzyme activity. Na_2HPO_4 has a buffering capacity KH_2PO_4 and K_2HPO_4 has a buffering capacity that could reduce the pH fluctuation caused by volatile fatty acids (VFAs) accumulation during the fermentation process. Nitrogen in the form of peptone is required for the synthesis of nucleic acid, protein and enzyme in which an appropriate concentration of nitrogen could enhance bacterial growth and activity.

Optimum environmental factors affecting hydrogen production have been investigated by various statistical methods using various kinds of carbon sources such as glucose, xylose, and lignocellulosic materials (Sittijunda et al., 2012; Wang et al., 2008; Geng et al., 2010; Jitrwung et al., 2011; Saraphirom et al., 2010; Khamtib et al., 2011; Prasertsan et al., 2009). However, information on using waste glycerol to produce hydrogen by *C. pasteurianum* is still limited. In our previous study similar optimization was carried for process parameters pH, temperature and glycerol concentration. Accordingly, this study attempts to optimize media compositions used to produce hydrogen from waste glycerol employing RSM with Plackett-Burman and CCD.

Plackett–Burmam design followed by Central Composite Design (CCD) was employed to optimize different medium components for the production of hydrogen by free cells of *C. pasteurianum*. The variables having significant effect on hydrogen yield were selected from Plackett–Burman design, which were further optimized using CCD design.

4.2 MATERIALS AND METHODS

4.2.1 Materials

Microbial culture of *Clostridium pasteurianum* MTCC 116 (ATCC 6013)was procured from Microbial Type Culture Collection (MTCC), Chandigarh, India. Pure glycerol was procured from Merck, Germany. All other medium components and chemicals used in this study were procured from HiMedia Pvt. Ltd., India.

4.2.2 Synthesis of crude glycerol

The crude glycerol was produced in our laboratory by alkali catalyzed methanolysis of soybean oil. The details of transesterification reaction are as follows: molar ratio (12:1), oil (60 mL), methanol (30 mL), NaOH catalyst (0.54 g, 1% w/v),

temperature (65°C), reaction time (1 h). After completion of the reaction, the reaction mixture was kept standing in the separating funnel for 18–20 h. The mixture separated into two layers, viz. upper layer of biodiesel and lower layer of glycerol. Approximately, 27 mL of crude glycerol was produced from the transesterification reaction. The quantities of alkali and alcohol contaminants in crude glycerol were determined as follows: 0.85% w/v of NaOH (calculated by acid base titration) and 0.26% w/v methanol (determined using gas chromatograph).

4.2.3 Inoculum preparation

Freeze dried cultures of *Clostridium pasteurianum* were maintained in Reinforced Clostridial Medium (RCM). The composition of RCM in 1 L of distilled water was as follows: yeast extract 5.0 g, beef extract 10.0 g, peptone 10.0 g, glucose 5.0 g, starch 1.0 g, sodium chloride 5.0 g, sodium acetate 3.0 g, cysteine hydrochloride 0.5 g, agar 0.5 g. The pH of the medium was adjusted to 6.8 ± 0.2 using 1 M NaOH. The medium was inoculated and kept in a rotary incubator shaker (Make: Lab Companion; Model: SI–300R) at 37°C, 150 rpm for 24 h. The 24 h culture was used for streaking over agar plate having same medium composition with 15 g/L of agar, and the culture was kept at 37°C in a desiccator containing anaerobic gas pack. The culture broth was used as stock and was sub–cultured every month.

4.2.4 Batch fermentation

The cells from stock culture were grown in fresh RCM medium prior to inoculation under anaerobic conditions (Khanna et al., 2013). Batch experiments were set up by transferring inoculum from mid log phase of culture in 100 mL serum bottle containing BSH (a modified form of Basal solution for hydrogen production) (Chen et al., 2005, Junghare et al., 2012) medium with working volume of 60 mL comprising 6

mL (10% v/v) of *Clostridium pasteurianum* inoculum, 1.2 mL of 3% (w/v) L–cysteine HCl as a reducing agent, and 52.8 mL of fermentation medium (BSH) including substrate glycerol (10 g/L). Resazurin dye (0.1%w/v) was added into medium as an indicator of anaerobic conditions. The BSH medium comprised of following components (concentration, g/L): peptone (2), yeast extract (1), K_2HPO_4 (0.230), KH_2PO_4 (4.035), NaCl (2) in addition to 10 mL trace solution and 10 mL vitamin solution. Trace element solution comprised of following components (concentration, g/L): $MnO_4 \cdot 7H_2O$ (0.01), $ZnSO_4 \cdot 7H_2O$ (0.05), H_3BO_3 (0.01), $N(CH_2COOH)_3$ (4.5), $CaCl_2 \cdot 2H_2O$ (0.01), Na_2MoO_4 (0.01), $CoCl_2 \cdot 6H_2O$ (0.2), $AlK(SO_4)_2$ (0.01), $MgCl_2 \cdot 6H_2O$ (0.2), Fe_2Cl_3 (0.1), $CuCl_2 \cdot 6H_2O$ (0.05). The composition of vitamin solution was as follows (concentration, g/L): riboflavin (0.025), citric acid (0.02), folic acid (0.01) and para–amino benzoic acid (0.01). The initial pH of the medium was adjusted to 7 using 1M NaOH. Prior to inoculation, the medium was flushed with pure nitrogen (99.99%) for 15 min, sealed with rubber stoppers, crimped and autoclaved at 121°C, 15 psi for 15 min. The bottles were then inoculated with 10% v/v inoculum and incubated at 37°C and 150 rpm. All treatments were carried out in duplicate. Aliquots of fermentation broth were withdrawn periodically to assess the quantity of glycerol consumed. Similarly samples from gaseous phase were collected periodically to quantify H_2 and CO_2 content.

4.2.5 Analytical methods

Glycerol was quantified by HPLC analysis using a Rezex RCM Monosaccharide calcium–column (300 mm × 8 µm × 7.8 mm, Phenomenex, India) thermostated at 35°C with the help of external column oven (Model– HCO–02, PCI analytics Pvt. Ltd., India). The HPLC apparatus comprised of a pump (Series 200, Perkin Elmer), a refractive index detector (Series 200, Perkin Elmer) and a vacuum degasser (Series 200, Perkin Elmer).

Ultra–pure water (18.2 MΩ·cm resistivity at 25°C) was used as the mobile phase at a flow rate of 0.5 mL/min. Reaction mixture samples were centrifuged (12,000 rpm, 20 min) and filtered through a 0.2 µm membrane filter, and diluted appropriately prior to injection into HPLC. Standard calibration plots were used to determine residual concentration of glycerol in the samples of reaction mixture.

The composition of product gas of glycerol fermentation was determined using Gas Chromatograph (Make: Thermo scientific, Model: Ceres800 plus) with thermal conductivity detector (TCD) and Porapak Q (60/80 mesh) column employing argon as carrier gas at a flow rate of 30mL/min. The operational temperature at the column oven was 45°C and the injector and detector temperatures were maintained at 200°C. Gas samples were taken from the bottles and used to determine the contents of hydrogen and carbon dioxide. Hydrogen gas production was calculated from the headspace measurements and the total volume of gas produced for each time interval using the mass balance equation.

$$V_{H,i} = V_{H,i-1} + C_{H,i}(V_{G,i}-V_{G,i-1}) + V_H (C_{H,i}-C_{H,i-1}) \quad (4.1)$$

$V_{H,i}$ and $V_{H,i-1}$ are the cumulative hydrogen gas volumes at current (i) and previous time interval (i-1), respectively; $V_{G,i}$ and $V_{G,i-1}$ are total biogas volume at the current and previous time intervals; $C_{H,i}$ and $C_{H,i-1}$ are the fraction of hydrogen gas in the headspace at the current and previous time intervals; V_H is the volume of headspace of vials. The removed biogas volume for analysis was also taken into account during hydrogen mass balance.

4.2.6 Experimental design for medium optimization

4.2.6.1 Plackett–Burman design

The Plackett–Burman design was applied to evaluate significance of seven variables (i.e. yeast extract, K_2HPO_4, KH_2PO_4, peptone, NaCl, mineral solution and vitamin solution in twelve experimental runs. Each parameter was tested at two levels coded as (–1) for lower level and (+1) for higher level, as depicted in Table 4.1. These medium components and their limits were selected based on the published literature .MINITAB (Release 15.1, PA, USA, Trial Version) was used for experimental design analysis and data processing. Placket–Burman design is a two–level factorial design that follows first–order polynomial equation:

$$Y = \beta_0 + \sum_{i=1}^{n} \beta_i X_i \qquad (4.2)$$

Notations: Y– response variable (Hydrogen (%v/v)), β_0– model intercept, β_i– linear coefficient and X_i – optimization variable (or medium component) (Plackett and Burman, 1946). Each experimental run was carried out in triplicate to access reproducibility, and the average response value in each experiment was considered for analysis. The analysis of variance was carried out with a confidence interval of 95%. The significant variables from this result were further analyzed using central composite design (CCD) of experiments.

4.2.6.2 Central composite design

The central composite design is commonly used to study significant interaction effect between variables. Four significant medium components from previous Plackett–Burman design, viz. peptone, yeast extract, NaCl and K_2HPO_4 at five coded levels (–α, –1, 0, +1, +α) were used for the experiments, as described in Table 4.4. The experimental

design constituted 31 individual runs ($=2^k+2k+n_0$), where 'k' is the number of independent variables, and n_o is the number of replicate runs at the center point of the variable. The experimental runs were generated using Minitab statistical software (Release 15.1, Trial Version).

Table 4.1. Factors and levels used in Plackett–Burman design matrix for production of hydrogen from crude glycerol

Factors (g/L)	Levels	
	Low (–α)	High (+α)
(X_1) – Peptone	1	4
(X_2) – Yeast extract	0.5	2
(X_3) – NaCl	0.5	2
(X_4) – K_2HPO_4	0.1	1
(X_5) – KH_2PO_4	2	8
(X_6) – Vitamin solution (mL/L)	2	10
(X_7) – Mineral solution (mL/L)	2	10

4.2.6.3 Statistical analysis and model fitting

The experimental data given in Table 4.2Bwas fitted to the following quadratic model containing coefficients corresponding to individual and interactive effects of parameters:

$$Y = \beta_0 + \sum_{i=1}^{k} \beta_i X_i + \sum_{i=1}^{k} \beta_{ii} X_i^2 + \sum_{i \neq j} \sum_{i} \beta_{ij} X_i X_j \qquad (4.3)$$

Notation: Y – measured response variable (% Hydrogen), k – number of factors or medium components, β_o – intercept (or regression constant), β_i – linear coefficient, β_{ii} – quadratic coefficient, and β_{ij} – interaction coefficient. The coded values (x) of the actual experimental variables were determined using eq. 4.4:

$$X = (x_i - x_o)/\Delta x \qquad (4.4)$$

where, i = 1, 2, 3…, X is the dimensionless value of the variables; x_o is the value of the variable x at center point and Δx is the step change. The significance of each factor in

fitted model was determined by signal to noise ratio and by the analysis of variance (ANOVA). ANOVA of the linear, quadratic and interaction regression coefficients (i.e., F– value and p– value. The F– and p– values of linear and interaction coefficients essentially exhibit the individual and interactive effects of the independent variables on the response variable, i.e. % H_2. p– values of linear and interaction coefficients indicate nature of interaction between independent variables. The interactive effect of the factors was studied by plotting response surface plots and the corresponding contour plots.

4.2.6.4 Validation experiments

For the assessment of the accuracy of the optimum medium composition predicted by the statistical analysis, glycerol fermentation experiments have been conducted using the medium composition resulting from statistical analysis. Fermentation experiments have been carried out using both pure as well as crude glycerol. Reproducibility of fermentation results was checked by performing all validation experiments in triplicate.

4.3 RESULTS AND DISCUSSION

4.3.1 Plackett–Burman design for screening of significant medium components

The results of initial screening of medium components using Plackett–Burman design are given in Table 4.2. The experimental and predicted values for % H_2 (v/v) match very well. The statistical analysis of Plackett–Burman design is given in Table 4.3A and B. The values of the first–order model coefficients for all seven variables along with *t* value and *p*–value are depicted in Table 4.3A, while the ANOVA of the model is given in Table 4.3B. The *t*–value limit for analysis is 2.78 as shown in the Pareto plot (Fig. 4.1). The *t*–value for yeast extract, NaCl, peptone and K_2HPO_4 are higher than this limit, which points towards their significance. KH_2PO_4 and mineral solution has a negative effect on H_2 production as depicted from both Pareto plot and negative Placket–

Burman model coefficient. The overall regression coefficient for the model is R^2 = 0.9797, with adjusted R^2 = 0.9441 shows the model fits very well to the data. The model equation for hydrogen (%v/v) could be written as:

$$Y = 30.87 + 2.72\,X_1 + 8.74\,X_2 + 5.37\,X_3 + 2.53\,X_4 - 1.19\,X_5 + 0.19\,X_6 - 1.13\,X_7 \quad (4.5)$$

Table 4.2: Plackett–Burman design matrix with coded values and %v/v hydrogen

Run order	X_1	X_2	X_3	X_4	X_5	X_6	X_7	% Hydrogen (v/v)	
								Experimental	Predicted
1	1	–1	1	–1	–1	–1	1	28.00± 0.945	27.55
2	1	1	–1	1	–1	–1	–1	41.11± 1.142	41.62
3	–1	1	1	–1	1	–1	–1	38.79 ± 2.224	39.47
4	1	–1	1	1	–1	1	–1	36.48 ± 2.052	35.27
5	1	1	–1	1	1	–1	1	37.48 ± 1.339	36.97
6	1	1	1	–1	1	1	–1	46.00 ± 3.067	45.32
7	–1	1	1	1	–1	1	1	42.00 ± 2.241	45.03
8	–1	–1	1	1	1	–1	1	26.16 ± 1.112	24.78
9	–1	–1	–1	1	1	1	–1	17.16 ± 2.205	16.71
10	1	–1	–1	–1	1	1	1	12.50± 3.043	14.83
11	–1	1	–1	–1	–1	1	1	32.27± 1.156	29.24
12	–1	–1	–1	–1	–1	–1	–1	12.50± 3.028	13.64

Table 4.3: Statistical analysis of results from Plackett–Burman experimental design.

(A) Model coefficients, *t*–and *p*–value for each variable

Model term	Effect	Coefficient Estimate	Computed *t*–value	*p*–value
Intercept		30.87	38.84	0.000*
X_1	5.45	2.72	3.43	0.027*
X_2	17.47	8.74	10.99	0.000*
X_3	10.74	5.37	6.75	0.003*
X_4	5.05	2.53	3.18	0.034*
X_5	–2.38	–1.19	–1.50	0.209
X_6	0.39	0.19	0.25	0.816
X_7	–2.27	–1.13	–1.43	0.226

* Significant *p* values, $p \leq 0.05$; $R^2 = 0.9797$; Predicted $R^2 = 0.8169$; Adjusted $R^2 = 0.9441$

(B) ANOVA for the model

Term	Sum of squares	DF	Mean square	*F*–value	*p*–value
Model	1460.48	7	208.64	27.52	0.003
X_1	89.05	1	89.05	11.75	0.027
X_2	916.13	1	916..13	120.85	0.000
X_3	345.72	1	345.72	45.61	0.003
X_4	76.66	1	76.66	10.11	0.034
X_5	16.97	1	16.97	2.24	0.209
X_6	0.47	1	0.47	0.06	0.816
X_7	15.48	1	15.48	2.04	0.226
Residual error	30.32	4	7.58		
Total	1490.80	11			

DF – degree of freedom; SS – sum of squares; MS – mean square

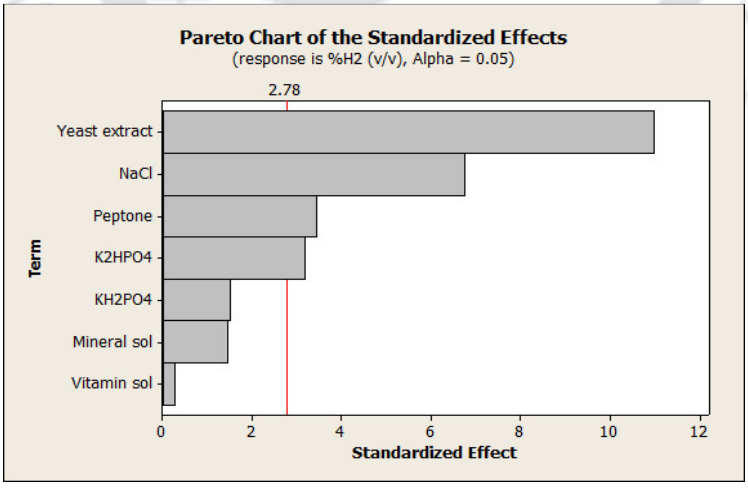

Figure 4.1: Pareto plot for Plackett–Burman analysis

4.3.2 Central composite design for optimization of medium components

The central composite design (CCD) was used to optimize the resulted significant variables from Plackett–Burman design. Plackett–Burman study revealed that, peptone, yeast extract, NaCl and K_2HPO_4 has significant effect on hydrogen production. The full factorial CCD matrix of these variables is given in Table 4.4.

Fitting of the experimental data of response variable (i.e. % v/v H_2 content of product gas) to the quadratic regression model using coded values of independent variables listed in Table 4.4yielded following equation:

$$Y = 45.171 + 1.767X_1 + 2.779X_2 + 3.663X_3 + 2.353X_4 - 1.497X_1X_2 + 0.159X_1X_3 + 1.086X_1X_4 - 1.216X_2X_3 + 1.431X_2X_4 + 2.101X_3X_4 - 2.523X_1^2 - 1.898X_2^2 - 3.480X_3^2 - 4.188X_4^2 \quad (4.6)$$

The values of the response variable predicted by the quadratic response model have also been given in Table 4.4. It could be seen from Table 4.4that experimental and model predicted values of the response variable are in close agreement, which indicates the best fit of the model to experimental data. The statistical analysis of the quadratic response model is given in Table 4.5A that lists the coefficients of the model (given in eq. 4.6) along with their *p*– and *t*–values.

Analysis of variance (ANOVA) of the quadratic model is given in Table 4.5B. ANOVA results show that regression model was highly significant ($p < 0.01$), while the lack of fit was not significant ($p > 0.05$). Coefficient of determination (R^2) was 0.963, which indicated that 96.3% variation in the response variable could be explained using the model. $R^2 = 0.963$ also indicated best fit of the model to the experimental data, which is also corroborated by close agreement of the experimental and model–predicted values of response variable.

Table 4.4. Central composite design matrix of three medium components in coded and actual (in parenthesis, g/L) values along with experimental and predicted values for hydrogen (%v/v)

Run order	Peptone $(X_1)^*$	Yeast Extract $(X_2)^*$	NaCl $(X_3)^*$	K_2HPO_4 $(X_4)^*$	% Hydrogen (v/v)	
					Experimental	Predicted
1	–1 (1.75)	–1 (0.875)	–1 (0.87)	–1 (0.325)	22.01±0.577	24.58
2	+1 (3.25)	–1 (0.875)	–1 (0.87)	–1 (0.325)	28.39±0.822	28.62
3	–1 (1.75)	+1 (1.625)	–1 (0.87	–1 (0.325)	31.16±0.239	32.71
4	+1 (3.25)	+1 (1.625)	–1 (0.87)	–1 (0.325)	30.49±0.207	30.75
5	–1 (1.75)	–1 (0.875)	+1 (1.62)	–1 (0.325)	31.77±0.423	29.82
6	+1 (3.25)	–1 (0.875)	+1 (1.62)	–1 (0.325)	33.12±0.674	34.49
7	–1 (1.75)	+1 (1.625)	+1 (1.62)	–1 (0.325)	30.54±0.631	33.08
8	+1 (3.25)	+1 (1.625)	+1 (1.62)	–1 (0.325)	30.99±0.341	31.76
9	–1 (1.75)	–1 (0.875)	–1 (0.87)	+1 (0.775)	20.75±0.102	20.05
10	+1 (3.25)	–1 (0.875)	–1 (0.87)	+1 (0.775)	28.52±0.654	28.43
11	–1 (1.75)	+1 (1.625))	–1 (0.87)	+1 (0.775)	32.83±0.647	33.90
12	+1 (3.25)	+1 (1.625)	–1 (0.87)	+1 (0.775)	34.27±0.287	36.29
13	–1 (1.75)	–1 (0.875)	+1 (1.62)	+1 (0.775)	31.50±0.812	33.69
14	+1 (3.25)	–1 (0.875)	+1 (1.62)	+1 (0.775)	44.19±0.478	42.72
15	–1 (1.75)	+1 (1.625)	+1 (1.62)	+1 (0.775)	42.84±0.567	42.68
16	+1 (3.25)	+1 (1.625)	+1 (1.62)	+1 (0.775)	45.84±0.782	45.71
17	–α (1.00)	0 (1.250)	0 (1.25)	0 (0.550)	33.84±0.723	31.54
18	+α (4.00)	0 (1.250)	0 (1.25)	0 (0.550)	38.84±0.561	38.61
19	0 (2.50)	–α (0.500)	0 (1.25)	0 (0.550)	31.84±0.671	32.02
20	0 (2.50)	+α (2.000)	0 (1.25)	0 (0.550)	45.84±0.357	43.14
21	0 (2.50)	0 (1.250)	–α (0.50)	0 (0.550)	26.12±0.421	23.92
22	0 (2.50)	0 (1.250)	+α (2.00)	0 (0.550)	38.90±0.231	38.58
23	0 (2.50)	0 (1.250)	0 (1.25)	–α (0.100)	26.12±0.543	23.71
24	0 (2.50)	0 (1.250)	0 (1.25)	+α (1.000)	33.23±0.612	33.12
25	0 (2.50)	0 (1.250)	0 (1.25)	0 (0.550)	45.00±0.412	45.17
26	0 (2.50)	0 (1.250)	0 (1.25)	0 (0.550)	45.80±0.723	45.17
27	0 (2.50)	0 (1.250)	0 (1.25)	0 (0.550)	46.00±0.831	45.17
28	0 (2.50)	0 (1.250)	0 (1.25)	0 (0.550)	46.70±0.301	45.17
29	0 (2.50)	0 (1.250)	0 (1.25)	0 (0.550)	43.00±0.436	45.17
30	0 (2.50)	0 (1.250)	0 (1.25)	0 (0.550)	45.70±0.510	45.17
31	0 (2.50)	0 (1.250)	0 (1.25)	0 (0.550)	44.00±0.626	45.17

Table 4.5. Results of central composite design for optimization of fermentation parameters

(A) The coefficients of quadratic regression model and their *t*– and *p*– values

Model term	Coefficient	*t*–value	*p*–value Prob >*F*
Intercept (A_0)	45.171	58.024	0.000*
Linear coefficients			
Peptone (X_1)	1.767	4.204	0.001*
Yeast extract (X_2)	2.779	6.611	0.000*
NaCl (X_3)	3.663	8.713	0.000*
K_2HPO_4 (X_4)	2.353	5.599	0.000*
Square coefficients			
Peptone (X_1^2)	–2.523	–6.551	0.000*
Yeast extract (X_2^2)	–1.898	–4.929	0.000*
NaCl (X_3^2)	–3.480	–9.035	0.000*
K_2HPO_4 (X_4^2)	–4.188	–10.875	0.000*
Interaction coefficients			
Peptone and Yeast extract ($X_1 \times X_2$)	–1.497	–2.909	0.010*
Peptone and NaCl ($X_1 \times X_3$)	0.159	0.310	0.761
Peptone and K_2HPO_4 ($X_1 \times X_4$)	1.086	2.110	0.051
Yeast extract and NaCl ($X_2 \times X_3$)	–1.216	–2.363	0.031*
Yeast extract and K_2HPO_4 ($X_2 \times X_4$)	1.431	2.781	0.013*
NaCl and K_2HPO_4 ($X_3 \times X_4$)	2.101	4.081	0.001*

(B) ANOVA for quadratic model

Source	DF	SS	MS	*F*–value	*p*–value Prob >*F*
Regression	14	1788.70	127.76	30.12	0.000*
Linear	4	715.47	178.86	42.16	0.000*
Square	4	890.87	222.72	52.50	0.000*
Interaction	6	182.36	30.39	7.16	0.001*
Residual (Error)	16	67.88	4.24		
Lack of fit	10	58.06	5.80	3.55	0.088
Pure error	6	9.81	1.64		
Total	30	1856.58			

*Significant p values, $p \leq 0.05$; $R^2 = 0.963$; Predicted $R^2 = 0.813$; Adjusted $R^2 = 0.931$

The *t*–test,*F*–values and *p*–values of quadratic model coefficients indicate relative significance of corresponding independent variables. A large *t*–stat value and *p*–value < 0.05 indicates significance of the coefficient and the corresponding independent variable. Relative *F*–values of linear, interaction and quadratic coefficient indicate significance of the individual effects of independent variables and the magnitude of interaction between them. As per ANOVA results given in Table 4.5B, *F*–value of overall regression is 30.12, while *F*–value of linear coefficient is 42.16. *F*–value of 7.16 for interaction coefficients is much smaller than *F*–value for linear coefficients, which implies relatively standalone or unrelated effect of independent variables on the % v/v H_2 content of product gas. *p*–values of all linear and quadratic coefficients are < 0.05 with large absolute *t*–values, which indicates that all variables have significant effect on % v/v H_2 content of product gas. The *t*–values of interaction coefficients are relatively smaller than linear and square coefficients indicating their relative less significance. Moreover, *p*–values of interaction coefficients between peptone and NaCl; and peptone and K_2HPO_4 concentration is > 0.05, which further confirms that the interaction between these variables is insignificant or in other words, these variables have independent effect on the response variable. The *p*–value of the interaction coefficient between yeast extract–NaCl; yeast extract–K_2HPO_4 and NaCl–K_2HPO_4 is < 0.05, which signifies that these variables have an inter–related effect on response variable. Relatively small *F*–value of 3.55 for The Lack of Fit with *p*–value of 0.088 implies that Lack of Fit is not significant as compared to the pure error, or in other words the model was significant.

The contour plots (Fig. 4.2 A, B, C, D) reveal interactions among any two independent variables on the response variable (% v/v H_2 content of product gas). The contour plots (which essentially are graphical representation of regression eq. 4.6) represent infinitive number of combinations of two test variables, with the third variable

maintained at its zero (or center point) level. The shapes of response surface contours, whether elliptical, circular, or saddle point, explain the magnitude of interaction between independent variables (Tanyildizi et al., 2005; Ravikumar et al., 2005). For strong interactions among the variables, the contour plots have perfectly elliptical shape. The surface confined in the smallest contour represents parameter space for maximum value of response variable.

A peculiar facet of the contour plots is that each of these plots has a clear highest point, which means that the maximum hydrogen production could be achieved inside the design boundary. The contour plots of peptone vs. NaCl have circular shape, which points to relatively individual effect (or insignificant interactions) between the parameters. This is also corroborated by p–value > 0.05 for the interaction coefficients for these variables, as noted earlier. On the other hand, the contour plots between K_2HPO_4 vs NaCl, K_2HPO_4 vs yeast extract, NaCl vs. yeast extract and yeast extract vs. peptone has elliptical shape, which reveals significance of interaction between these variables. This result is also corroborated by the ANOVA results, i.e. p–value < 0.05 for the interaction coefficient of these factors. In the given range of optimization parameters, the highest H_2 content of 48.10% v/v in product gas is obtained for peptone, 2.7g/L; yeast extract, 1.48 g/L; NaCl, 1.46g/L; K_2HPO_4, 0.68 g/L as depicted from the desirability function plot shown in Fig.4.3A

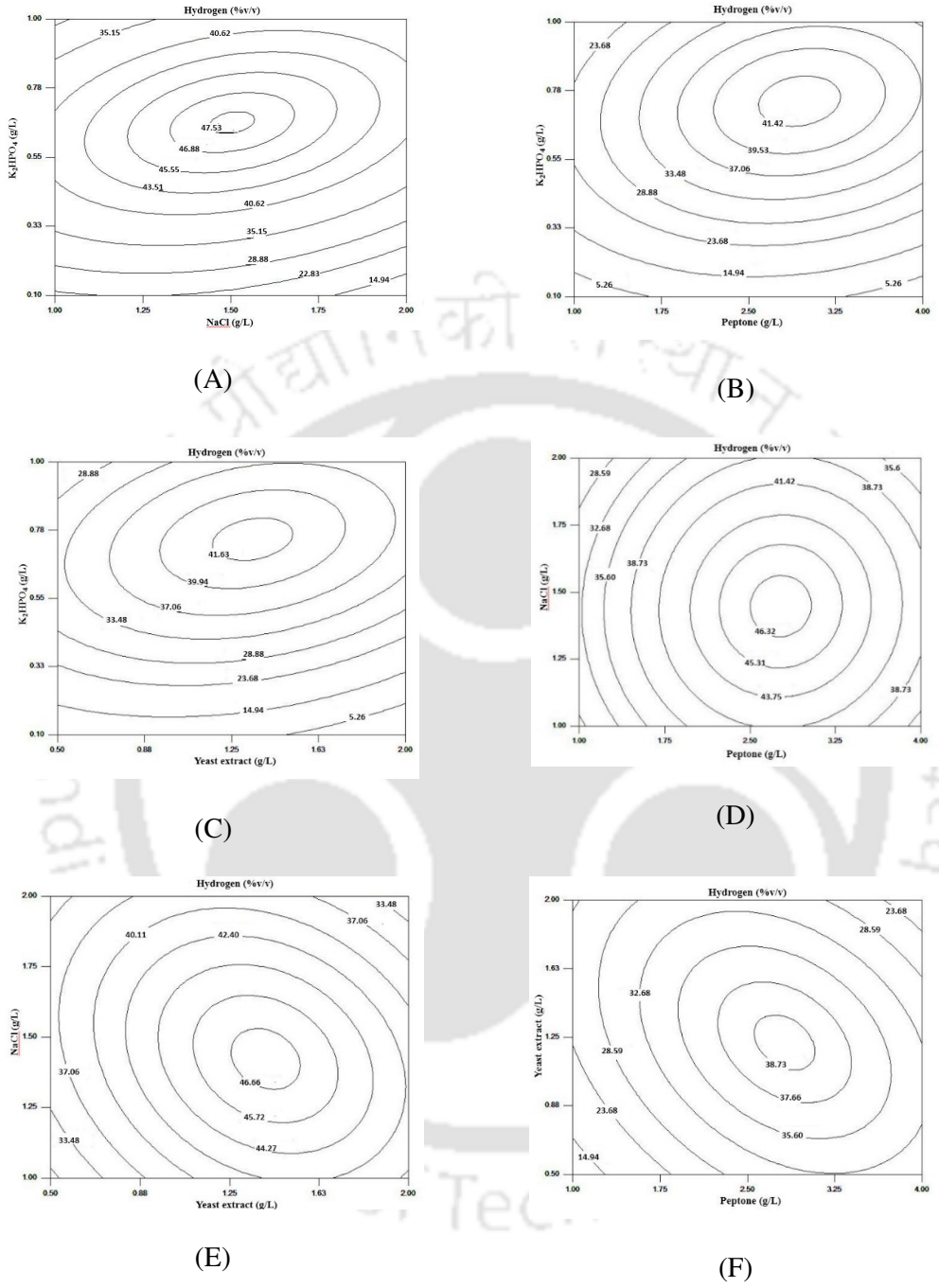

Figure 4.2. Contour plots depicting interactions among different optimization parameters for H_2 production (A) K_2HPO4 and NaCl (B) K_2HPO4 and peptone (C) K_2HPO4 and yeast extract (D) NaCl and peptone (E) NaCl and peptone (F) yeast extract and peptone

4.3.3 Validation of experiments for biohydrogen production with optimized medium

The desirability function plot showing optimum concentration of medium components is shown in Fig. 4.3A. As noted earlier, validation of the statistical analysis of medium composition for glycerol fermentation was done by conducting fermentation experiments with optimum medium compositions predicted by the CCD analysis. Fig. 4.3B depicts the profile of production of H_2 in these experiments using crude glycerol as substrate with *C. pasteurianum.* The final hydrogen content in the product gas achieved with crude glycerol was 47.45 %v/v, which is in close agreement with the prediction of CCD analysis (48.10 %v/v). This gave a measurable yield of 0.745 mol H_2/mol glycerol which showed ~26% increment compared to our previous report which used un-optimized fermentation medium.

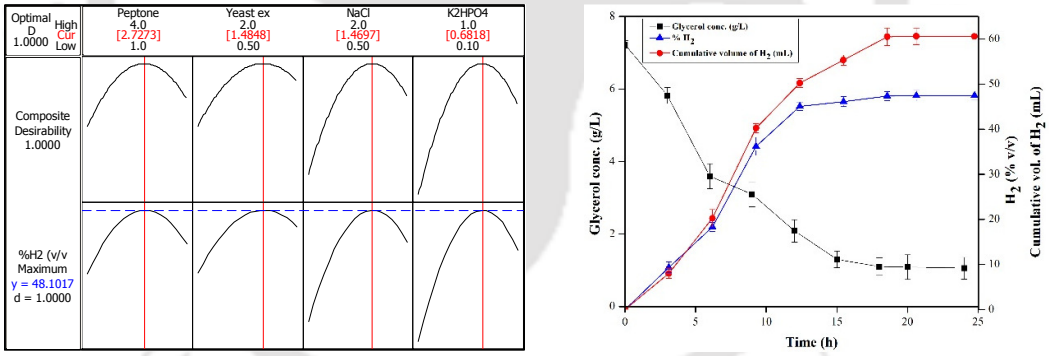

(A) (B)

Figure 4.3. Results of validation experiments (A) Desirability function plot showing the optimum levels of medium components (B) Time profiles of substrate consumption (crude glycerol, g/L), Cumulative volume of H_2 (mL)and H_2 concentration (% v/v) in product gas with

4.3.4 Analysis of effect of medium components

The statistical optimization of fermentation medium components has revealed yeast extract, NaCl, peptone and K_2HPO4 as the significant components. In this section, an attempt is made to identify their influence on the fermentative hydrogen production process. Yeast extract is a good complex nutritional source of amino-nitrogen, vitamins, and other unknown growth factors for many microbial organisms (Smith et al., 1975). The main functional components in yeast extract (Johnson et al., 1981) that are used by Clostridia are p-aminobenzoic acid, vitamin B_{12}, pyridoxamine, and biotin. Yeast extract is also necessary for the growth of the hydrogen producer *C. thermopalmarium* (Sohet al., 1991). Zhang et al., 2014 explained the importance of yeast extract on pH of the medium which is an important process parameter for fermentative hydrogen production and also affirmed that the yeast extract of high concentration (more than 2.0 g/L) might promote the role of hydrogen consumption at the latter part of the fermentation by activation of uptake hydrogenase. In this study, the optimized yeast extract value 1.48 g/L falls in this range and hence has a significant effect on H_2 production by *C. pasteurianum*. Similar studies were reported which also supported the significance of yeast extract on hydrogen production by clostridia (Geng et al., 2010; Ferchichi et al., 2005). Further, Li et al. (2011) have demonstrated that three amino acids (glycine, serine and tyrosine) in yeast extract accelerate the production of alcohol–dependent enzymes such as glycerol dehydrogenase, the immediate enzyme in glycerol metabolism. Peptone is another source of nitrogen which is required for cell growth and maintenance.

Beneficial effect of NaCl has already been supported in our previous work (Sarma et.al., 2016) as Na+ ions work towards faster trans-membrane transport of

nutrients and substrate to intracellular region, which essentially improves enzymatic reactions in glycerol metabolism resulting in higher hydrogen production. Xiaolong et al. (2006)have studied the effect of sodium ion concentration on hydrogen production from sucrose and the optimum sodium ion concentration reported is in the range of 1–2 g/L. Xiaolong et al. (2006)have also reported that Na+ concentrations above 4 g/L showed marked reduction in hydrogen production. This reduction is attributed to adverse effect of high Na+ concentration on microbial enzyme activities such as dehydrogenase activity, alkaline phosphatase and adenosine tri phosphate. Khanna et al. (2011) have assessed the effect of sodium ions on hydrogen production and concentration upto 250mM of sodium ion is beneficial for growth of hydrogen producing bacteria.

K_2HPO4 in the medium acts as a source of both potassium and phosphate which are important growth enhancing nutrients. Moreover, K_2HPO4 also acts as a buffering agent and it helps in maintenance of pH of the fermentation broth at a desired value (Yalcin and Ozbas, 2008) and pH is a significant factor for biohydrogen production process (Sarma et al. 2016).

4.4 CONCLUSIONS

This study attempted to optimize hydrogen production from crude glycerol using *Clostridium pasteurianum*. Hydrogen production was revealed to be influenced by medium components that augment activity and substrate promiscuity of hydrogenase and other enzymes involved in glycerol metabolism. Peptone is a source of nitrogen which is required for cell growth and maintenance, whereas K_2HPO4 help maintain pH of the medium which is very essential for production of fermentative hydrogen. Yeast extract,

which provides growth factors and amino acids accelerating production of alcohol degrading enzyme, was also revealed as essential component of the medium.

References

Chen, W.M., Tseng, Z.J., Lee, K.S., Chang, J.S., 2005. Fermentative hydrogen production with *Clostridium butyricum* CGSS isolated from anaerobic sewage sludge. Int J Hydrogen Energ. 30, 1063-1070.

Ferchichi, M., Crabbe, E., Hintz, W., Gil, G-H., Almadidy, A., 2005. Influence of culture parameterson biological hydrogen production by *Clostridium saccharoperbutyl-acetonicum* ATCC 27021. World J Microbiol. Biotechnol. 21, 855-862.

Geng, A., He, Y., Qian, C., Yan, X., Zhou, Z., 2010. Effect of key factors on hydrogen production from cellulose in a co-culture of *Clostridium thermocellum* and *Clostridium thermopalmarium*. Bioresour. Technol. 101, 4029–4033.

Jitrwung, R., Yargeau, V., 2011. Optimization of media composition for the production of biohydrogen from waste glycerol. Int. J. Hydrogen Energ. 36, 9602–9611.

Johnson, M.J., Peterson, W.H., Fred, E.B., 1931. Oxidation and reduction relations between substrate and products in the acetone butyl alcohol fermentation. J. Biol. Chem.91, 569–591.

Junghare, M., Subudhi, S., Lal, B., 2012. Improvement of hydrogen production under decreased partial pressure by newly isolated alkaline tolerant anaerobe, *Clostridium butyricum* TM-9A: Optimization of process parameters. Int J Hydrogen Energy. 37, 3160-68.

Khamtib, S., Plangklang, P., Reungsang, A., 2011. Optimization of fermentative hydrogen production from hydrolysate of microwave assisted sulfuric acid pretreated oil palm trunk by hot spring enriched culture. Int J Hydrogen Energ. 36,14204-14216.

Khanna, N., Kotay, S.M., Gilbert, J.J., Das, D., 2011. Improvement of biohydrogen production by *Enterobacter cloacae* IIT–BT 08 under regulated pH. J. Biotechnol. 152, 9–15.

Khanna, S., Goyal, A., Moholkar, V.S., 2013a. Effect of fermentation parameters on bio–alcohols production from glycerol using immobilized *Clostridium pasteurianum*: an optimization study. Prep. Biochem. Biotechnol. 43, 828–847.

Li, M., Liao, X., Zhang, D., Du, G., Chen, J., 2011. Yeast extract promotes cell growth and induces production of polyvinyl alcohol‐degrading enzymes. Enzyme Res. 2011, 179819. doi:10.4061/2011/179819.

Prasertsan, P., O-Thong, S., O-Thong, N.K., 2009. Optimization and microbial community analysis for production of biohydrogen from palm oil mill effluent by thermophilic fermentative process. Int J Hydrogen Energ. 34, 7448-7459.

Plackett, R.L., Burman, J.P., 1946. The design of optimum multifactorial experiments. Biometrika. 33, 305‐325.

Ravikumar, K., Pakshirajan, K., Swaminathan, T., Balu, K., 2005. Optimization of batch process parameters using response surface methodology for dye removal by a novel adsorbent. Chem. Eng. J. 105, 131–138.

Saraphirom, P., Reungsang, A., 2010. Optimization of biohydrogen production from sweet sorghum syrup using statistical methods. Int J Hydrogen Energ. 35(24), 13435-13444.

Sarma, S., Dubey, V.K., Moholkar, V.S., 2016. Kinetic and thermodynamic analysis (with statistical optimization) of hydrogen production from crude glycerol using *Clostridium pasteurianum*. Int. J. Hydrogen Energ. 33, 1471–1482.

Sittijunda, S., Reungsang, A., 2012. Biohydrogen production from waste glycerol and sludge by anaerobic mixed cultures. Int. J. Hydrogen Energ. 37, 13789–13796.

Smith, T.J., Hillier, A.J. and Lee, G.J. (1975) The nature of thestimulation of the growth of Streptococcus lactis by yeast extract.Journal of Dairy Research 42, 123–138.

Soh, A. L. L., Ralambotiana, H., Ollivier, B., Prensier, G., Tine, E. & Garcia, J.-L. (1991). *Clostridium thermopalmarium* sp. nov., amoderately thermophilic butyrate-producing bacterium isolatedfrom palm wine in Senegal. Syst Appl Microbiol 14,135±139.

Tanyildizi, M.S., Ozer, D., Elibol, M.,2005. Optimization of α–amylase production by *Bacillus sp.* using response surface methodology. Process. Biochem. 40, 2291–2296.

Wang, J., Wan, W., 2008. Optimization of fermentative hydrogen production process by response surface methodology. Int. J. Hydrogen Energ. 33, 6976–6984.

Xiaolong, H., Minghua, Z., Hanqing, Y., Qinqin, S., Lecheng, L., 2006. Effect of sodium ion concentration on hydrogen production from sucrose by anaerobic hydrogen–producing granular sludge. Chinese J. Chem. Eng. 14, 511–517.

Yalcin, S.K., Ozbas, Z.Y., 2008. Effects of ammonium sulfate concentration on growth and glycerol production kinetics of two endogenic wine yeast strains. Indian

J.Biotechnol. 7, 89-93.

Zhang, L., Ban, Q., Li, J., Xu, Y. 2014. Assessment of Effects of Yeast Extract on Bio-hydrogen Production from Anaerobic Activated Sludge. Int J Agricult. Biol. 6, 1189-1193

Chapter 5

Genetic Engineering of *Clostridium pasteurianum* for Improved Hydrogen Production from Crude Glycerol

5.1 INTRODUCTION

Clostridium pasteurianum is a mesophilic, strictly anaerobic, Gram-positive bacterium that possesses the metabolic capacity to ferment glycerol as a sole source of carbon and energy, yielding a mixture of gases (hydrogen and carbon dioxide), acids (acetic and butyric), and alcohols (ethanol, butanol, and 1,3-propanediol) (Biebl et al., 2001 and Dabrock et al., 1992). Unlike the past industrial workhorses, *C. acetobutylicum* and *C. beijerinckii*; *C. pasteurianum* has garnered nominal attention as a potential host for the production of biofuel. There was a lack of available genetic tools to alter molecular pathways in *Clostridium pasteurianum* mainly due to difficulties in genetic

accessibility of the organism This is largely due to the current inability to transfer DNA to *C. pasteurianum*, in addition to lack of a genome sequence for this organism. Based on early genetic studies, it appears efforts were in place to conduct genetic manipulation of *C. pasteurianum*, since a method for producing and regenerating protoplasts was developed (Clarke et al., 1979) and a Type-II restriction endonuclease was identified as a potential barrier to gene transfer (Richards et al., 1988). In contrast to Gram-negative bacteria, Gram-positive cells possess an extensive exterior network of peptidoglycan which physically restricts passage of exogenous DNA into the cell. For this reason, electrotransformation of Gram-positive species is generally less efficient than Gram-negative strains (Trevors et al., 1992). Poor electrotransformation efficiency of Gram-positive bacteria is further compounded within the clostridia due to the unusually high production of non-specific cell-wall-associated nucleases (Mermelstein et al., 1992). A number of highly-specific clostridial Type-II restriction endonucleases have also been identified (Jennert et al., 2000; Mermelstein et al., 1992; Klapatch et al., 1996), including CpaAI from *C. pasteurianum* ATCC 6013 (Richards et al., 1988), highlighting the importance of DNA protection via methylation of the transforming DNA. Unidentified restriction-modification systems are likely the underlying cause of electrotransformation recalcitrance that has been observed with certain species, such as *C. butyricum* (Gozalez-Pajuelo et al., 2005). But recently several recent strategies have been employed in an attempt to alter the central metabolism of *C. pasteurianum* to enhance its productivity. It is clear that metabolic engineering will play a central role in the development of *C. pasteurianum* as an efficient industrial producer. To this end, an electroporation-mediated method of transformation was recently established (Pyne et al., 2013), allowing gene transfer to *C. pasteurianum*. Such efficient plasmid transfer paves the way to

rational metabolic engineering strategies, including gene disruption, knockdown, and overexpression techniques (Papoutsakis et al., 2008; Pyne et al., 2014), very few of which have been explored using *C. pasteurianum* (Pyne et al., 2015; Schwarz et al., 2017).

5.1.1 *hydA*- Iron only hydrogenase

Hydrogenase is the key enzyme involved in catalyzing the reversible reaction of protons to molecular hydrogen (H_2). Hydrogenase was first described by Stephenson and Stickland in 1931 and since then extensive research has been conducted on the structure, function and mechanism of hydrogenase. Hydrogenases are characterized by the metal atoms present in their active site which plays an important role in the enzyme activity and based on this hydrogenases can be categorized into three distinct classes as [NiFe], [Fe-Fe] and [Fe] hydrogenase. Among these, [NiFe] constitute the largest number of hydrogenases found in bacteria and archaea. It has a bimetallic active site with nickel and an iron atom. [NiFe] hydrogenases are membrane bound enzymes, characterized by a dual function of H_2 formation and consumption refered to as uptake hydrogenases widely found in cyanobacteria such as Nostoc and Anabena (Kim et al., 2011). Unlike the second group, [FeFe]-hydrogenases are monomeric and contain only one catalytic subunit with a two iron atoms, is found in both eukaryotes and prokaryotes. This group of hydrogenase is particularly involved in H_2 production lacking H_2 consumption activity. And lastly the [Fe]-hydrogenases or [Fe]-only-hydrogenases which are only found in methanogenic Archaea (Calusinska et al., 2010). It catalyzes CO_2 reduction with H_2 to methane (Vignais and Colbeau, 2004). In bacteria, hydrogenases regulate the H^+ levels in the cells and thus, are actively involved in redox regulation and in

maintaining the proton motive force. Clostridia rely foremost on [FeFe]-hydrogenases but a few species possess [Fe]-hydrogenase and [NiFe]-hydrogenase (Calusinska et al., 2010). In *C. pasteurianum,* 4 hydrogenases were found in the genome (CLPA_c00280, CLPA_c07060-70, CLPA_c33960 and CLPA_c37830) (Poehlein et al., 2015). With CLPA_c07060 and CLPA_c07070 *C. pasteurianum* seems to possess a rare [NiFe]-hydrogenase with the genes encoding the small and large subunit, respectively. The BLAST searches and the reports by Pyne et al. (2014) affirms the respective gene of CLPA c00280 as *hydA*. Further knock-down of *hydA* by Schwarz et al., 2017 clearly show that deletion of the hydrogenase encoded by CLPA c00280 is tightly involved with the fermentative pathway in *C. pasteurianum*. Metabolic engineering strategies has been applied to hydrogenases mostly for increasing solvent production or decreasing other by-product formation such as acids. Many reports are focused on knock-down or deletion of hydrogenase which involves *hydA* knock-down via anti-sense RNA in *C. pasteurianum* (Pyne et al., 2015), attempted disruption of *C. acetobutylicum hydA* (Cooksley et al., 2012), deletion of the hydrogenase maturase gene *hydG* in *C. thermocellum* (Biswas et al., 2015). Previous work for improvement of hydrogen generation in clostridia involves over-expression of iron-only hydrogenase gene (*hydA)* in *C. paraputrificum* (Morimoto et al., 2005, Klein et al., 2010). Over-expression of hydrogenase in *C. acetobutylicum* DSM 729 did not show any influence on fermentation pattern and it was concluded that intracellular hydrogenase concentration does not limit hydrogen formation in this strain (Klein et al., 2010). Therefore the role of *hydA* as the key enzyme in hydrogen formation varies from organism to organism. However in *C. pasteurianum* the key role of *hydA* in the fermentative pathway was identified by Schwarz et al., 2017. Therefore, attempts to overexpress the *hydA* were carried out in this study.

To my knowledge there is no report of *hydA* over-expression in *C. pasteurianum* in terms of increasing hydrogen yield. This study presents the fermentation pattern of *C. pasteurianum* with overexpressed *hydA*.

5.1.2 *dhaD1:dhaK*- Glycerol dehydrogenase and dihydroxyacetone kinase

Under anerobic conditions bioconversion of glycerol is mediated through the *dha* system which is composed of four enzymes viz., glycerol dehydrogenase, dihydroxyacetone kinase, glycerol dehydratase and 1, 3-propanediol oxidoreductase (Forage et al., 1982a, 1982b).These enzymes are involved in two parallel pathways of anaerobic micro-organisms namely, oxidative and reductive pathway. The oxidative pathwayleads from glycerol to pyruvate to enter the fermentative pathway. The second pathway is reductive and goes from glycerol via 3-hydroxypropionaldehyde (3-HPA) to 1,3-PDO (Biebl et al., 1999; Malaviya et al., 2012).

In the oxidative branch glycerol dehydrogenase (*dhaD or gldA*) converts glycerol to dihydroxyacetone using NAD^+ and dihydroxyacetone is phosphorylated by dihydroxyacetone kinase (*dhaK*) in a coupled reaction with pyruvate kinase to dihydroxyacetone-phosphate which enters glycolysis and fermentation. This metabolic branch consumes glycerol and produces by-products such as ethanol, butanol, acetic acid, butyric acid, hydrogen, succinic acid and also provides energy and NADH to drive the reductive pathway for 1,3-propanediol formation.

Metabolic flux analysis showed that the glycolytic flux during anaerobic fermentation of glycerol was exclusively controlled by glycerol dehydrogenase and dihydroxyacetone kinase in *Escherichia coli (Cintolesi et al., 2012).*Various efforts to engineer glycerol catabolism and downstream metabolic pathways for production of

various value-added products, including fuels, chemicals, and biomaterials have been reported in the literature. Glycerol dehydrogenase and dihydroxyacetone kinase are the significant enzymes that play key role in glycerol uptake pathway. These enzymes has been metabolically explored in microorganisms particularly for fermentative production of 1,3-propanediol (1,3-PDO), 1,2-propanediol (1,2-PDO), and 2,3-butanediol (2,3-BDO) from glycerol (Wong et al., 2014; Yang et al., 2013; Jung et al., 2011; Clomburg et al., 2011; Maervoet et al., 2016). Overexpression of *dhaD* or *gldA* has resulted in improved yield of 1,2-propanediol in *E.coli* and *S. cerevisiae* (Jung et al., 2011; Clomburg et al., 2011). Yazdani and Gonzalez showed that simultaneous overexpression of *dhaKLM* and *gldA* increased glycerol utilization and ethanol synthesis (Yazdani and Gonzalez, 2008). Glycerol consumption is partially strengthened by overexpression of the glycerol uptake genes: glycerol dehydrogenase (*gldA*) and dihydroxyacetone kinase (*dhaKLM*) in *E. coli* which enhanced ethanol yield under microaerobic condition (Wong et al., 2014). Moreover, it has been reported that there are two genes encoding glycerol dehydrogenase in *Klebsiella pneumoniae* viz., *dhaD* and *gldA* (Wang et al., 2014). Similarly, in *C. pasteurianum* glycerol dehydrogenase is encoded by two genes *dhaD1* and *dhaD2* which was depicted from the complete genome of *C. pasteurianum.* In this study we have cloned the *dhaD1* gene

In this study, we have used crude glycerol synthesized in laboratory scale from soybean oil (Sarma et al., 2016) as the substrate for H_2 production. Our previous study on metabolic flux analysis (Sarma et al., 2017) explained that doubling the glycerol uptake flux channeled metabolic flux towards pyruvate node thereby increasing the flux towards efficient generation of hydrogen. This could be initiated by overexpression of the immediate genes of glycerol utilization pathway viz., *dhaD* and *dhaK*. The genes for

glycerol dehydrogenase (*dhaD*), dihydroxyacetone kinase (*dhaK*), glycerol dehydratase, and 1,3-propanediol oxidoreductase (*dhaT*) are encoded in one and the same regulon named *dha* (Forage and Lin, 1982; Tong et al., 1991). To my knowledge there is no report on over-expression of *dhaD1* and *dhaK* in *C. pasteurianum* in terms of increasing hydrogen yield. This study presents the fermentation pattern of *C. pasteurianum* with overexpressed *dhaD1-dhaK*.

In the work presented here, we have engineered *C. pasteurianum* by overexpression of combination of key genes *dhaD1, dhaK* and *hydA* for enhanced glycerol utilization and hydrogen production respectively. This attempt was made based on our previous studies on metabolic flux analysis of *C. pasteurianum* with glycerol as the substrate (Sarma et al., 2017) which proposed two theoretical approaches viz., doubling the glycerol uptake rate and elimination of butyrate pathway enhances the flux towards H_2.

5.2 MATERIALS AND METHODS

5.2.1 Aerobic strains and culture conditions

Escherichia coli was cultured in LB-medium consisting of, per litre: tryptone,10 g; yeast extract, 5 g; NaCl, 5 g; agar (for plates only), 10 g. Cultures were typically grown at 37˚C and liquid cultures were shaken at 200 rpm. Antibiotics were used in following concentrations: erythromycin (500 μg/mL), kanamycin (50 μg/mL) and chloramphenicol (25 μg/mL in agar plates or 12.5 μg/mL in liquid media).

5.2.2 Anaerobic strains and culture conditions

Clostridium pasteurianum-H4 (DSM 525) were grown anaerobically at 37˚C in artificial atmosphere of N2:H2:CO2 in an 80:10:10 volume% ratio in an anaerobic

workbench (Don33 Whitley, Yorkshire, UK) using medium pre-reduced over-night under the same conditions. Antibiotics were used in the following concentrations: erythromycin (50 μg/mL) and thiamphenicol (25 μg/mL). Initially Schwarz et al., 2017 tested various strains for DNA transformation by the electroporation protocol published by Pyne et al., 2013 as *C. pasteurianum* DSM 525, DSM 526, DSM 9989, DSM12136 and ATCC 6013. Type-strain DSM 525 had a success rate of 8 cfu/µg which is very low efficiency. Based on the fact that *C. pasteurianum* DSM 525 could repeatedly be transformed with low efficiencies it was hypothesised that the few transformants were most likely a result of the presence of rare mutant variants within the culture that are highly competent for DNA transfer. Thus Schwarz et al., 2017 proposed screening methods to screen hypertransformable *C. pasteurianum* DSM 525 strains and *C. pasteurianum* H4 is one of them which was used throughout for this study.

Table 5.1. Strains and plasmids used in this study.

Name	Properties	Reference
C. pasteurianum DSM 525	Wild type strain	DSMZ
C. pasteurianum DSM525-H4	Hypertransformable strain based on DSM 525	Schwarz et al., 2017
E. coli TOP10	Strain used for initial screening of clones	
E. coli TOP10xCR1	Strain harbouring plasmid CR1 with M. BepI methylase	Schwarz et al., 2017
pMTL82251	*E. coli-Clostridium* shuttle vector (pBP1, ermB, ColE1 traJ, MCS, TCpa fdx	Heap et al., 2009
Q5_pMTL82251_Pgl	231 bp fragment comprising promoter from glycerol operon of *C. pasteurianum* (Pgl) cloned into the NotI/NdeI recognition sites of pMTL82251	Minton and group.
Q5_pMTL82251_ Pgl _*hydA*	1795 bp fragment comprising of *hydA* gene of *C. pas*teurianum cloned into NdeI/NheI recognition sites of Q5_pMTL82251_Pgl	This study
Q5_pMTL82251_ Pgl _*dhaD-K* :	2936 bp fragment comprising of *dhaD1-dhaK* gene from glycerol operon (oxidative path) of *C. pasteurianum* cloned into NdeI/FspI recognition sites of Q5_pMTL82251_Pgl	This study

5.2.3 Medium used

RCM Agar Reinforced Clostridial Growth Medium was used as solid medium for *C. pasteurianum* cultures. The composition of RCM is per litre: yeast extract, 3 g; 'Lab Lemco' powder (beef extract), 10 g; peptone, 10 g; glucose, 5 g; soluble starch, 1 g; NaCl, 5 g; Na-acetate, 3 g; cystein hydrochloride, 0.5 g; agar, 15 g; pH 6.8.

2xYT 2xYT was used as liquid medium. For one litre the following was added to H_2O: tryptone, 16 g; yeast extract, 10 g; NaCl, 5 g; adjust pH to pH 6.2; autoclave. After autoclaving add 100 mL sterile 50 % glucose solution (or glycerol).

Biebl Medium was produced according to Biebl (2001) with SL7 micronutrient solution according to Biebl and Pfennig (1981). For one litre of medium the following was added to H_2O: KH_2PO_4, 0.5 g; K_2HPO_4, 0.5 g; $(NH_4)2SO_4$, 5 g; $MgSO_4 \cdot 7H_2O$; $CaCl_2 \cdot 2H_2O$, 0.02 g; $FeSO_4 \cdot 7H_2O$, 9.14 mg and, if glycerol was fermented, 1 g yeast extract. This mixture was adjusted to pH 6.2 with HCl and sterilised by autoclaving. After autoclaving 2 mL trace element solution SL7 and 120 mL of a 500 g/L sterile stock of carbon source (glucose or glycerol) was added and depending on culture condition 250 µL of a 0.1 mg/mL biotin stock (filter sterilised, only needed if no yeast extract was used), 20 mL of an autoclaved 250 g/L $CaCO_3$ stock and 1 mL of an autoclaved 2 mg/mL stock of resazurin (if redox indication was required). Trace element SL7 solution consists of, per litre: $MnCl_2 \cdot H_2O$, 100 mg; $ZnCl_2$, 70 mg, H_3BO_3, 60 mg; $NaMoO_4 \cdot 2H_2O$, 40 mg; $CoCl_2 \cdot 6H_2O$, 28.7 mg; $CuCl_2 \cdot 2H_2O$, 20 mg; $NiCl_2 \cdot 6H_2O$, 20 mg; HCl (25 %), 1 mL. The mixture was sterilized by filtration through a 0.2 µm filter.

BSH Medium The BSH (a modified form of Basal solution for hydrogen production) (Chen et al., 2005, Junghare et al., 2012) optimized medium comprised of following components (concentration, g/L): peptone (2.7), yeast extract (1.48), K_2HPO_4 (0.68), KH_2PO_4 (4.035), NaCl (1.46),in addition to 10 mL trace solution and 10 mL vitamin solution. Trace element solution comprised of following components (concentration, g/L): $MnO_4 \cdot 7H_2O$ (0.01), $ZnSO_4 \cdot 7H_2O$ (0.05), H_3BO_3 (0.01), $N(CH_2COOH)_3$ (4.5), $CaCl_2 \cdot 2H_2O$ (0.01), Na_2MoO_4 (0.01), $CoCl_2 \cdot 6H_2O$ (0.2), $AlK(SO_4)_2$ (0.01), $MgCl_2 \cdot 6H_2O$ (0.2), Fe_2Cl_3 (0.1), $CuCl_2 \cdot 6H_2O$ (0.05). The composition of vitamin solution was as follows (concentration, g/L): riboflavin (0.025), citric acid (0.02), folic acid (0.01) and para–amino benzoic acid (0.01). The initial pH of the medium was adjusted to 7 using 1 M NaOH. BSH medium with working volume of 50 mL comprising 3% (w/v) L–cysteine HCl as a reducing agent, substrate glycerol (6%).and resazurin dye (0.1%w/v) was added into medium as an indicator of anaerobic conditions.Prior to inoculation, the medium was flushed with pure nitrogen (99.99%) for 15 min, sealed with rubber stoppers, crimped and autoclaved at 121°C, 15 psi for 15 min. The bottles were then inoculated and incubated at 37°C and 150 rpm. All treatments were carried out in duplicate. Aliquots of fermentation broth were withdrawn periodically to assess the quantity of glycerol consumed. Similarly samples from gaseous phase were collected periodically to quantify H_2 and CO_2 content.

5.2.4 Serum flask cultures

For growth experiments, 100 mL serum flasks were used with 50 mL growth medium. The serum flasks were sterilized by autoclaving with a cotton stopper and aluminum foil in the top. The growth medium and the butyl-rubber stoppers were sterilized separately and was then filled into the serum bottles. The bottles with medium

were transferred into the anaerobic cabinet for at least 24h to reduce before inoculation. Pre-cultures were grown in falcon tubes with 20 mL growth medium inside the cabinet. The first tube was inoculated with a loop of culture from plate and left to grow for a few hours before it was serial diluted up to 10^{-3}. The next day the optical density (OD_{600}) was measured and the over-night culture grown to mid-exponential phase was selected to inoculate the serum bottle main culture inside the cabinet. For Biebl medium with glycerol an inoculum of 0.1 was aimed for. Once inoculated the bottles were closed with sterile butyl-rubber stoppers and transferred out of the cabinet for incubation at 37˚C. Samples for OD, pH and solvent analysis were taken by sterilizing the top of the butyl-rubber stopper with an alcohol swab and then taking the sample with a syringe through the rubber. Similarly samples from gaseous phase were collected periodically to quantify H_2 content.

5.2.5 Standard molecular biology methods

Standard protocols described by the respective supplier were followed for plasmid DNA purification (NEB Biolabs Monarch Plasmid Miniprep Kit #T1010L); genomic DNA purification (GenElute™ Genomic DNA Extraction Kit (Sigma Aldrich, UK)); gel extraction (NEB Biolabs Monarch Gel Extraction Kit #T1020L); PCR clean up (Jena Bioscience PCR Purification Kit # PP-201L). Dream Taq Green PCR Master Mix (Thermo Scientific™, UK) was used for routine and analytical PCR with 20 µl reaction volume according to supplier's instructions. Phusion® High-Fidelity DNA Polymerase (NEB, UK) was used for amplification of fragments subsequently used in cloning procedures according to supplier's instructions. Colony PCR of *E.coli* cells was performed by picking half of a colony from plate and resuspended in 10 µl

DreamTaqGreen PCR Master Mix with appropriate primers. The initial denaturing step was prolonged to 10 min at 98°C. However the colony PCR protocol for clostridial clones varied from that of gram negative cells. One colony was picked from plate and resuspended in a 50 µl of colony lysis buffer (20mM Tris-HCl, pH8; 2mM EDTA; 1%Triton-X 100) and heated in a microwave oven for 2 mins, followed by vortexing. 1µL of this mixture was added as a template DNA to 9 µl of Phusion® High-Fidelity DNA Polymerase PCR mix with appropriate primers. The initial denaturing step was prolonged to 10 min at 98°C. Standard protocols of cloning and transformation into *E. coli* were followed. FastDigest™ (Thermo Scientific™, UK) restriction enzymes were used throughout this work according to supplier's instructions but incubation time was increased to 1 h. Ligations were carried out with Quick Ligation™ Kit (NEB, UK) according to supplier's instructions and incubated for at least 1 h at room temperature. Based on the available sequence information against the published *C. pasteurianum* DSM 525 genome (Poehlein et al., 2015) oligonucleotide primers were designed (Table 5.2) to amplify the *hydA* and *dhaD1-dhaK* gene.

Table 5.2. Oligonucleotides used in this study. Underlined sequences indicate added restrictions sites.

Oligonucleotide	Sequence 5' to 3'
hydA_F	GGGAATTCCATATGAAAACAATAATTATAAATGGTGTAC AG
hydA_R	CTAGCTAGCGATCAACTTATATTAGCAAGAAATGAACTT TTTGCCAGCATTATGAAAATATTGTTTTTTCATAAGCTAG CTAG
6Q_hydA_F	GAACGGCGCGCGCGTTA
ShydA	GGAAGATGTGTTAATGCCTGTG
S82251_R	CTAAGGATTCAGAACGGCGCGCGCGCCGTTCTGAATCCT TAG
traj-F	GGAGGATTACAACGGCGCT
82XXX-LR	ATCCAGGGTGCTATCTTCG
DhaD1K_Pgs_F	TTGATAAAGGAGGATTACATATGAGAAAAGCATTTATTT GTCCAACTAAATAT
DhaD1K_R	CCATTCAGGCTGCCTACTTTATAACCTCTGAAATCTCTGT GAATATTACAC
9C_DhaKsco-F	ACTTTATAACCTCTGAAATCTC

5.2.6 Plasmid methylation and plasmid transfer into *C. pasteurianum*

For high frequency transformation into *C. pasteurianum* strain, plasmid DNA was *in vivo* methylated by propagation in the dam+, dcm+ *E. coli* hostCR1, an *E. coli* Top10 strain harbouring the plasmid pCR1, comprising a RSF1030-derived RSF origin of replication (Som and Tomizawa,1982, Novagen, Merck KGaA, Darmstadt, Germany), a kanamycin resistance marker and a gene encoding the M.BepI methyltransferase of *Brevibacterium epidermidis* under the transcriptional control of the *C. sporogenes fdx* promoter (P_{Cspfdx}). As the *E.coli* host employed (Top10) was dam+, the activity of the restriction enzyme *Cpa*II, a *Mbo*I/*Dpn*II-type restriction endonuclease previously

identified as *Cpa*I (Richards et al., 1988), was of no consequence. Here we used *in vivo* methylation by M. BepI which methylates the external cytosine (5'-mCGCG-3') of the *Cpa*AII recognition site (Lunnen et al., 1988). Methylated plasmids 0.5–5 µg DNA) were electroporated into *C. pasteurianum* as detailed below.

5.2.7 Preparation of electro-competent *C. pasteurianum*

C. pasteurianum was transformed with an optimised protocol based on the protocol published by Pyne et al. (2013). In short: (i) diluted over-night cultures were grown; (ii) 100 ml main-culture was inoculated to OD_{600} = 0.05; (iii) culture was grown to OD_{600} = 0.3-0.4 when sucrose was added to 0.4M final concentration and glycine was added to give an end concentration of 1.25 w/v%; (iv) culture was further grown to OD_{600} = 0.6-0.8; (v) culture was washed once in ice-cold sucrose-magnesium-phosphate (SMP) buffer (270 mM sucrose, 1 mM $MgCl_2$, 5 mM NaH_2PO_4, pH 6.5) after which the pellet was taken up in 3000 µl SMP buffer, enough for five transformations.

5.2.8 Transformation of electro-competent *C. pasteurianum*

For the electro-transformation 580 µl of competent cells, 30 µl ethanol (100 %)and 5 µg methylated plasmid DNA of plasmid of interest were added to a 4 mm cuvette. Inside the anaerobic cabinet the culture was electroporated with an exponential decay pulse of 1800 V without parallel resistance (Pyne et al., 2013). Transformations were immediately recovered in 10 ml 2x YTG overnight before plating dilutions on plates with antibiotics.

5.2.9 Analytical methods

The concentrations of metabolites in the samples withdrawn from fermentation

broth were quantified by HPLC analysis using a Hi–Plex H column (300 mm × 8 µm × 7.7 mm, Agilent, India) thermostated at 60°C with the help of external column oven (Model: HCO–02, PCI analytics Pvt. Ltd., India). 0.01 M H_2SO_4 in ultra–pure water (18.2 MΩ·cm resistivity at 25°C) was used as the mobile phase at a flow rate of 0.5 mL/min. Residual glycerol content of the fermentation samples was quantified by HPLC analysis using a Rezex RCM Monosaccharide calcium–column (300 mm × 8 µm × 7.8 mm, Phenomenex, India) thermostated at 35°C with the help of external column oven (Model– HCO–02, PCI analytics Pvt. Ltd., India). Ultra–pure water (18.2 MΩ·cm resistivity at 25°C) was used as the mobile phase at a flow rate of 0.5 mL/min. The HPLC apparatus comprised of a pump (Series 200, Perkin Elmer), a refractive index detector (Series 200, Perkin Elmer) and a vacuum degasser (Series 200, Perkin Elmer). Reaction mixture samples were centrifuged (12,000 rpm, 20 min) and filtered through a 0.2 µm membrane filter, and diluted appropriately prior to injection into HPLC. Standard calibration plots were used to determine concentrations of the metabolites and glycerol in the samples of fermentation mixture. The composition of product gas from glycerol fermentation was determined using Gas Chromatograph (Make: Thermo scientific, Model: Ceres800 plus) with thermal conductivity detector (TCD) and Porapak Q (60/80 mesh) column employing argon as carrier gas at a flow rate of 30 mL/min. The operational temperature of the column oven was 45ºC, and the injector and detector temperatures were maintained at 200ºC. Gas samples were withdrawn from fermentation serum bottles and the molar/volumetric content of H_2 and CO_2 in the gas was determined. Hydrogen gas production was calculated from measurement of headspace of fermentation bottles (above surface of fermentation mixture).

The total volume of gas produced in each time interval can be determined using the mass balance equation.

$$V_{H,i} = V_{H,i-1} + C_{H,i}(V_{G,i} - V_{G,i-1}) + V_H (C_{H,i} - C_{H,i-1})$$

$V_{H,i}$ and $V_{H,i-1}$ are the cumulative hydrogen gas volumes at present (i) and previous (i–1)time interval, respectively; $V_{G,i}$ and $V_{G,i-1}$ are total product gas volume at the current and previous time intervals; $C_{H,i}$ and $C_{H,i-1}$ are the volume or mole fractions of hydrogen gas in the headspace at the current and previous time intervals; V_H is the volume of headspace of vials. The volume of product gas used for analysis was also taken into account during hydrogen mass balance.

5.3 RESULTS AND DISCUSSION

5.3.1 Construction of recombinant hydrogenase from *C. pasteurianum*

In *C. pasteurianum* it was possible to overexpress the putative main hydrogenase *hydA* (CLPA_c00280) which shows 71% identity with the well described *C. acetobutylicum hydA* (Santangelo et al., 1995). The gene was amplified (Fig. 5.1A) from genomic DNA of *C. pasteurianum* DSM 525(H4) (Schwarz et al., 2017) with primers hydA_F and hydA_R (Table 5.2). The *hydA* gene was then cloned into a pMTL80000 modular shuttle plasmid developed by Heap et al., 2009. The plasmid pMTL82251 was used and slightly modified by deletion and insertion of few bases followed by insertion of the glycerol promoter (Pgl_GL) from *C. pasteurianum* glycerol operon (CLPA_c22720 to CLPA_c22820) and was renamed as Q5_pMTL_82251_Pgl_GL by Minton and group. Both the plasmid and the amplified *hydA* was digested by NdeI and NheI (Fig. 5.1B) and ligated overnight. The ligation mixture was transformed into *E.coli* TOP10 cells using calcium chloride heat shock method (Ausubel et al. 1987). The erythromycin resistant colonies were selected on the LB agar plate supplemented with

500 µg/mL erythromycin and positive clones were screened by colony PCR followed by DNA sequencing (Fig. 5.1C). After successful screening of positive clones carrying *hydA* the plasmid DNA was protected against restriction by *in vivo* methylation with *E. coli* carrying plasmid pMTL-CR1 expressing the M.BepI methylase. The methylated plasmids are then transformed into *C. pasteurianum* by electroporation and the erythromycin resistant colonies were selected on the freshly prepared RCM agar plate supplemented with 40 µg/mL erythromycin. Positive clones of *C. pasteurianum* carrying *hydA*-Q5_pMTL_82251_GL plasmid were screened by colony PCR with primers 82XXX-LR and traj_F (primers in the plasmid backbone) amplifying a band of 2385 bp (Fig. 5.2D) against the clones with empty Q5_pMTL_82251_GL plasmid (without *hydA* insert) with a band of 861 bp (Fig. 5.2D).

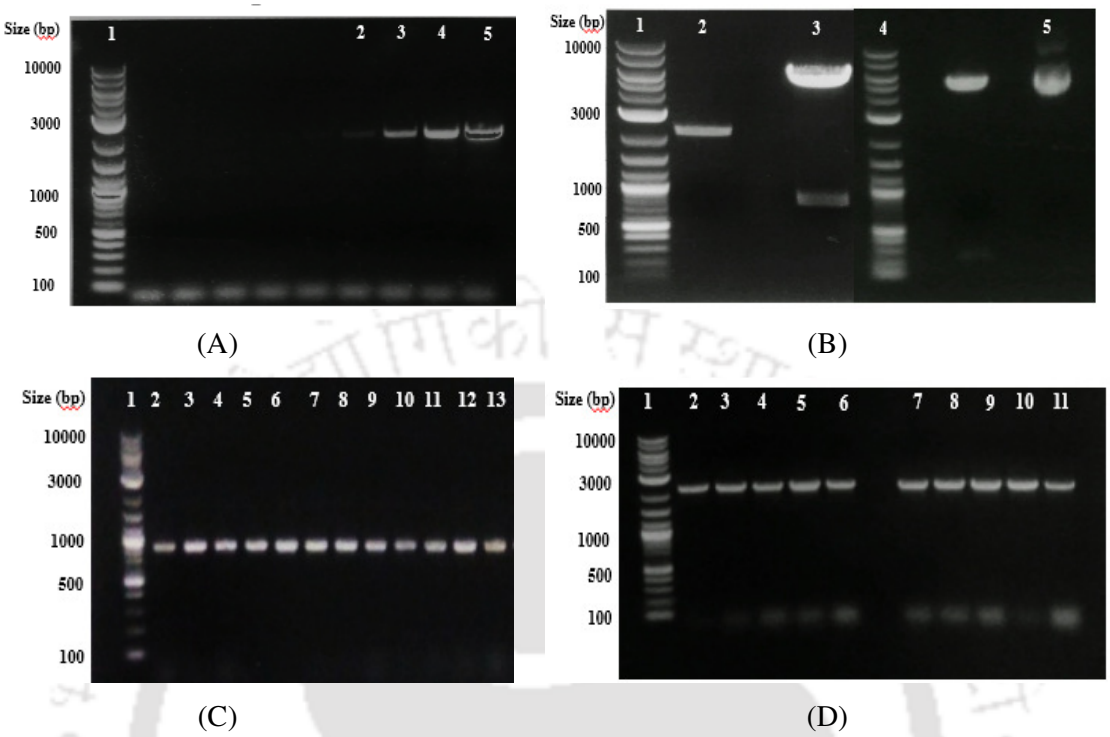

Figure 5.1. Cloning and overexpression of *hydA* in Q5_pMTL82251_GL vector. (**A**) PCR amplification of *hydA* from *C. pasteurianum* genomic DNA. Lane 1: 2-log DNA ladder, Lane 2-5: Gradient PCR amplified band of *hydA* showing size of around 2100 bp. (**B**) Restriction digestion of insert and plasmid with NdeI and NheI. Lane 1,4: 2-log DNA ladder, Lane 2,3: Digested hydA insert and Q5_pMTL82251_GL vector respectively, Lane 5: Undigested Q5_pMTL82251_GL vector. (**C**) Clone confirmation by colony PCR of *C. pasteurianum* harbouring empty-Q5_pMTL82251_GL plasmid giving a band of 861bp. Lane 1: 2-log DNA ladder; Lanes 2 to 13: PCR product. (**D**) Clone confirmation by colony PCR of *E. coli* and *C. pasteurianum* harbouring *hydA*-Q5_pMTL82251_GL plasmid giving a band of 2385bp. Lane 1: 2-log DNA ladder; Lanes 2-6: PCR product of *hydA* amplified from *E.coli* TOP10, Lanes 7-11: PCR product of *hydA* amplified from *C. pasteurianum* H4.

5.3.2 Construction of recombinant glycerol dehydrogenase-dihydroxyacetone kinase from *C. pasteurianum*

The *dhaD1-dhaK* (2936 bp) gene is amplified (Fig. 5.2A) from genomic DNA of *C. pasteurianum* DSM 525 (H4) by using primers DhaD1K_Pgs_F and DhaD1K_R. The vector Q5_pMTL82251_GL was digested with NdeI and FspI (5241 bp) (Fig. 5.2B) and

the cloning was carried out by using the NEB Gibson Assembly Cloning Kit (NEB #E5510). The ligation mixture was transformed into *E. coli* TOP10 cells using calcium chloride heat shock method (Ausubel et al. 1987). The erythromycin resistant colonies were selected on the LB agar plate supplemented with 500 µg/mL erythromycin and the positive clones in *E.coli* TOP10 were screened by colony PCR with primers 9C_DhaK_sco_F and 82XXX-LR (Table 5.2) amplifying a band of 1272 bp (Fig. 5.2C) followed by DNA sequencing. After successful screening of positive clones carrying *dhaD1-dhaK* the plasmid DNA was methylated by transformation into *E. coli* carrying plasmid pMTL-CR1 expressing the M.BepI methylase. The methylated plasmids are then transformed into *C. pasteurianum* by electroporation and the erythromycin resistant colonies were selected on the freshly prepared RCM agar plate supplemented with 40 µg/mL erythromycin. Positive clones of *C. pasteurianum* carrying *dhaD-dhaK*-Q5_pMTL_82251_GL plasmid were screened by colony PCR with primers 82XXX-LR and traj_F amplifying a band of 3526 bp (Fig. 5.2D) against the clones with empty Q5_pMTL_82251_GL plasmid (without *dhaD-dhaK* insert) with a band of 861bp (Fig. 5.1 C).

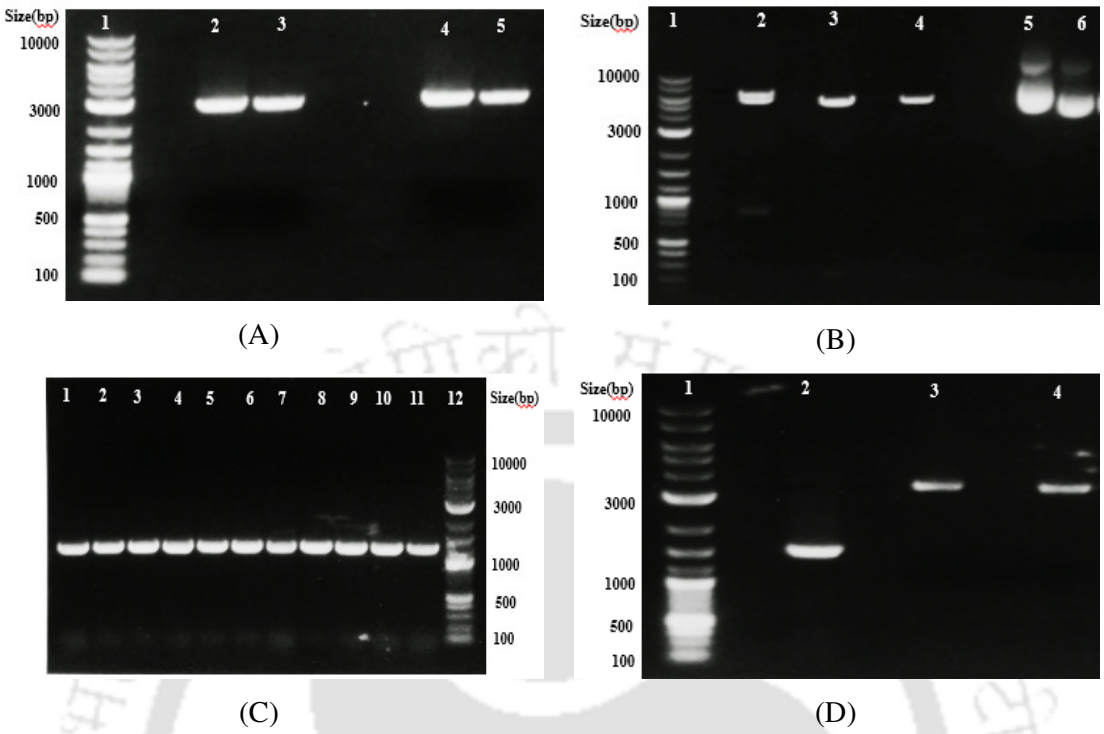

Figure 5.2. Cloning and overexpression of *dhaD1-dhaK* in Q5_pMTL82251_GL vector. (**A**) PCR amplification of *dhaD1-dhaK* from *C. pasteurianum* genomic DNA. Lane 1: 2-log DNA ladder, Lane 2-5: PCR amplified band of *dhaD1-dhaK* showing size of around 2936 bp. (**B**) Restriction digestion of plasmid with NdeI and FspI. Lane 1: 2-log DNA ladder, Lane 3,4: Digested Q5_pMTL82251_GL vector, Lane 5,6: Undigested Q5_pMTL82251_GL vector. (**C**) Clone confirmation by colony PCR of *E. coli* harbouring *dhaD1-dhaK*_Q5_pMTL82251_GL plasmid with primers 9C_DhaK_sco_ F and 82XXX-LR giving a band of 1272 bp. Lanes 1-11: PCR product, Lane 12: 2-log DNA ladder. (**D**) Clone confirmation by colony PCR of *C. pasteurianum* harbouring *dhaD1-dhaK*_Q5_pMTL82251_GL plasmid giving a band of 3526 bp. Lane 1: 2-log DNA ladder; Lane 2: PCR product with 9C_DhaK_sco_F and 82XXX-LR primers, Lanes 3,4: PCR product 82XXX-LR and traj_F primers.

5.3.3 Batch Fermentation

To analyze the fermentation patterns of hydrogenase (*hydA*), dihydroxyacetone kinase and glycerol dehydrogenase (*dhaD1K*) overexpression, *C. pasteurianum hydA*$^{++}$, *C. pasteurianum dhaD1K*$^{++}$ and *C. pasteurianum* DSM525 H4 wild type were grown in 100 ml serum flasks with 50 ml Biebl medium (Biebl et al., 2001) or BSH medium

(Basal solution for hydrogen production) (Chen et al., 2005, Junghare et al., 2012) with pure and crude glycerol as the substrate. The crude glycerol fermentation profiles are described in Fig. 5.3and 5.4. Both Biebl and BSH fermentation medium was used for the fermentation experiments with pure and crude glycerol as substrate and compared. The BSH medium was optimized in our previous study and the optimized medium is used in the present study for glycerol fermentation by recombinant and wild type strains of *C. pasteurianum.* The fermentation data presented in Table 5.3 and 5.4 infers nearly similar profiles with both the fermentation medium which suggest that both of them are suitable for fermentative hydrogen production from glycerol. The biomass profiles are also nearly similar suggesting that the medium components of both the medium are significant for the growth and metabolism of *C. pasteurianum* cells.

5.3.3.1 Hydrogenase overexpressed phenotype

Pure and crude glycerol with a final concentration of 60 g/L was used for fermentation. Glycerol is not entirely exhausted in the cultures of either strain. However consumption in the *dhaD1K*$^{++}$ strain is much faster than the wild type and the *hydA*$^{++}$ strain. This is due to the high activity of the immediate glycerol intake enzymes viz. glycerol dehydrogenase and dihydroxyacetone kinase. The *hydA* recombinant produced higher amount of acetate and negligible amount of lactate and butyrate as compared with the wild type. The lactate production reduced to 56% and butyrate to 75% of the wild type production (Table 5.3). The final acetate concentration after 27 h of fermentation in the *hydA* recombinant increased by 45% of that of wild type. Further stoichiometrically, higher hydrogen production is associated with higher acetate production and from this study it could be inferred that highest hydrogen is produced in the *hydA*$^{++}$ strain which

again produces higher amount of acetate. Thus, it could be concluded that improvement in the hydrogen gas production in the *hydA*$^{++}$ strain was caused by reduction in the amount of lactic acid and enhancement in the amount of acetic acid. It seems apparent that the enhanced hydrogenase activity caused over-oxidation of NADH to NAD+, and consequently the depletion of NADH to reduce pyruvic acid to lactic acid. Similar observations were also reported by Morimoto et al. (2005) for hydrogen production by *C. paraputrificum*. Butyrate production was observed in WT strain but it decreased in both the overexpressed strains after 24 h (Fig. 5.4E). Similar butyrate profiles were observed by Schwarz et al. (2017). The solvent profiles of *hydA*$^{++}$ strain suggested that there was a reduction in all the solvents viz. 1,3-propanediol, ethanol and butanol as compared to the WT strain. Although the total amount of solvent produced during fermentation is higher than the total acids but the total acids increased to 71.41 mM and total solvents decreased to 163.10 mM in the *hydA*$^{++}$ strain compared to the WT. Thus *hydA*$^{++}$ strain is associated with increase in acid and hydrogen production along with decreased solvents compared to the wild type. This is in accordance with that hydrogen is produced in acedogenic phase and reduces during solvetogenic phase of fermentation. A marked increase of 80% in the cumulative hydrogen volume in the *hydA*$^{++}$ strain is observed as compared to the wild type. This corresponds to a yield of 1.1 moles of H_2 per mole of glycerol after 24 h of fermentation using crude glycerol.

The overexpression of *hydA* thus resulted in increase in hydrogen production in *C. pasteurianum* along with changes in the formation of other fermentation products. The results clearly demonstrate that hydrogenase is the rate limiting enzyme of hydrogen production in *C. pasteurianum* which is in accordance with findings of Morimoto et al.,

2005 but in contrast with the findings of Klein et al., 2010 which reports overexpression of hydrogenase has no effect on hydrogen and other metabolites in *C. acetobutylicum*.

5.3.3.2 *dhaD1-dhaK* overexpressed phenotype

Fermentation experiments were carried out with the *C. pasteurianum dhaD1K* overexpressed strain (*dhaD1K*$^{++}$) with crude and pure glycerol (60g/L) as the substrate. Higher glycerol consumption could be observed in the fermentation experiments with both crude and pure glycerol with *dhaD1K* recombinant strain (Table 5.3 and 5.4). The overexpression of *dhaD1K* gene resulted in higher production and activity of glycerol dehydrogenase and dihydroxyacetone kinase enzymes, which resulted in increased glycerol metabolism and simultaneous increase in the product yields. Similar reduction in lactate and butyrate was observed and acetate production increased compared to the wild type. This strain showed an interesting solvent profile with almost 68% increase in 1,3-PDO and 13.5% increased in butanol production compared to the WT. The higher 1,3-PDO production reveals that the overexpression of the immediate enzymes of glycerol metabolism has redirected the pathway towards 1,3-PDO formation rather than towards acetyl-CoA. Due to higher solvent production in this strain, the hydrogen production is slightly reduced as compared to the *hydA* recombinant strain. The fermentation profiles reveal that the cumulative hydrogen volume increased by 75% in the *dhaD1K*$^{++}$ strain, which correspond to a yield of 0.93 moles of H_2 per mole of glycerol.

From these results it could be concluded that under anaerobic conditions combined overexpression of glycerol dehydrogenase and dihydroxyacetone kinase in *C. pasteurianum* showed an increased 1,3-PDO production along with hydrogen as

compared to the wild type. The importance of *dhaD* and *dhaK* in 1, 3-PDO production has been widely explored in *K. pneumonia* but no such report exist to determine its significance in hydrogen production in any of the species. Horng et al. (2010) disrupted *dhaD* and *dhaK1* in *K. pneumoniae*, which significantly lowered 1,3-propanediol production in the mutant than the wild strain. These results are consistent with the findings of Wei et al., 2014, that the *DhaK1* or *dhaK2* mutation inhibited *dha* regulon expression and *DhaK3* mutation reduced glycerol utilization compared to the wild strain. Luo et al. (2011) knocked out *dhaD* in *K. pneumoniae*, and the mutant also shows poor 1,3-propanediol product ability. They suggested that this phenomenon is due to the unbalanced NADH. Thus these findings ascertain that *dhaD* and *dhaK* has significant role in glycerol utilization and *dha* regulon expression which has been supported by our present findings that overexpression of these genes regulate the production of propanediol and hydrogen. The biomass data presented in Table 5.2 and table 5.3 shows a slight increase in biomass of the recombinant strains as compared to the wild type. This observation indicated that combined overexpression of *dhaD1K* affected glycerol uptake rate through the oxidative pathway of *dha* regulon. Increased glycerol uptake regulated energy utilization by the cell thereby increasing the cell growth. On the other hand a marginal increment in biomass content further ascertain that major fraction of carbon is utilized in the formation of cell metabolites rather than cell growth which resulted in increase in yield of acetate, butanol, 1,3-propanediol and hydrogen.

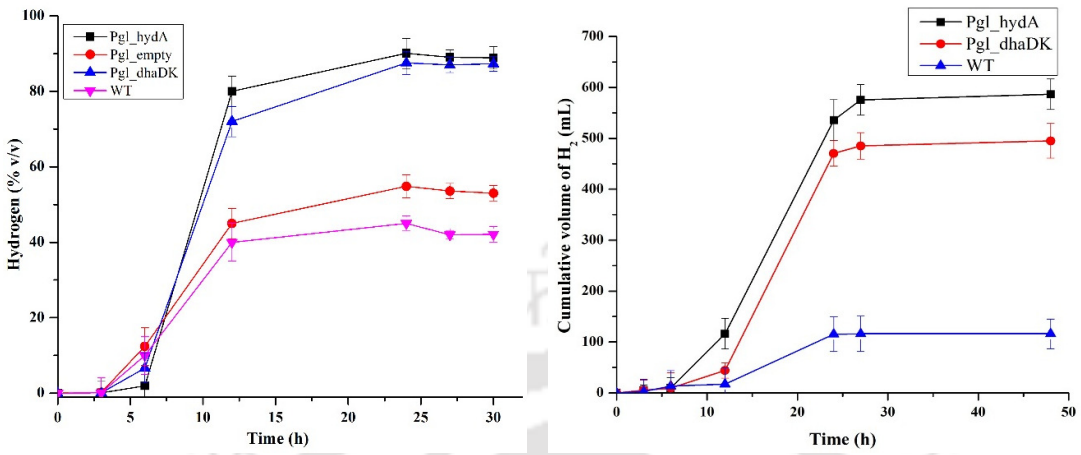

(A) **(B)**

Figure 5.3 Time profiles of hydrogen production from crude glycerol fermentation by *C. pasteurianum*-H4(WT); *C. pasteurianum*-H4-*hydA* (Pgl_hydA); *C. pasteurianum*-H4-*dhaDK* (Pgl_dhaDK) and *C. pasteurianum*-H4(Pgl_empty). (A) % H_2 v/v (B) Cumulative volume of H_2

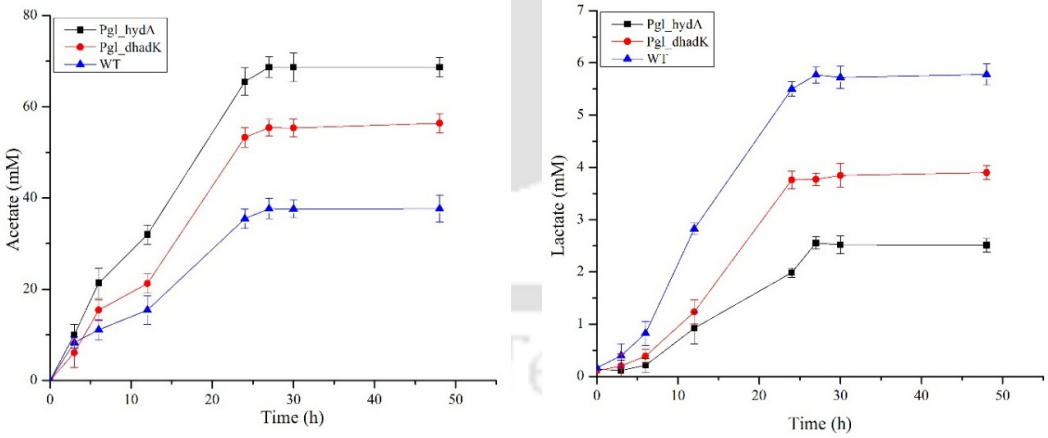

(A) **(B)**

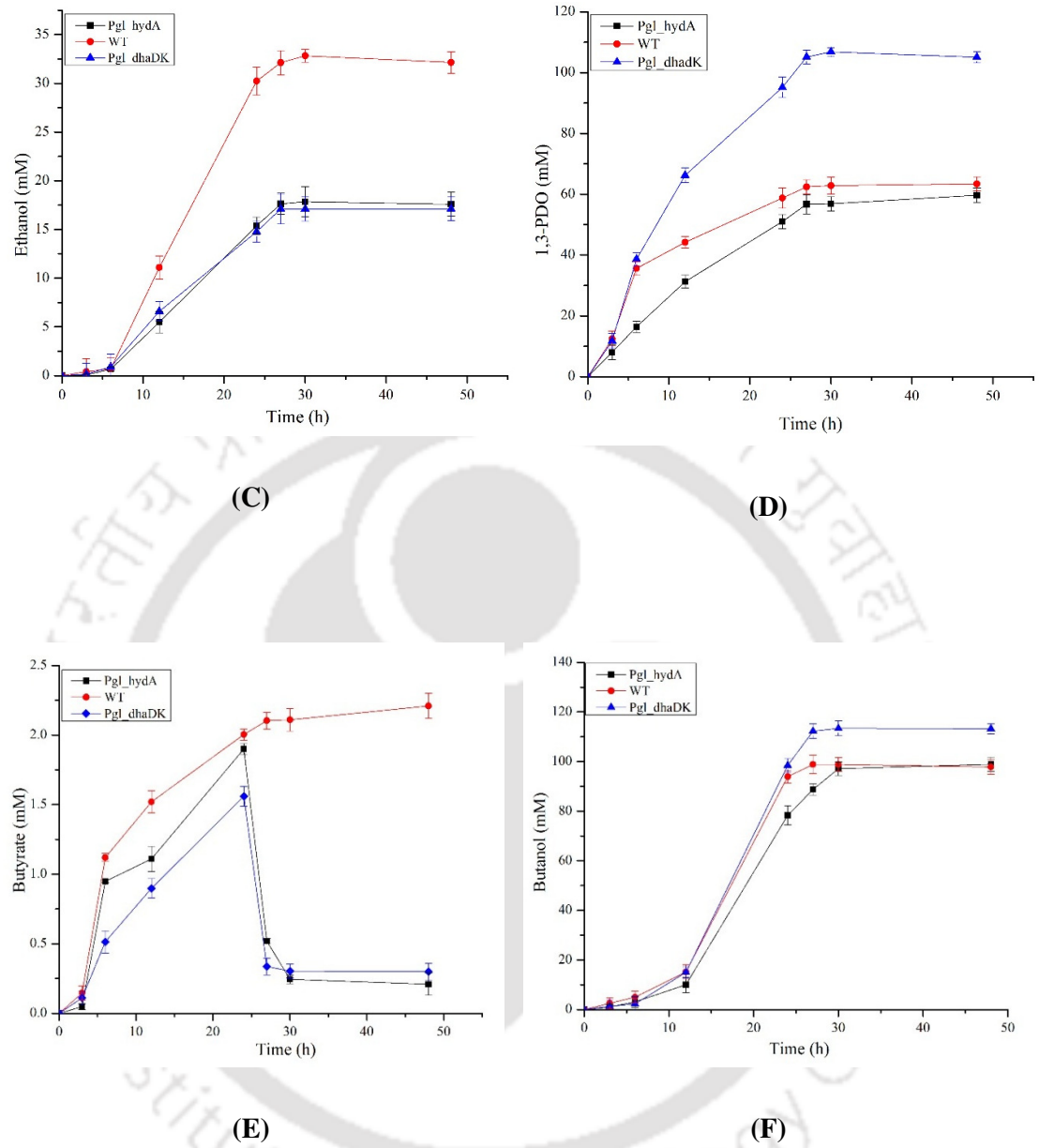

Figure 5.4 Solvent and acid profiles for crude glycerol fermentations of *C. pasteurianum DSM525-H4*(WT); *C. pasteurianum-H4-hydA* (Pgl_hydA); *C. pasteurianum-H4-dhaDK* (Pgl_dhaDK); (A) Acetate;(B) Lactate; (C) Ethanol; (D) 1,3-Propanediol; (E) Butyrate; (F) Butanol

Table 5.3. Product and substrate profiles of *hydA*$^{++}$, *dhaD1K*$^{++}$ overexpressed crude glycerol fermentations with wild type (WT) as control in serum bottles.

Carbon source	60g/L (650 mM) crude glycerol					
Medium	Biebl			BSH		
Strain	*hydA*$^{++}$	*dhaD1K*$^{++}$	WT	*hydA*$^{++}$	*dhaD1K*$^{++}$	WT
Product concentrations [mM]						
Carbon source used[mM]	420.54±5.4	450.11±2.3	390.31±3.1	418.34±2.5	445.66±3.4	350.23±2.6
Lactate	2.51±0.2	3.90±0.1	5.7±0.3	5.45±0.5	5.73±0.2	7.19±0.2
Acetate	68.69±1.1	55.39±0.8	37.68±0.4	64.82±1.1	51.12±0.5	36.12±0.5
Butyrate	0.51±0.0	0.33±0.7	2.10±0.5	11.27±0.8	10.53±0.4	12.10±1.0
1,3-Propanediol	56.70±1.2	105.10±0.8	62.40±0.7	53.21±1.1	86.33±0.2	60.40±0.3
Ethanol	17.6±0.3	17.11±0.6	32.12±1.2	15.61±1.1	10.56±0.4	10.12±0.7
Butanol	88.8±1.5	112.23±1.1	98.83±0.8	44.21±1.4	63.21±1.1	66.43±0.7
CO2	76.21±2.3	76.34±3.2	65.56±2.1	75.45±3.1	75.34±1.8	63.7±4.4
Biomass	38.21±0.3	39.81±0.4	35.32±0.1	37.54±0.3	39.44±0.2	34.12±0.1
Carbon recovery (%)	89.02	93.87	92.24	83.06	84.24	90.79

Table 5.4. Product and substrate profiles of *hydA*$^{++}$, *dhaD1K*$^{++}$ overexpressed pure glycerol fermentations with wild type (WT) as control in serum bottles.

Carbon source	60g/L (650 mM) pure glycerol					
Medium	Biebl			BSH		
Strain	*hydA*$^{++}$	*dhaD1K*$^{++}$	WT	*hydA*$^{++}$	*dhaD1K*$^{++}$	WT
Product concentrations [mM]						
Carbon source used[mM]	408.91±2.1	440.34±3.2	375.54±1.4	380.91±1.2	410.34±2.5	340.54±3.2
Lactate	2.44±0.3	4.22±0.1	4.58±0.6	4.78±1.1	5.43±1.0	7.32±0.5
Acetate	61.12±0.3	45.21±0.4	31.13±0.4	55.23±0.1	43.21±1.1	28.67±1.0
Butyrate	0.56±0.3	1.56±0.8	1.12±0.3	7.87±0.2	7.63±1.3	8.34±1.1
1,3-Propanediol	45.34±0.8	93.44±0.5	58.06±0.6	26.25±1.3	73.44±0.5	61.28±1.1
Ethanol	22.11±1.0	23.12±0.8	35.40±0.4	10.89±0.5	12.67±1.1	12.23±0.4
Butanol	71.87±0.1	115.13±2.1	106.12±0.2	60.87±0.4	61.12±0.0	58.12±1.2
CO2	74.54±3.2	71.32±2.5	63.34±1.4	71.12±3.5	76.34±2.8	62.21±3.2
Biomass	36.12±0.3	38.67±0.1	33.42±0.7	35.23±0.2	36.53±0.3	32.15±0.2
Carbon recovery (%)	85.46	92.68	93.50	83.33	85.58	89.28

5.4 CONCLUSIONS

In this chapter we have attempted successfully the overexpression of three key genes responsible for hydrogen production from glycerol. To our knowledge no studies have been reported for the homologous overexpression of these genes (*hydA, dhaD1-dhaK*) in *C. pasteurianum*and its effect on fermentative hydrogen production. This study reveals that *hydA* plays a crucial role in increasing the yield of hydrogen by simultaneous increase in acetic acid and reduced lactic acid. Similarly, overexpression of *dhaD1K* also enhanced the glycerol metabolism and hydrogen production compared to the wild type strain, thereby explaining its importance in the glycerol hydrogen pathway.

Acknowledgements

This work was partly funded by Department of Biotechnology, India and British Council, United Kingdom under the Newton Bhaba PhD Placement Programme 2017-18. A part of this chapter was carried out at Synthetic Biology Research Centre, Centre for Biomolecular Sciences, The University of Nottingham, UK under the supervision of Prof. Nigel P. Minton. We gratefully acknowledge valuable discussions and suggestions from Prof. Minton and his research group.

References

Biebl, H., Pfennig, N., 1981. Isolation of members of the family Rhodospirillaceae in t*he prokaryotes*, Springer. 267–273.

Biebl, H., Menzel, K., Zeng, A.P., Deckwer,W. D., 1999. Microbial production of 1,3–propanediol. Appl. Microbiol. and Biotechnol. 52(3), 289–297.

Biebl, H., 2001. Fermentation of glycerol by *Clostridium pasteurianum* - batch and continuous culture studies. J of Industrial Microbiol. Biotechnol. 27(1), 18–26.

Biswas, R., Zheng, T., Olson, D.G., Lynd, L.R., Guss, M.G., 2015. Elimination of hydrogenase active site assembly blocks H_2 production and increases ethanol yield in *Clostridium thermocellum*. Biotechnol. for Biofuels. 8, 1–10.

Calusinska, M., Happe, T., Joris, B., Wilmotte, A., 2010. The surprising diversity of clostridial hydrogenases: a comparative genomic perspective. Microbiol. 156(6), 1575–1588.

Chen, W.M., Tseng, Z.J., Lee, K.S., Chang, J.S.,2005. Fermentativehydrogen production with *Clostridium butyricum* CGSSisolated from anaerobic sewage sludge. Int J Hydrogen Energ. 30, 1063-1070.

Cintolesi, A., Clomburg, J.M., Rigou, V., Zygourakis, K., Gonzalez, R., 2012. Quantitative analysis of the fermentative metabolism of glycerol in *Escherichia coli*. Biotechnol. Bioeng. 109, 187–198.

Clarke, D.J., Fuller, F.M., Morris, J.G., 1979. Proton-translocating adenosine-triphosphatase of the obligately anaerobic bacterium *Clostridium pasteurianum*.1. ATP phosphohydrolase activity. Eur J Biochem. 98, 597–612.

Clomburg, J.M., Gonzalez, R., 2011. Metabolic engineering of *Escherichia coli* for the production of 1,2-propanediol from glycerol. Biotechnol Bioeng. 108, 867–879.

Cooksley, C.M., Zhang, Y., Wang, H., Redl, S., Winzer, K., Minton, N.P., 2012. Targeted mutagenesis of the *Clostridium acetobutylicum* acetone-butanol-ethanol fermentation pathway. Metab. Eng. 14, 630–641.

Dabrock, B., Bahl, H., Gottschalk, G., 1992. Parameters affecting solvent production by *Clostridium pasteurianum.* Appl. Environ. Microbiol. 58, 1233–1239.

Forage, R.G., Lin, E., 1982a. DHA system mediating aerobic and anaerobic dissimilation of glycerol in *Klebsiella pneumoniae* NCIB 418. J of Bacteriol. 151, 591-599.

Forage, R.G., Foster, M.A., 1982b. Glycerol fermentation in *Klebsiella pneumoniae*: functions of the coenzyme B12-dependent glycerol and diol dehydratases. J of Bacteriol. 149, 413-419.

Horng, Y.T., Chang, K.C., Chou, T.C., Yu, C.J., Chien, C.C., Wei, Y.H., Soo, P.C., 2010. Inactivation of dhaD and dhaK abolishes by-product accumulation during 1,3-propanediol production in Klebsiella pneumonia. J Industrial Microbiol. Biotechnol., 37, 707-716.

Jennert, K.C.B., Tardif, C., Young, D.I., Young, M., 2000. Gene transfer to *Clostridium cellulolyticum* ATCC 35319. Microbiology-(UK). 146, 3071–3080.

Junghare, M., Subudhi, S., Lal., B., 2012. Improvement of hydrogen production under decreased partialpressure by newly isolated alkaline tolerant anaerobe,*Clostridium butyricum* TM-9A: Optimization of processparameters. Int J Hydrogen Energy. 37, 3160–3168.

Jung, J.Y., Yun, H.S., Lee, J., Oh, M.K., 2011. Production of 1,2-Propanediol from glycerol in *Saccharomyces cerevisiae*. J. Microbiol. Biotechnol. 21, 846–853.

Kim, D-H., Kim, M-S., 2011. Hydrogenases for biological hydrogen production. Bioresour. Technol. 102, 8423–8431.

Klapatch, T.R., Demain, A.L., Lynd, L.R., 1996. Restriction endonuclease activity in

Clostridium thermocellum and *Clostridium thermosaccharolyticum*. Appl Microbiol Biotechnol. 45, 127–131.

Klein, M., Ansorge-Schumacher, M.B., Fritsch, M., Hartmeier, W., 2010. Influence of hydrogenase overexpression on hydrogen production of *Clostridium acetobutylicum* DSM 792. Enzyme and Microbial Technol. 46(5), 384–390.

Luo, L.H., Seo, J.W., Oh, B.R., Seo, P.S., Heo, .Y., Hong, W.K., Kim, D.H., Kim, C.H., 2011. Stimulation of reductive glycerol metabolism by overexpression of an aldehyde dehydrogenase in a recombinant *Klebsiella pneumoniae* strain defective in the oxidative pathway. J Industrial Microbiol. Biotechnol. 38, 991-999.

Malaviya, A., Jang, Y. S., Lee, S. Y., 2012. Continuous butanol production with reduced byproducts formation from glycerol by a hyper producing mutant of *Clostridium pasteurianum*. Appl. Microbiol. Biotechnol. 93(4), 1485–1494.

Maervoet, V.E.T., Maeseneire, S.L.D., Avci, F.G., Beauprez, J., Soetaert W.K., Mey, M.D., 2016. High yield 1,3-propanediol production by rational engineering of the 3-hydroxypropionaldehyde bottleneck in *Citrobacter werkmanii*. Microbial Cell Factories. 15, 23–31.

Mermelstein, L.D., Welker, N.E., Bennett, G.N., Papoutsakis, E.T., 1992. Expression of cloned homologous fermentative genes in *Clostridium acetobutylicum* ATCC 824. Bio/Technology. 10,190–195.

Morimoto, K., Kimura, T., Sakka, K., Ohmiya, K., 2005. Overexpression of a hydrogenase gene in *Clostridium paraputrificum* to enhance hydrogen gas production. FEMS

Microbiol. Lett. 246, 229–234.

Papoutsakis, E.T., 2008. Engineering solventogenic clostridia. Current opinion in biotechnology. 19(5), 420–429.

Poehlein, A., Grosse-Honebrink, A, Zhang, Y., Minton, N.P., Daniel, R., 2015. Complete genome sequence of the nitrogen-fixing and solvent producing *Clostridium pasteurianum* DSM 525. Genome announcements. 3(1), e01591–14.

Pyne, M.E., Moo-Young, M., Chung, D.A., Chou, C.P., 2013. Development of an electrotransformation protocol for genetic manipulation of *Clostridium pasteurianum*.Biotechnol. for Biofuels, 6(1),50.

Pyne, M.E., Moo-Young, M., Chung, D.A., Chou, C.P., 2014. Expansion of the genetic toolkit for metabolic engineering of *Clostridium pasteurianum*: chromosomal gene disruption of the endogenous CpaAI restriction enzyme. Biotechnol. for biofuels. 7(1), 1.

Pyne, M.E., Moo-Young, M., Chung, D.A., Chou, C.P., 2015. Antisense-RNA-mediated gene downregulation in *Clostridium pasteurianum*. Fermentation. 1 (1), 113–126.

Richards, D.F., Linnett, P.E., Oultram, J.D., Young, M., 1988. Restriction endonucleases in *Clostridium pasteurianum* ATCC 6013 and *C. thermohydrosulfuricum* DSM 568. Microbiol. 134, 3151–3157.

Santangelo, J.D., Durre, P., Woods, D.R., 1995. Characterization and expression of the hydrogenase-encoding gene from *Clostridium acetobutylicum* P262. Microbiol. 141(1), 171–180.

Sarma, S., Anand, A., Dubey, V.K., Moholkar, V.S., 2017. Metabolic flux network analysis of hydrogen production from crude glycerol by *Clostridium pasteurianum*. Bioresour. Technol. 242, 169–177.

Schwarz, K., Grosse-Honebrink, A., Derecka, K., Rotta, C., Zhang, Y., Minton, N.P., 2017. Towards improved butanol production through targeted geneticmodification of *Clostridium pasteurianum*. Metabolic Engineering, doi:10.1016/j.ymben.2017.01.009

Tong, I.T., Liao, H.H., Cameron, D.C., 1991. 1,3-Propanediol production by Escherichia coli expressing genes from the *Klebsiella pneumoniaedha* regulon. Appl. Environ. Microbiol. 57, 3541–3546.

Trevors, J.T., Chassy, B.M., Dower, W.J., Blaschek, H.P., 1992. Electrotransformation of bacteria by plasmid DNA. In Guide to electroporation and electrofusion. Edited by Academic Press Inc. 265–283.

Vignais, P.M., Colbeau, A., 2004. Molecular biology of microbial hydrogenases. Current Issues in Mol. biol. 6(2), 159–188.

Wang, Y., Tao, F., Xu, P., 2014. Glycerol dehydrogenase plays a dual role in glycerol metabolism and 2,3-Butanediol formation in *Klebsiella pneumonia*. J Biol. Chem. 289, 6080–6090.

Wei, D., Wang, M., Jiang, B., Shi, J., Hao, J. 2014. Role of dihydroxyacetone kinases I and II in the *dha* regulon of *Klebsiella pneumonia*. J. Biotechnol. 177, 13–19.

Wong, M.S., Li, M., Black, R.W., Le, T.Q., Puthli, S., Campbell, P., Monticello. D.J., 2014. Microaerobic conversion of glycerol to ethanol in *Escherichia coli*. Appl. Environ. Microbiol. 80, 3276–3282.

Yang, T.W., Rao, Z.M., Zhang, X., Xu, M.J., Xu, Z.H, Yang, S.T., 2013. Fermentation of biodiesel-derived glycerol by *Bacillus amyloliquefaciens*: effects of co-substrates on 2,3-butanediol production. Appl Microbiol Biotechnol. 97, 7651–7658.

Yazdani, S.S., Gonzalez, R., 2008. Engineering *Escherichia coli* for the efficient conversion of glycerol to ethanol and co-products. Metab. Eng.10, 340–351.

Chapter 6

Conclusions and Future Direction

6.1 Overview

This thesis has presented the research on enhanced hydrogen production via optimization of process parameters and media which has highlighted relative individual significance of different process parameters on H_2 production. Further this thesis also presents analysis of the metabolic pathway of glycerol metabolism for hydrogen production by MFA tool which has given insights into individual role of rate limiting enzymes involved in hydrogen production. The effect of process intensification tool in the form of ultrasound was also analysed in this study, which essentially boosts yield of hydrogen. The *in silico* results obtained by MFA were further exemplified by constructing recombinant strains harbouring the specific genes encoding the key enzymes for hydrogen production. In essence this study has presented a comprehensive account of the complete mechanism involved in

hydrogen pathway and has explored all possible aspects to enhance fermentative hydrogen production from crude glycerol.

In this final chapter, we present an overview of the main results of preceding chapters. These results, when viewed and analyzed at a glance, give an idea of potential of the bioprocess of glycerol conversion to hydrogen.

In **Chapter 2**, we have presented kinetic and thermodynamic analysis along with optimization of process parameters of crude glycerol fermentation for hydrogen production. Prior to the main experiments, preliminary experiments with "one variable at a time (OVAT)" approach have been conducted for determination of optimum incubation time, inoculum size, incubation temperature, initial pH of fermentation, initial glycerol concentration. These results have been used to design the main CCD experiments. Fermentation parameters have been optimized using Central Composite Design (CCD) of experiments as: pH = 6.7, temperature = 36°C, crude glycerol concentration = 7.4 g/L. Kinetic and thermodynamic analysis has been done using Haldane substrate inhibition model, Arrhenius plots and Eyring equation. Kinetic parameters V_{max} and K_m increase, while K_I reduces for crude glycerol, as compared to pure glycerol. Moreover, activation energy (217 kJ/mol) and ΔG (103 kJ/mol) for crude glycerol are lesser than pure glycerol. Consequently, hydrogen yield in crude glycerol fermentation (0.627 mol H_2/ mol glycerol with 44% v/v H_2 in product gas) is significantly higher than pure glycerol. Role of Na^+ ions in improving crude glycerol fermentation has been experimentally confirmed. Kinetic and thermodynamic parameters for crude glycerol fermentation determined in this study have quantitatively substantiated its potential for biohydrogen production.

In **Chapter 3**, we have attempted to get insight into ultrasound induced enhancement in biohydrogen production from glycerol fermentation using metabolic flux analysis (MFA). A pseudo steady state metabolic flux network model was constructed and analyzed using experimentally measured glycerol uptake rate and fluxes of four metabolites, viz. acetate, butyrate, succinate and 1,3–PDO. Batch mode fermentation of glycerol has been carried out with mechanical shaking (control experiments) and sonication (test experiments) using pre–optimized conditions of pH, temperature and initial glycerol concentration. Comparative analysis of the metabolic fluxes in the control experiments and ultrasound–assisted (or test) experiments has given insight into the influence of ultrasound on glycerol metabolism and H_2 yield. Glycerol consumption increased by ~50% under sonication. Biohydrogen yield showed marked rise of ~40% with application of ultrasound. Butyrate and 1, 3–PDO were the major products of glycerol metabolism. Sonication had major influence on carbon fluxes at the acetyl–CoA node. MFA results revealed enhanced flux towards butyrate under sonication, which was manifested in higher butyrate to acetate (B/A) ratio in products and greater H_2 generation. Biohydrogen production was also a microbial growth associated process. Finally, two theoretical alternatives for further enhancement of biohydrogen production were assessed with MFA, viz. enhancement of glycerol uptake and blocking of butyrate pathway.

In Chapter 4, we have addressed the statistical optimization of medium components for production of hydrogen from crude glycerol by a combination of Plackett-Burman (PB) and Central Composite Design (CCD). % H_2 (v/v) was used as the response variable for all experiments. Initial screening of seven medium components using PB design revealed the significant effect of four medium components viz. yeast

extract, NaCl, peptone and K_2HPO_4which was supported by the Pareto plot and significant p-value of the parameters. These four components were further optimized using CCD method of optimization to find out their optimum values. The significant individual and interactive effect of these components were corroborated by the ANOVA results and the corresponding contour plots. The optimum values of these medium components depicted from the desirability function plot are peptone, 2.7g/L; yeast extract, 1.48 g/L; NaCl, 1.46g/L; K_2HPO_4, 0.68 g/L. The validation of the statistical analysis of medium composition for glycerol fermentation was done by conducting fermentation experiments with optimum medium compositions predicted by the CCD analysis which resulted in the final H_2 content of 47.45 %v/v, which is in close agreement with the prediction of CCD analysis (48.10 %v/v). These components augment the activity of enzymes involved in glycerol metabolism and are beneficial for hydrogen production. The main functional components in yeast extract that are used by Clostridia are p-aminobenzoic acid, vitamin B_{12}, pyridoxamine, and biotin, necessary for the growth of the hydrogen producers. The amino acids (glycine, serine and tyrosine) present in yeast extract accelerates the production of alcohol–dependent enzymes such as glycerol dehydrogenase, the immediate enzyme in glycerol metabolism. Peptone is another source of nitrogen which is required for cell growth and maintenance. NaCl is a rich source of Na+ ions which also has beneficial effect on hydrogen production supported by our previous studies and other studies reported in Chapter 1. Na+ ions work towards faster trans-membrane transport of nutrients and substrate to intracellular region, which essentially improves enzymatic reactions in glycerol metabolism resulting in higher hydrogen production.K_2HPO4 in the medium acts as a source of both potassium and phosphate which are important growth enhancing nutrients. Moreover, K_2HPO4 also

acts as a buffering agent and it helps in maintenance of pH of the fermentation broth at a desired value and pH is a significant factor for biohydrogen production process.

In Chapter 5, we have explored the genetic engineering approaches to enhance hydrogen yield in *C. pasteurianum* from glycerol. In this study, we have dealt with homologous overexpression of *dhaD1-dhaK* and *hydA* gene in *C. pasteurianum* for enhanced glycerol utilization and hydrogen production respectively. This attempt was made based on our previous studies on metabolic flux analysis of *C. pasteurianum* with glycerol as the substrate (Chapter 3) which proposed two theoretical approaches viz., doubling the glycerol uptake rate and elimination of butyrate pathway enhances the flux towards H_2.A marked increase of 80% in the cumulative hydrogen volume in the *hydA*$^{++}$ strain is observed as compared to the wild type. This corresponds to a yield of 1.1 moles of H_2 per mole of glycerol after 24 h of fermentation using crude glycerol. Analysis of other co-products of this fermentation revealed some interesting facts. The *hydA* recombinant produced higher amount of acetate and negligible amount of lactate and butyrate as compared with the wild type. Improvement in the hydrogen gas production in the *hydA*$^{++}$ strain was caused by reduction in the amount of lactic acid and enhancement in the amount of acetic acid. It seems apparent that the enhanced hydrogenase activity caused over-oxidation of NADH to NAD+, and consequently the depletion of NADH to reduce pyruvic acid to lactic acid. The solvent profiles of *hydA*$^{++}$ strain suggested that there was a reduction in all the solvents viz. 1,3-propanediol, ethanol and butanol as compared to the WT strain. The fermentation profiles reveal that the cumulative hydrogen volume increased by 75% in the *dhaD1K*$^{++}$ strain which correspond to a yield of 0.93 moles of H_2 per mole of glycerol. Higher glycerol consumption could be observed with *dhaD1K* recombinant strain along with 68% increment in 1, 3-PDO

production. The higher 1,3-PDO production reveals that the overexpression of the immediate enzymes of glycerol metabolism has redirected the pathway towards 1,3-PDO formation rather than towards acetyl-CoA. Due to higher solvent production in this strain the hydrogen production is slightly reduced as compared to the *hydA* recombinant strain.

7.2 SUGGESTIONS FOR FUTURE WORK

The present thesis aims in enhancement of hydrogen yield from crude glycerol by various intensification techniques which includes statistical optimization of medium components and process parameters, analysis of glycerol mediated hydrogen pathway in *C. pasteurianum* by metabolic flux analysis, application of ultrasonication and concluding by genetic engineering of *C. pasteurianum*. Thus this thesis work provides an intensive detailed study on hydrogen production from crude glycerol emphasizing on both physical and genetic approaches to improve the production yield of H_2.The results of this thesis can be further used for the development of a large/industrial scale process. The results of flux analysis and genetic engineering has revealed the significance of few genes in hydrogen production which also makes us more curious towards exploring and identifying the roles of more such rate limiting or inhibiting genes involved in the glycerol mediated H_2 pathway in order to redirect the pathway solely towards hydrogen production. Further research on this pathway may help in increasing the hydrogen yield near to the theoretical yield. Some suggestions to work further in this area can be given as follows:

1. All the experiments in this thesis were conducted in laboratory scale. These studies can be conducted in large-scale process by using bioreactors which will provide insight into real time values.

2. The ultrasound enhanced processes need further optimization with higher frequencies. The ultrasound frequency for present study was kept constant (37 kHz), experiments with different frequencies will be able to ascertain individual contribution of ultrasound to the process. Further in depth assessment of influence of sonication on the structure of different enzymes of glycerol metabolic pathway. Further to evaluate the mechanism involved behind this intensification, studies on proteomic and transcriptomic analysis of the test and control can be done which would provide a detailed perception of the process.

3. The extraction, purification and characterization of the enzyme hydrogenase, glycerol dehydrogenase and dihydroxyacetone kinase from the recombinant strains constructed in this study.

4. Blocking the pathways of other byproducts is one of the essential method to redirect the pathway towards the production of a particular product and increase the yield. This is possible by generating knock-outs of the corresponding genes such as solvent and acid associated genes in *C. pasteurianum,* could help in further improvement of hydrogen yield.

RESEARCH OUTPUTS

PUBLISHED IN PEER REVIEWED INTERNATIONAL JOURNALS

OUT OF THESIS

1. Shyamali Sarma, Avinash Anand, Vikash Kumar Dubey, Vijayanand S. Moholkar. 2017.

Metabolic flux network analysis of hydrogen production from crude glycerol by *Clostridium pasteurianum*. Bioresour. Technol. 242, 169–177.

2. Shyamali Sarma, Vikash Kumar Dubey, Vijayanand S. Moholkar. 2016. Kinetic and thermodynamic analysis (with statistical optimization) of hydrogen production from crude glycerol using Clostridium pasteurianum. Int. J. Hydrogen Energ. 33, 1471–1482.

Manusrcipt under preparation

1. Shyamali Sarma, Vikash Kumar Dubey, Vijayanand S. Moholkar. Optimization of media composition for hydrogen gas production from crude glycerol using *Clostridium pasteurianum*. MTCC 116 (ATCC 6013) by dark fermentation.

2. Shyamali Sarma, David Ortega, Nigel P. Minton, Vikash Kumar Dubey, Vijayanand S. Moholkar. Homologous overexpression of hydrogenase, glycerol dehydrogenase and dihydroxyacetone kinase genes for improved glycerol metabolism and enhanced hydrogen production from crude glycerol by *Clostridium pasteurianum* DSM 525-H4.

Award

Newton Bhaba PhD placement fellowship 2016-17 coordinated by DBT, India and British Council,UK in the University of Nottingham,UK

OTHER PUBLICATIONS

1. Shuchi Singh, Mayank Agarwal, Shyamali Sarma, Arun Goyal, Vijayanand S. Moholkar. 2015. Mechanistic insight into ultrasound induced enhancement of simultaneous saccharifica- tion and fermentation of *Parthenium hysterophorus* for ethanol production Ultrasonics sonochemistry 26, 249-256.

2. Shuchi Singh, Shyamali Sarma, Mayank Agarwal, Arun Goyal, Vijayanand S. Moholkar. 2015. Ultrasound enhanced ethanol production from *Parthenium hysterophorus*a mechanistic investigation. Bioresource technology 188, 287-294.

CONFERENCES PRESENTATIONS

1. Poster Presentation: "Homologous overexpression of key enzymes of *Clostridium pasteurianum*for enhanced biohydrogen production based on metabolic flux analysis" at Research Conclave, organized by IIT Guwahati, Assam, India held from 8-11 March, 2018.

2. Poster Presentation: "Optimization of process parameters for hydrogen production from crude glycerol by *Clostridium pasteurianum* using Response Surface Methedology" at theInternational conference on New Horizons in Biotechnology organized by NIIST, Trivandrum, India held from 22-25 Nov., 2015.